SYSTEMATIC OPTIMIZATION AND EXPERIMENTAL VALIDATION OF SIMULATED MOVING BED CHROMATOGRAPHY SYSTEMS FOR TERNARY SEPARATIONS AND EQUILIBRIUM LIMITED REACTIONS

A Thesis
Presented to
The Academic Faculty

by

Gaurav Agrawal

In Partial Fulfillment
of the Requirements for the Degree
Doctor of Philosophy in the
School of Chemical and Biomolecular Engineering

Georgia Institute of Technology
August 2014

SYSTEMATIC OPTIMIZATION AND EXPERIMENTAL VALIDATION OF SIMULATED MOVING BED CHROMATOGRAPHY SYSTEMS FOR TERNARY SEPARATIONS AND EQUILIBRIUM LIMITED REACTIONS

Approved by:

Dr. Yoshiaki Kawajiri, Advisor
School of Chemical and Biomolecular Engineering
Georgia Institute of Technology

Dr. Athanasios Nenes
School of Chemical and Biomolecular Engineering
Georgia Institute of Technology

Dr. Matthew Realff
School of Chemical and Biomolecular Engineering
Georgia Institute of Technology

Dr. Andreas S. Bommarius
School of Chemical and Biomolecular Engineering
Georgia Institute of Technology

Dr. Martha Grover
School of Chemical and Biomolecular Engineering
Georgia Institute of Technology

Dr. Panagiotis Tsiotras
School of Aerospace Engineering
Georgia Institute of Technology

Date Approved: 1 July 2014

ACKNOWLEDGEMENTS

There are many people to thank who have helped me along the way in doing this work. First, I want to thank my adviser, Dr. Yoshiaki Kawajiri, who was a consistent source of wisdom, direction, and encouragement throughout graduate school. I learned much about numerical optimization and simulated moving bed chromatography from him. He also helped me to grow as a technical writer and speaker. I am honored to be his student.

I'm grateful to my Ph.D. committee, who reviewed and approved this thesis, and gave me many insightful comments from their expertise. They also reviewed my Ph.D. proposal and checked my progress along the way to help me stay on course.

I'm grateful to my colleagues, Dr. Balamurali Sreedhar, Jungmin Oh, Pakkapol Kanchanalai and Huayu Li who helped me in various ways, and we also had many fruitful discussion about this research. I'm also thankful to all the members of the Kawajiri Research Group for being friendly co-workers, and helping me to prepare for some tough presentations. I'm also thankful to the ChBE 2010 entering class, many of whom have been friends to me in graduate school.

I'm thankful to all the faculty and staff at the School of Chemical and Biomolecular Engineering at the Georgia Institute of Technology for working together to create a vibrant academic community.

The financial support from The Dow Chemical Company and Semba Biosciences are also gratefully acknowledged.

TABLE OF CONTENTS

LIST OF TABLES

LIST OF FIGURES

SUMMARY

Simulated Moving Bed (SMB) chromatography is a separation process where the components are separated due to their varying affinity towards the stationary phase. Over the past decade, many modifications have been proposed in SMB chromatography in order to effectively separate a binary mixture. However, the separation of multi-component mixtures using SMB is still one of the major challenges. Although many different strategies have been proposed, previous studies have rarely performed comprehensive investigations for finding the best ternary separation strategy from various possible alternatives. Furthermore, the concept of combining reaction with SMB has been proposed in the past for driving the equilibrium limited reactions to completion by separating the products from the reaction zone. However, the design of such systems is still challenging due to the complex dynamics of simultaneous reaction and adsorption.

The first objective of the study is to find the best ternary separation strategy among various alternatives design of SMB. The performance of several ternary SMB operating schemes, that are proposed in the literature, are compared in terms of the optimal productivity obtained and the amount of solvent consumed. A multi-objective optimization problem is formulated which maximizes the SMB productivity and purity of intermediate eluting component at the same time. Furthermore, the concept of optimizing a superstructure formulation is proposed, where numerous SMB operating schemes can be incorporated into a single formulation. This superstructure approach has a potential to find more advantageous operating scheme compared to existing operating schemes in the literature.

The second objective of the study is to demonstrate the Generalized Full Cycle (GFC) operation experimentally for the first time, and compare its performance to the JO process. A Semba Octave^{TM} chromatography system is used as an experimental SMB unit to implement the optimal operating schemes. In addition, a simultaneous optimization and model correction (SOMC) scheme is used to resolve the model mismatch in a systematic way. We also show a systematic comparison of both JO and GFC operations by presenting a Pareto plot of the productivity achieved against the desired purity of the intermediate eluting component experimentally.

The third objective of the study is to develop an simulated moving bed reactor (SMBR) process for an industrial-scale application, and demonstrate the potential of the ModiCon operation for improving the performance of the SMBR compared to the conventional operating strategy. A novel industrial application involving the esterification of acetic acid and 1-methoxy-2-propanol is considered to produce propylene glycol methyl ether (PMA) as the product. A multi-objective optimization study is presented to find the best reactive separation strategy for the production of the PMA product. We also present a Pareto plot that compares the ModiCon operation, which allows periodical change of the feed composition and the conventional operating strategy for the optimal production rate of PMA that can be achieved against the desired conversion of acetic acid.

CHAPTER I

INTRODUCTION

In any chemical or bioprocessing industry, the need to separate and purify a product from a complex mixture is an important step in the production line. As a result, the separation techniques have received considerable attention over the past few decades for the purification of various natural and biological products, especially in the pharmaceutical industry, where there is a high demand to produce high-purity chemicals. The separation techniques that are based on adsorption principles have been found to be more versatile, with the many types of adsorbent materials that are now available, than other industrial separation techniques [21]. Preparative chromatography, in particular, is a promising option of separation because of its capability to separate a mixture even when the components differ very little in terms of affinity towards the stationary phase.

Chromatography is a powerful separation process for a multitude of reasons. Firstly, it can separate complex mixtures with great precision. The purity requirements of the products are often easier to meet in chromatography compared to other separation methods. Secondly, chromatography can be used to separate delicate products since the conditions under which it is performed are not typically severe. For these reasons, chromatography is quite well suited to a variety of uses in the field of biotechnology, such as separating the mixtures of proteins.

Chromatography, as of today, has developed into an invaluable laboratory tool for the separation and identification of numerous compounds. It is in fact one of the most versatile and widespread technique used in the modern analytical chemistry. Chromatography is also now acknowledged as an industrial unit operation for the

extraction and the purification of fine chemicals, particularly those used as pharmaceutical intermediates [21].

The following sections explain the basic principle of chromatography and its extension to simulated moving bed (SMB). In addition, the concept of reactive chromatography and its application as simulated moving bed reactor (SMBR) are also discussed.

1.1 Principle of chromatography

Chromatography is an adsorptive separation process, where the components are separated due to their varying affinity towards the adsorbent. It is mostly used for homogeneous molecular mixtures. The homogeneous mixture phase is, in most cases, a fluid (liquid) phase with dissolved substances and the additional second phase is an adsorbent (solid) phase. The mixture of substances to be separated (feed), the solvent which is used for their dissolution and transport (desorbent), and the adsorbent (stationary/solid phase) are summarized as the chromatographic system.

Figure 1.1 illustrates the batch chromatography process for the separation of a binary mixture [7]. In this procss, the feed mixture consists of two components A and B, where A is less retained, and B is more retained. A sample of this feed mixture is injected into the column and then the desorbent is fed upstream for moving these components. The weakly retained component (A) moves faster in the column while the strongly retained component (B) moves slower. Over time, both components separate from each other and their fractions are collected at different times at the outlet of column. A detector can also be used in this process to track the effluents concentrations online. In this operation, complete separation of both the components can be achieved although the operating cost may be high considering the solvent consumption and the long production times. Therefore, such batch operation may not be suitable for large-scale productions.

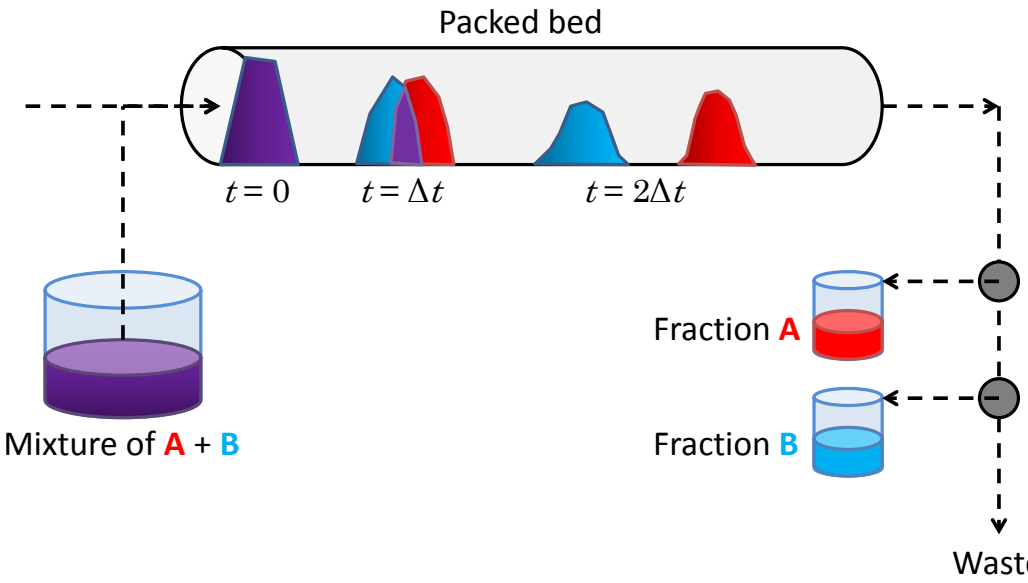

Figure 1.1: Illustrating the principle of chromatography for a binary separation system. The fractions of A and B elute at different times from the outlet of the column [7].

Simulated moving bed (SMB) process, on the other hand, is an extension of batch chromatography that performs chromatography in a continuous and counter-current fashion.

1.2 Simulated moving bed chromatography

The simulated moving bed (SMB) process is based on a flow scheme that takes advantage of continuous and counter-current movement of the liquid and stationary phases without actual movement of the solid. As shown in Figure 1.2, the standard SMB unit consists of multiple chromatographic columns which are interconnected in a cyclic conformation. The feed and desorbent are supplied continuously and at the same time extract and raffinate streams are withdrawn through the outlet ports. The feed mixture consists of two components which are separated by utilizing the difference in their affinity towards the adsorbent phase. The faster moving component is recovered from the raffinate outlet while the slower moving component is recovered through the extract outlet. The counter-current motion of the stationary phases is

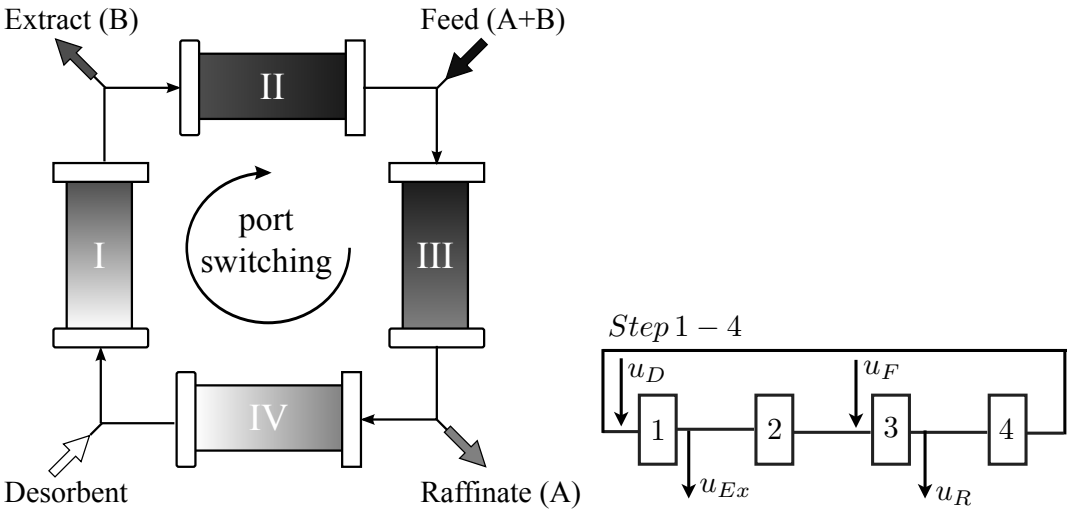

(a) Conceptual illustration (b) Standard schematic

Figure 1.2: Four-zone SMB configuration for separation of a binary mixture. (a) Illustrating the concept of binary separation (b) The standard schematic representation followed in this study.

achieved by switching both inlet and outlet ports simultaneously at a regular interval in the direction of liquid flow. Since SMB is a continuous and cyclic operation, it enables higher throughput and incurs less desorbent consumption compared to the batch chromatography.

The operating conditions of SMB must be determined to achieve the desired performance. The two inlet streams, feed and desorbent and two outlet streams, extract and raffinate divide the entire SMB system into four zones. The flow rate in each zone can be controlled independently, and hence there are four control parameters. The zone velocities are in general selected such that zone II and III separates component A from B while zone I and IV regenerates the columns by desorbing both of the adsorbed components. Furthermore, the counter-current motion of the stationary phase is simulated by switching the inlet and outlet ports in the direction of liquid flow. This switching time of the ports is also a control parameter. In a standard SMB, all these control parameters are considered constant with time and

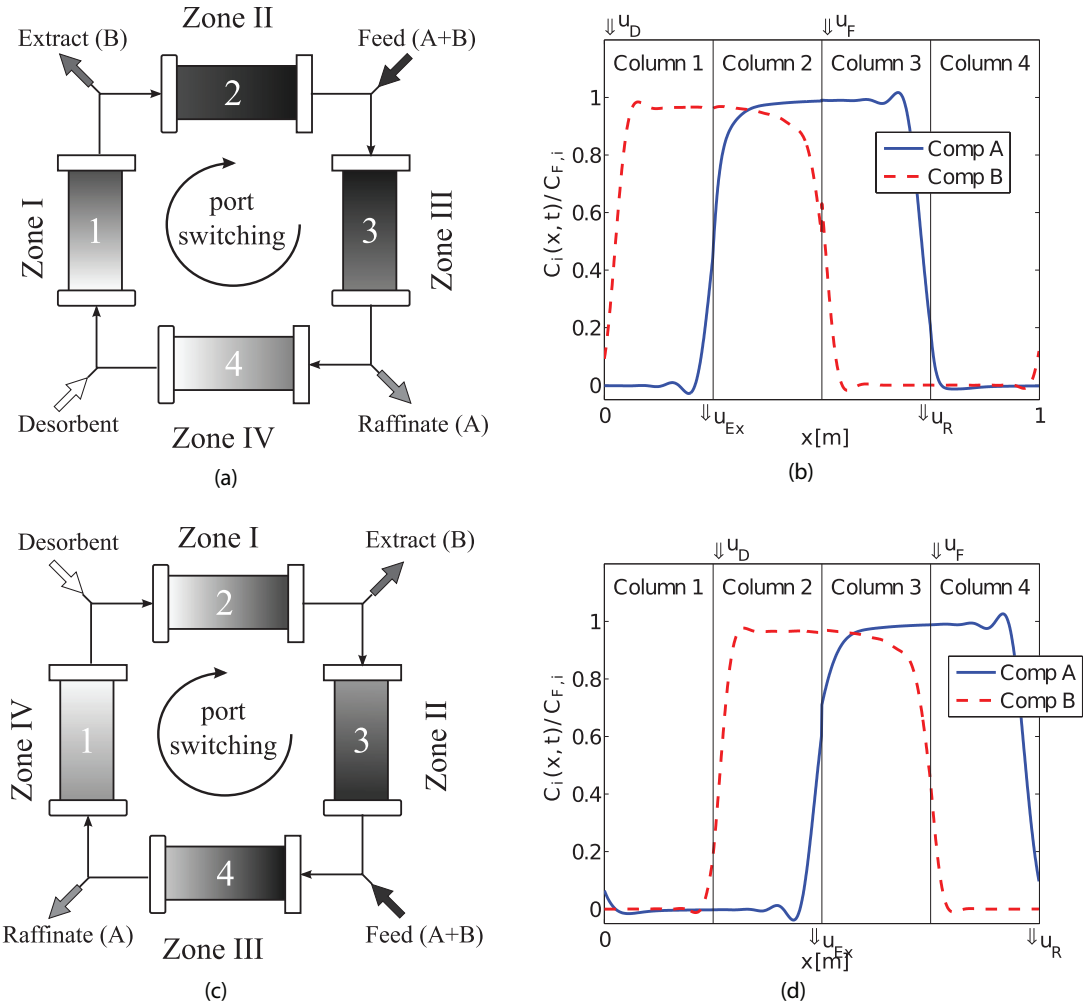

Figure 1.3: Schematic of SMB process with the internal concentration profiles at cyclic steady state for two consecutive steps. (a) Step 1, (b) the normalized internal concentration profiles at the beginning of Step 1, (c) Step 2, (d) the normalized internal concentration profiles at the beginning of Step 2.

treated as operating conditions. Since these operating conditions influence both purity and recovery obtained in the product outlets, the optimal performance of the SMB systems depends on the identification of the optimal operating conditions. The optimization strategies that are used for obtaining the optimal operating conditions of SMB systems are discussed in Chapter 3.

In the SMB systems, the counter-current movement of the solid phase is simulated by discrete shifting of inlet and outlet ports. Due to this discrete shifting, the SMB systems arrives at a cyclic steady state (CSS). At the CSS, the concentration profiles

still change inside the columns; however the snapshots of internal concentration profiles at the beginning and at the end of the step are identical, apart from a shift of exactly one column length [37]. Figure 1.3 illustrates this concept of CSS by showing the internal concentration profiles for two consecutive steps of the SMB operation at the cyclic steady state. In Step 1, the feed mixture is fed between columns 2 and 3 and the desorbent is supplied between columns 1 and 4. Thus, the faster moving component (A) moves to column 3 and recovered from the raffinate outlet while the slower moving component (B) is left behind in the columns 1 and 2 and thus withdrawn from the extract outlet (see Figure 1.3(b)). After both the products are collected from the product outlets, the SMB system switches to Step 2. In this step, the positions of all the inlet and outlet ports are switched clockwise by one column length (Figure 1.3(c)). As a result, the feed is fed between columns 3 and 4 and desorbent is supplied between columns 1 and 2. Similarly, the raffinate and extract outlet streams are also switched to the outlet of columns 4 and 2, respectively. The concentration profiles at the beginning of Step 2 are shown in Figure 1.3(d). As can be seen from the Figures 1.3(b) and (d), the internal concentration profiles at the beginning of Step 2 are exactly identical to Step 1, except for the shift of one column length. Thus, the SMB system is at a cyclic steady state. This cyclic operation of SMB is constantly repeated to recover pure products continuously from the raffinate and the extract outlet. This standard SMB configuration with four zones has been extensively studied by various research groups and established strategies to determine the design and operation are available today [12, 68, 84, 77, 52, 71, 21, 30].

SMB systems are an efficient mean of performing large-scale chromatographic separations and thus have been successfully applied in various areas such as sugar, petrochemical and pharmaceutical separations [71, 21, 23, 74]. Since SMB enables high throughput and low desorbent consumption compared to conventional chromatography, there has been a continuous effort to find modified SMB schemes that

allow for higher productivity yet meeting the same product specifications. Examples of such modifications are the processes called Varicol, which allows asynchronous movement of injection and withdrawal ports [46], PowerFeed, where the external flow rates (u_F, u_D, u_{Ex}, u_R) are varied within one switching interval t_{sw} [37, 94], Partial Feed, where the feed is partially injected within one switching interval [93] , ISMB, where the first part of the step is similar to standard four-zone SMB without recycle while the second part is just circulating the liquid along the columns with no inflow or outflows [81], ModiCon, where the feed flow rate remains constant however feed concentration is altered during one switching interval t_{sw} [73]. However, these modified SMB operations are limited to the separation of binary mixtures.

One of the major disadvantage of SMB is that it is unable to fractionate multiple components into more than two product streams. This issues is addressed in the first objective of this work, which is to explore the potential of SMB systems for the separation of multi-component mixtures. The objectives of this project and a review of past studies on multi-component mixtures are given in Chapter 4.

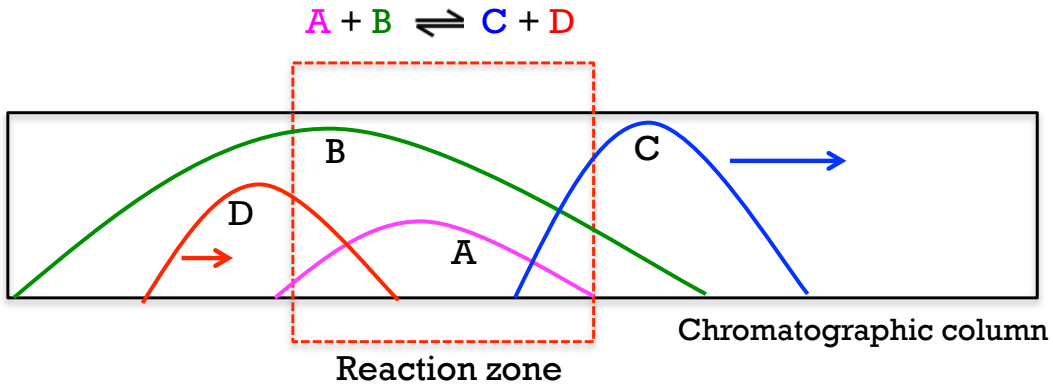

Figure 1.4: Schematic of reactive chromatography unit for the production of component C through the reaction of A and B.

1.3 Reactive chromatography

The reactive chromatography process is based on the concept of integrating both separation and reaction inside a chromatographic column (see Figure 1.4). In this process, the limiting reactant (A) is injected as a sharp pulse into the column and then the excess reactant (B) is supplied. The two components react inside the column forming products that are fractionated at the outlet of the column. The weakly adsorbed component (C) moves faster in comparison to the strongly adsorbed component (D). Such a mechanism facilitates the reversible reaction to go beyond thermodynamic equilibrium by continuously separating the products from the reaction zone. As a consequence, there is more product formation in these systems and the products can be recovered at high purities due to their separation from the reactants. Furthermore, the integration of both reaction and separation units into one single unit reduces both capital and operating costs. However, this batchwise operation may not be suitable for large-scale productions.

Simulated moving bed reactor (SMBR), on the other hand, is an extension of this process that performs reactive chromatography in a continuous and counter-current fashion. The SMBR system is described in the next Section.

1.4 Simulated moving bed reactor

Simulated moving bed reactor (SMBR) is an extension of the reactive chromatography process that performs it in a continuous and counter-current fashion. The SMBR unit, as shown in Figure 1.5, consists of multiple chromatographic columns that are interconnected in a cyclic conformation. These columns are packed using a resin that can functions both as a catlayst and an adsorbent. The schematic in Figure 1.5 is drawn for a second order reversible reaction that is equilibrium limited ($A + B \rightleftharpoons C + D$). Here, the feed is a mixture of components A and B while the

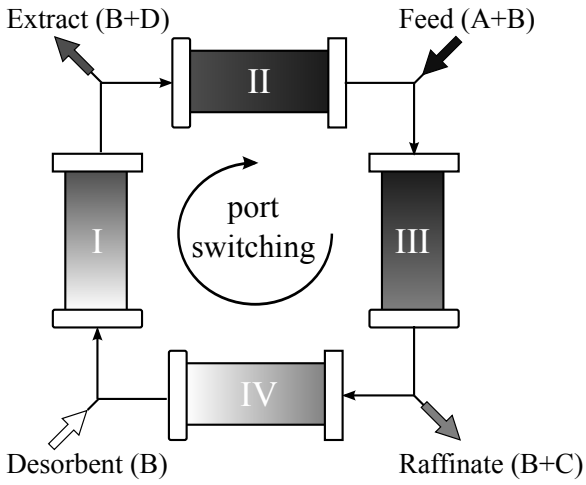

Figure 1.5: Schematic of simulated moving bed reactor unit for the production of component C through the reaction of A and B ($A + B \rightleftharpoons C + D$).

desorbent only consists of component B. Both feed and desorbent are supplied continuously and at the same time extract and raffinate streams are withdrawn through the outlet ports. Component A reacts with B under catalyzed conditions forming C and D. As this reaction proceeds inside the SMBR, both components C and D are continuously removed thus shifting the equilibrium in the forward direction. The faster-moving component, C, is recovered from the raffinate outlet while the strongly retained component, D, is recovered through the extract outlet.

The operating conditions of SMBR must be determined to achieve the desired performance. The two inlet streams, feed and desorbent, and two outlet streams, extract and raffinate, divide the entire SMBR system into four zones. The flow rate in each zone can be controlled independently, and hence there are four degrees of freedom. The zone velocities are in general selected such that zone II and III become the reaction plus separation zones while zone I and IV regenerates the columns [21]. Furthermore, the counter-current motion of the solid phase is simulated by switching both inlet and outlet ports simultaneously in the direction of liquid flow. The two consecutive switching of the ports defines a step and the time for which this step lasts is also a degree of freedom. In a four-column SMBR, four consecutive steps complete

a full cycle and it brings the SMBR system back to its original configuration. This cyclic operation of SMBR is constantly repeated to extract pure products from the raffinate and the extract outlets. The number of operating parameters that affect the performance of SMBR is five: four zone flow rates and the switching time. In a standard SMBR, all of these control parameters are considered constant with time and treated as operating conditions. Similar to the design of SMB systems, the optimal performance of the SMBR systems also depends on the identification of the optimal operating conditions. The optimization strategies that are used for obtaining the optimal operating conditions of SMBR systems are also discussed in Chapter 3.

CHAPTER II

SCOPE OF THESIS

The work presented in this thesis is based on available mathematical modeling and the optimization methods for the simulated moving bed (SMB) and simulated moving bed reactor (SMBR) processes. There are three main objectives:

1. Identify the best separation strategy for the separation of a ternary mixture among various alternative designs of SMB

2. Experimentally validate both JO and Generalized Full Cycle operations for separation of sugars

3. Develop an SMBR process for industrial-scale production of propylene glycol ethers

The first objective is the topic of Chapter 4, where the performance of several SMB operating schemes, that are used for the separation of a ternary mixture, are compared. A variety of operating schemes such as SMB cascade, Eight-zone, Five-zone, Four-zone and JO process are included in this study. The performance of these systems is compared in terms of the maximum productivity that can be attained in the SMB system and the amount of solvent consumed. This comparison is performed by formulating a multi-objective optimization study that maximizes the SMB productivity and the purity of intermediate eluting component at the same time. In addition, the concept of superstructure formulation is proposed where numerous SMB operating schemes can be incorporated into a single formulation. Based on this concept, the Generalized Full Cycle (GFC) and Full superstructure formulation are presented in this study, which are optimized by considering a large number of SMB

configurations. It is demonstrated that this approach has a potential to find the best ternary separation strategy among various alternatives designs of SMB. The emphasis of this study is on separation of a ternary mixture however the analysis could be extended for any multi-component separation system.

The second objective is the topic of Chapter 5, which focuses on combining both computational and experimental sides of SMB chromatography. In Chapter 4, it is shown (through a computational study) that the JO and the GFC operations are promising to obtain a higher productivity of the SMB process in comparison to the other existing operations. In this chapter, optimized operations of both JO and GFC operations are experimentally validated. A Semba Octave^{TM} chromatography system is used as an experimental SMB unit for implementing the optimal operating conditions. In addition, the separation of sugars is chosen as the chromatographic system for the validation of operating strategies. When the optimal operating conditions obtained from the model optimization are implemented on the experimental unit, a model mismatch is observed in the products purity and recovery values. To resolve this model mismatch in a systematic way, in this study, a simultaneous optimization and model correction (SOMC) scheme has been proposed and implemented. The SOMC scheme arrives at the optimal operating conditions which satisfy the optimal productivity as well as the desired purity and recovery of products experimentally.

The final objective is the topic of Chapter 6, which extends the optimization studies of the SMB systems to the SMBR systems. SMBR operations can provide economic benefit for equilibrium limited reversible reactions. In such operations, in situ separation of the products drives the reversible reactions to completion beyond thermodynamic equilibrium and also enables in the continuous recovery of the products of high purity. In this study, a novel industrial application of SMBR process is developed. We consider the production of propylene glycol methyl ether acetate

(PMA) through the esterification of 1-methoxy-2-propanol (PM) and acetic acid using AMBERLYST^{TM} 15 as a catalyst and adsorbent. A multi-objective optimization study is presented to find the best reactive separation strategy for the production of the PMA product. The multiple objectives are to maximize the production rate of PMA and maximize the conversion of the esterification reaction. In addition, a ModiCon operating strategy is proposed, which is based on the cyclic modulation of the feed concentration. It is demonstrated that such a feed concentration gradient during the step time can manipulate the internal concentration profiles inside the SMBR. By introducing this strategy, it is shown that the performance of the SMBR system can be improved significantly compared to the conventional SMBR operating strategy. This work, to the best of our knowledge, implements the ModiCon strategy for the first time in reactive separation systems.

Altogether this work is focused on finding the best design and operation of the SMB and the SMBR systems based on a systematic approach. The mathematical models that are available in the literature and the deterministic nonlinear programming techniques are used to find the optimal SMB/SMBR configurations. This model based optimization approach can provide innovative solutions that are difficult to identify using human intuition. In addition, a systematic algorithm is developed to resolve the model mismatch while implementing the optimal operating conditions on the experimental unit. This study thus eliminates the need for trial-and-error methods which rely significantly on human intervention and experience to resolve the model mismatch.

CHAPTER III

MODELING AND OPTIMIZATION

This chapter is devoted to the detailed mathematical modeling and the optimization methods for the simulated moving bed (SMB) and simulated moving bed reactor (SMBR) processes. The mathematical modeling is based on the first principles.

3.1 Modeling of simulated moving bed

Over the last decades, several mathematical models have been proposed in the literature for modeling the SMB system. A summary of these models can be found in Schmidt-Traub et al. [71]. These models can be broadly classified in two categories: true moving bed (TMB) model and simulated moving bed (SMB) model. The TMB model simplifies the dynamics of the SMB process by neglecting the cyclic switching of the SMB system. This simplification reduces the computational effort significantly. However, the model based optimal design of SMB requires an accurate description of the dynamics of the SMB process. Therefore, various researchers in the past have employed the use of a detailed SMB model [9, 17, 29, 30, 41, 55, 84]. Dunnebier and Klatt [17] also compared various types of SMB models with different levels of complexity for the dynamic simulation of the SMB processes. It was shown that the a linear driving force (LDF) model, which assumes the linear driving force for the mass transfer rate in the solid phase, is capable of predicting the experimental data reasonably well, even for nonlinear isotherms. Further, Bentley et al. [9] have used this LDF model for the separation of nonlinear SMB systems and the predictions made by the model agreed with the experimental results. In this study, we employ the same LDF model for modeling the SMB system.

The isotherm system used in our study is linear and thus the LDF model is

expected to capture the dynamics of SMB process very accurately. In the LDF model, both axial dispersion and the diffusion into the adsorbent particles, which causes the band broadening, are lumped in the mass transfer coefficient. The modeling equations are as follows.

Mass balance in the liquid phase:

$$\epsilon_b \frac{\partial C_i^j(x,t)}{\partial t} + (1-\epsilon_b)\frac{\partial q_i^j(x,t)}{\partial t} + u^j(t)\frac{\partial C_i^j(x,t)}{\partial x} = 0. \tag{1}$$

where C_i^j and q_i^j are the concentration in the liquid and the solid phase, respectively, ϵ_b is the bed porosity, $u^j(t)$ is the superficial velocity of column, x is the axial distance and t is the time. The superscript j represents the jth column while subscript i refers to the component index.

Mass balance in the solid phase:

$$(1-\epsilon_b)\frac{\partial q_i^j(x,t)}{\partial t} = K_{m,i}(C_i^j(x,t) - C_i^{j,eq}(x,t)). \tag{2}$$

where $C_i^{j,eq}$ is the concentration in the liquid phase that is in equilibrium with the solid phase and $K_{m,i}$ is the liquid phase based mass transfer coefficient.

Adsorption equilibrium: the equilibrium between liquid and the solid phase is represented by linear isotherms.

$$q_i^j(x,t) = H_i\, C_i^{j,eq}(x,t)$$

$$i = 1,\ldots,N_{Comp}, \quad j = 1,\ldots,N_{Column} \tag{3}$$

where H_i is the henry constant. The symbols N_{Comp} refers to the total number of components and N_{Column} refers to the total number of columns.

The SMB system consists of multiple chromatographic columns that are interconnected in a cyclic conformation (see Figure 2(a)). Hence, we must satisfy the flow and mass balance equations at the connecting ports between any two columns. Since the inlet/outlet streams are different between jth and $(j+1)th$ column, the following

equations are written in their general form as:

$$u^{j+1}(t) = u^{j}(t) - (u_R^j(t) + u_{Ex}^j(t) + u_I^j(t)) + (u_D^{j+1}(t) + u_F^{j+1}(t)). \tag{4}$$

$$C_i^{j+1}(0,t)\, u^{j+1}(t) = C_i^j(L,t)\left(u^j(t) - u_{Ex}^j(t) - u_R^j(t) - u_I^j(t)\right) + C_{i,F}\, u_F^{j+1}(t). \tag{5}$$

where u_R^j, u_{Ex}^j, u_I^j, u_D^j and u_F^j are the velocities of raffinate, extract, intermediate stream outlet, desorbent and the inlet feed stream, respectively. $C_{i,F}$ is the concentration of ith component in the feed and L is the length of the column.

3.1.1 Treatment of CSS

In SMB operation the counter-current movement of the stationary phase is simulated by shifting both the inlet and outlet streams in the direction of liquid flow by valve switching. Due to this discrete shifting, SMB systems arrives at a cyclic steady state referred as CSS. There are multiple ways to formulate the CSS constraints. A single step formulation is considered where all the steps are identical except the shifting of inlet and outlet streams due to valve switching. The formulation is written as [37]:

$$\begin{aligned} C_i^j(x,0) &= C_i^{j+1}(x,t_{step}), \quad i = 1,\ldots,N_{Comp}, \quad j = 1,\ldots,N_{Column}-1 \\ q_i^j(x,0) &= q_i^{j+1}(x,t_{step}), \quad i = 1,\ldots,N_{Comp}, \quad j = 1,\ldots,N_{Column}-1 \end{aligned}$$

$$\begin{aligned} C_i^{N_{Column}}(x,0) &= C_i^1(x,t_{step}), \quad i = 1,\ldots,N_{Comp} \\ q_i^{N_{Column}}(x,0) &= q_i^1(x,t_{step}), \quad i = 1,\ldots,N_{Comp} \end{aligned}$$

On the other hand, a full cycle formulation is considered for operations in which the operation during all the four steps is different [59]. In the full cycle formulation, the concentration profiles are identical at the beginning and at the end of the cycle. The formulation is written as:

$$\begin{aligned} C_i^j(x,0) &= C_i^j(x,t_{cycle}), \quad i = 1,\ldots,N_{Comp}, \quad j = 1,\ldots,N_{Column} \\ q_i^j(x,0) &= q_i^j(x,t_{cycle}), \quad i = 1,\ldots,N_{Comp}, \quad j = 1,\ldots,N_{Column} \end{aligned}$$

3.2 Modeling of simulated moving bed reactor

In the past, several mathematical models have been proposed in the literature for modeling the SMBR system. A summary of these models can be found in Schmidt-Traub et al. [71]. These models can be broadly classified in two categories: true moving bed reactor (TMBR) model and simulated moving bed reactor (SMBR) model. The TMBR model simplifies the SMBR dynamics by assuming infinite number of columns and does not account for the discrete switching of inlet and outlet ports [56, 78]. This simplification reduces the computational effort significantly. However, the model based optimal design of SMBR requires an accurate description of the dynamics of the SMBR process. Therefore, various researchers have employed the use of a detailed SMBR model. Zhang et al. [95] and Yu et al. [91, 92] used an equilibrium dispersive SMBR model which assumes both liquid and solid phase to be in equilibrium by neglecting all the mass transfer effects. Zhang et al. [96] used an SMBR model based on linear adsorption isotherm and linear driving force approximation for the adsorption rate, where both axial dispersion and diffusion into adsorbent particles, which cause band broadening, were lumped into one mass transfer coefficient. Strohlein et al. [79] used an isothermal, lumped kinetic rate model with a linear driving force for the adsorption rate.

In this study, it was found that the complex dynamics of simultaneous reaction and adsoption inside the SMBR is difficult to capture by lumping both axial dispersion and diffusion into the adsorbent particles into the mass transfer coefficients. Hence, these two effects have to be accounted separately, and we adopt a transport dispersive model with a linear driving force for the adsorption rate [71]. Here, the axial dispersion phenomenon and diffusion into the adsorbent particles inside the columns are accounted separately using an overall axial dispersion coefficient and individual mass transfer coefficients for each component. The mass balance equations in the liquid and solid phases for component i in the jth adsorption column are written as

follows.

Mass balance in the liquid phase:

$$\frac{\partial C_i^j(x,t)}{\partial t} + \frac{1-\epsilon_b}{\epsilon_b} K_{m,i} \left(q_i^{j,eq}(x,t) - q_i^j(x,t)\right) + u^j \frac{\partial C_i^j(x,t)}{\partial x} = D_{ax} \frac{\partial^2 C_i^j(x,t)}{\partial x^2}. \quad (6)$$

where $C_i^j(x,t)$ and $q_i^j(x,t)$ are the concentration in the liquid and the solid phase at axial distance x and time t, respectively, $q_i^{j,eq}(x,t)$ is the concentration in the solid phase that is in equilibrium with the liquid phase, ϵ_b is the bed porosity, $K_{m,i}$ is the solid phase based mass transfer coefficient of the ith component, D_{ax} is the axial dispersion coefficient, u^j is the superficial velocity of the column, x is the axial distance and t is the time. The subscript i represents the component index while superscript j refers to the jth column.

Mass balance in the solid phase:

$$\frac{\partial q_i^j(x,t)}{\partial t} = K_{m,i}(q_i^{j,eq}(x,t) - q_i^j(x,t)) + \nu_i\, r^j(x,t). \quad (7)$$

where ν_i is the stoichiometric reaction coefficient of the ith component and $r^j(x,t)$ is the net reaction rate in the jth column at distance x and time t.

The equilibrium between solid and liquid phases is represented by the following linear adsorption isotherm equation [63]

$$q_i^{j,eq}(x,t) = H_i\, C_i^j(x,t). \quad (8)$$

where H_i is the Henry constant.

The above partial differential equations require boundary conditions, which are discussed below. The concentration at the inlet and outlet of the columns are expressed by using the well-known Danckwerts relations. Since the SMBR system consists of multiple chromatographic columns that are interconnected in a cyclic conformation (see Figure 1.5), the mass balance equations at the connecting ports between any two columns is a part of the boundary conditions.

Mass balance between jth and $(j+1)th$ column:

$$C_i^{j+1}(0,t)\,u^{j+1} = C_i^j(L,t)\left(u^j - u_{Ex}^j - u_R^j\right) + C_{i,F}\,u_F^{j+1} + C_{i,D}\,u_D^{j+1} + D_{ax}\left.\frac{\partial C_i^j(x,t)}{\partial x}\right|_{x=0}. \tag{9}$$

where u_R^j, u_{Ex}^j, u_D^j and u_F^j are the velocities of raffinate, extract, desorbent and the inlet feed stream, respectively. These values are positive only if raffinate, extract, desorbent, or feed is withdrawn or fed, and zero otherwise. The symbol $C_{i,F}$ and $C_{i,D}$ are the concentrations of ith component in the feed and desorbent, respectively and L is the length of the column.

The other boundary condition determines the concentration at the outlet of column.

$$\left.\frac{\partial C_i^j(x,t)}{\partial x}\right|_{x=L} = 0. \tag{10}$$

The flow balance at the inlet and outlet ports should also be satisfied to maintain the consistency of the flow. Thus, the following equations are implemented.

$$u^{j+1} = u^j - (u_R^j + u_{Ex}^j + u_I^j) + (u_D^{j+1} + u_F^{j+1}). \tag{11}$$

$$i = 1, \ldots, N_{Comp}, \quad j = 1, \ldots, N_{Column}$$

where the symbol N_{Comp} refers to the total number of components and N_{Column} is the total number of columns.

3.2.1 Treatment of CSS

In SMBR, the counter-current movement of the solid phase is simulated by discrete shifting of inlet and outlet ports. As a result, the SMBR systems arrives at a cyclic steady state (CSS). At the CSS, the concentration profiles still change inside the columns; however the snapshots of internal concentration profiles at the beginning and at the end of the step are identical, apart from a shift of exactly one column length [37]. Since SMBR is a symmetric operation i.e. all the steps are identical except

the shifting of inlet and outlet streams due to valve switching, we consider a single step formulation to write the CSS [3, 30, 37]. In this formulation, the concentration profiles at the beginning of the step in the jth column are identical to the concentration profiles at the end of the step in the $(j+1)th$ column. The formulation is written as:

$$C_i^j(x,0) = C_i^{j+1}(x,t_{step}), \quad i = 1,\ldots,N_{Comp},\ j = 1,\ldots,N_{Column}-1 \tag{12}$$

$$q_i^j(x,0) = q_i^{j+1}(x,t_{step}), \quad i = 1,\ldots,N_{Comp},\ j = 1,\ldots,N_{Column}-1 \tag{13}$$

$$C_i^{N_{Column}}(x,0) = C_i^1(x,t_{step}), \quad i = 1,\ldots,N_{Comp} \tag{14}$$

$$q_i^{N_{Column}}(x,0) = q_i^1(x,t_{step}), \quad i = 1,\ldots,N_{Comp} \tag{15}$$

where t_{step} is the step time.

3.3 Optimization Strategy

The methods that solves nonlinear programming (NLP) problems can be separated into two categories: the sequential and the simultaneous strategies. In the sequential methods, only the control variables are discretized and the resulting NLP is solved with control vector parametrization (CVP) methods. In this formulation, the control variables are represented as piecewise polynomials and optimization is performed with respect to the polynomial coefficients. For a given set of initial conditions and control parameters, the DAE model is then solved in a inner loop, while the parameters representing the control variables are updated on the outside using an NLP solver. Gradients of the objective function with respect to the control coefficients and parameters are calculated either from direct sensitivity equation of the DAE system or by integration of adjoint sensitivity equations [11].

The simultaneous approaches, on the other hand, deal with full discretization of state and control profiles and the state equations. Typically the discretization is performed by using collocation on finite elements, a high order implicit Runge-Kutta

method. The resulting set of equations and constraints leads to a large nonlinear program that is addressed with large scale NLP solvers. This approach is fully simultaneous and requires no nested calculations with DAE solvers. Moreover, both structure and sparsity of the KKT system can be exploited by modern NLP solvers such as IPOPT [88].

In this study, we use the simultaneous approach for optimization, where the spacial domains are discretized using central finite difference scheme, and the Radau collocation on finite elements is used for the temporal discretization [30]. These discretized equations are incorporated within a large-scale Nonlinear Programming (NLP) optimization problem, which is implemented into AMPL (A Mathematical Programming Language) modeling environment. The advantage of using AMPL is that it supports nonlinear programming and provides the automatic differentiation functionality which is used in many solvers. The resulting problem has large number of variables and linearized Karush-Kuhn-Tucker (KKT) condition tends to have a sparse structure [29]. Thus, it is crucial to choose a solver which can handle large number of variables and at the same time exploit the problem structure. To satisfy these requirements, we choose IPOPT 3.0 [88], an interior-point solver discussed in the Section 3.3.2.

The SMB/SMBR optimization problem is a large-scale, non-convex, partial differential equation (PDE) constrained problem which makes it extremely challenging to solve. Further, since there can be steep concentration profiles for highly efficient chromatographic columns, the numerical method can require larger number of finite elements to obtain accurate solutions. To deal with this challenge, we have used sophisticated methodologies such as collocation methods in order to reduce the problem size. The collocation methods are discussed in next section.

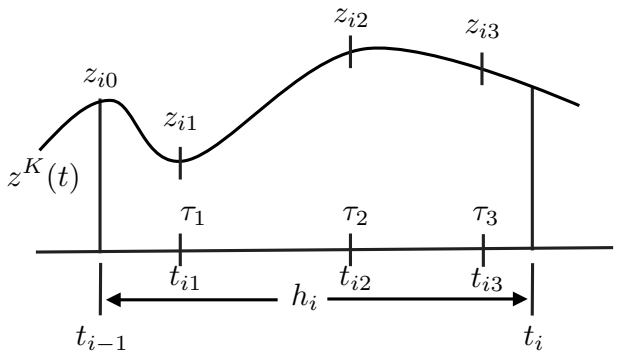

Figure 3.1: Polynomial approximation ($z^K(t)$) for the state profile across the i^{th} finite element [11]. Here we have three collocation points located at τ_1, τ_2 and τ_3 distances in the finite element.

3.3.1 Collocation methods

Collocation methods are high-order implicit Runge-Kutta methods, where the states are represented by piecewise polynomials inside each finite element (see Figure 3.1). The coefficients of the polynomial are determined by solving differential equations at the collocation points. The location of collocation points is based on the chosen collocation method. In this study, Gauss-Radau collocation method is considered for discretization in the time domain. The resulting collocation equations are algebraic equations that can be incorporated directly within an NLP formulation. The large-scale NLP formulation allows a great deal of sparsity and structure, along with flexible decomposition strategies to solve this problem efficiently. Moreover, convergence difficulties in the embedded DAE solver are avoided, and sensitivity calculations from the solver are replaced by direct gradient and Hessian evaluations within the NLP formulation [11].

There are a few other advantages of using collocation methods. Since the NLP formulation needs to deal with discontinuities in control profiles, a single-step method is preferred, as it is self-starting and does not rely on smooth profiles that extend over previous time steps. The collocation formulation requires smooth profiles only within the finite element. In addition, the high-order implicit discretization provides

accurate profiles with relatively few finite elements. As a result, the number of finite elements need not be excessively large, particularly for problems with many states and controls.

3.3.2 Interior-point methods

The interior-point methods are an alternative to active set strategies in order to solve nonlinear programming problems. The algorithm used by these methods is illustrated by the following example. Let's consider a general optimization problem given as:

$$\min_{x} f(x) \tag{16}$$

$$s.t.\ c(x) = 0,\ x \geq 0 \tag{17}$$

The interior point method transforms this general optimization problem into the following formulation [11]:

$$\min \Phi_{\mu_l}(x) = f(x) - \mu_l \sum_{i=1}^{n_x} ln(x_i) \tag{18}$$

$$s.t\ c(x) = 0,\ x > 0 \tag{19}$$

where the integer l is the sequence counter. Also, $\lim_{l\to\infty} \mu_l = 0$. In other words, the value of μ is progressively decreased in order to obtain a solution close to the optimum solution of general optimization problem. Since the logarithmic barrier term becomes unbounded at $x = 0$, the path generated by interior-point algorithm would always lie in a region that consists of strictly positive variables, $x > 0$.

In general, a newton based strategy is adopted along with the line search technique in order to solve KKT conditions obtained from the reformulated optimization problem. The dual variable are introduced into the KKT conditions along with the equations $X\,\mu = \mu\,e$. This substitution and linearization eases the nonlinearity of barrier terms. The KKT conditions of the system of Equations (18)-(19) are written as:

$$\nabla f(x) + \nabla c(x)\, v - u = 0, \tag{20}$$

$$X\, \mu = \mu\, e, \tag{21}$$

$$c(x) = 0 \tag{22}$$

where $X = diag\{x\}$, $e = [1, 1, \ldots, 1]^T$, and the solution vector $x(\mu) > 0$, *i.e.* it lies strictly in the interior. Given an iterate x^k, v^k, u^k with $x^k, u^k > 0$, search directions (d_x^k, d_v^k, d_u^k) are obtained from the following equation [11]:

$$\begin{bmatrix} W^k & \nabla c(x^k) & -I \\ \nabla c(x^k) & 0 & 0 \\ U^k & 0 & X^k \end{bmatrix} \begin{bmatrix} d_x^k \\ d_v^k \\ d_u^k \end{bmatrix} = - \begin{bmatrix} \nabla f(x^k) + \nabla c(x^k) v^k - u^k \\ c(x^k) \\ X^k\, u^k - \mu_l\, e \end{bmatrix} \tag{23}$$

where $W^k = \nabla_{xx} L(x^k, v^k)$, $L = \bar{f}(x) + c(x)^T\, v$ and $\bar{f}(x)$ is the objective function given by Equation (18). The matrix W^k, inside the interior-point methods, could be computed exactly or could be approximated using quasi-newton methods. Since interior-point methods can accept exact second order derivatives, they have fast convergence properties.

CHAPTER IV

COMPARISON OF VARIOUS TERNARY SIMULATED MOVING BED SEPARATION SCHEMES BY MULTI-OBJECTIVE OPTIMIZATION

4.1 Motivation

Since its development by UOP in the 1960s, simulated moving bed (SMB) chromatography has emerged as a continuous and effective separation technique for preparative and industrial scale chromatography. SMB systems are widely applied in many industrial applications such as sugar, food, petrochemical and pharmaceutical industries [23, 71, 74]. The SMB technology is well established, in particular, for a difficult separation of binary mixtures.

However, the application of SMB for multi-component separation is still considered one of the major challenges. Multi-component separation is a very important problem for bioseparation, such as protein purification. In such applications, the feed mixture may have a large number of components of similar chemical structures. There have been several concepts that are proposed in the literature to separate a multi-component mixture through various modifications keeping the advantages of SMB. The JO process was presented for ternary separation in which the feed is discontinuously added only during a part of the cycle and rest all other steps behaves similar to SMB with no feed. This process was commercialized by Japan Organo Company [48]. In addition, Mata et al. [49] had developed a pseudo SMB model for this JO process and discussed the effect of operating conditions and mass transfer coefficients on the process performance. Nicolaos et al. [58] studied several ternary

SMB configurations such as eight-zone, nine-zone and cascade of SMB in the framework of equilibrium theory. Kessler and Seidel-Morgenstern [34] analyzed various combination of 4-zone units using an equilibrium stage model in order to study their potential to separate ternary and quaternary mixtures. Wankat [89] developed seven cascades for SMB systems for ternary separation and determined desorbent to feed ratio for each cascade using the equilibrium model. Beste and Arlt [10] proposed a side-stream SMB which was later classified as five-zone SMB for separation of multi-component mixtures. Kim et al. [35] proposed an additional single-cascade system, the modified four-zone, along with five-zone SMB for ternary separations. Kurup et al. [41] compared these five-zone and modified four-zone SMB systems at optimal conditions for varying adsorption selectivity, mass-transfer resistance, and nonlinearity in adsorption isotherm parameters. Mun [57] proposed improvements in the five-zone SMB by simultaneous use of partial-feeding and partial-closing of the product ports, however, in these operating schemes, a step was further divided into sub steps. Such operations add complexity to the SMB system and are beyond the scope of this work. In addition, a few non-isocratic SMB methods are also developed in past as discussed by Wang et al. [90] and Aumann et al. [5]. Most of these modified SMB configurations (excluding non-isocratic methods) are discussed, in depth, later in this chapter.

The performance of SMB system highly depends on its operating conditions. Furthermore, by changing relative position of feed, desorbent, extract, intermediate and raffinate streams, a large number of SMB configurations can be created. Hence, the identification of optimal operating strategy for multi-component separation is indeed a challenging problem. Moreover, to incorporate these numerous SMB configurations into a single optimization problem and treating operating conditions as decision variables is very computationally extensive. Kawajiri and Biegler [29] proposed the concept of superstructure formulation where a number of SMB operating schemes could be incorporated. They also showed the potential of superstructure approach to

find more advantageous operating scheme compared to standard SMB or PowerFeed. Nevertheless, their study was limited only to binary separations. In this study, we extend this work for the separation of a ternary mixture. A Generalized Full Cycle (GFC) formulation and a full superstructure formulation are proposed based on the generalization of superstructure formulation. The optimal operating schemes obtained from these formulations are shown to be more advantageous than the existing operating schemes.

Although several ternary SMB operating strategies are presented in the literature, a comparison encompassing various operating schemes is rarely performed. Therefore, in this study , we also compare a number of operating schemes such as Five-zone, Four-zone, Eight-zone, JO and SMB cascade. The emphasis of this study is on separation of a ternary mixture however the analysis could be extended for any multi-component separation. The comparison of ternary operating strategies has been performed by formulating a multi-objective optimization problem, which is solved using deterministic nonlinear programming techniques as opposed to heuristic algorithms. We apply a full-discretization approach for optimization, where the spacial domains are discretized using central finite difference scheme, and the Radau collocation on finite elements is used for the temporal discretization [30]. The discretized equations are incorporated within a large-scale Nonlinear Programming (NLP) problem, which is solved using an interior-point solver IPOPT [88].

This chapter is organized as follows: Section 4.2 describes various modified SMB operating schemes in order to separate out a ternary mixture. Section 4.3 explains the mathematical model used for modeling the SMB system. Section 4.4 discusses the optimization problem formulation and the optimization strategy implemented in order to solve this problem. Section 4.5 presents comparison of ternary SMB operating schemes and discusses the optimal operating schemes obtained from the GFC and the full superstructure formulation. Section 4.6 concludes the chapter.

4.2 Operating schemes

We classify the existing modified SMB configurations, in order to separate a ternary mixture, into three categories:

- Five-zone and Four-zone SMB systems which are straightforward modifications of conventional four-zone SMB.
- the cascade of SMB's such as in the Eight-zone and SMB cascade systems.
- the full cycle SMB systems such as in the JO process where the entire cycle of SMB is modified.

We assume that the ternary mixture fed to the SMB system consists of components A, B and C with A as least adsorbable component, B as intermediate and C as most adsorbable component. Hence, the major constituents of raffinate, intermediate and extract stream outlets would be components A , B and C respectively. The Henry coefficients for these components are listed in Table 4.1. It is to be noted that the separation factor for components A and B (K_2/K_1) is larger compared to components B and C (K_3/K_2).

4.2.1 Modified conventional Four-zone SMB systems

4.2.1.1 Five-zone SMB

Five-zone operating scheme (Figure 4.1) is a slight modification of the conventional four-zone SMB configuration [10]. In this scheme, one of the separation zones in the conventional SMB is divided into two zones and a side stream is added for the recovery of intermediate component B. This splitting of zones depends on the kind of separation to be performed. For example, the separation zone before the feed inlet is splitted into two if the separation between components A and B is easier compared to components B and C [58]. Hence there exists three separation zones and two regenerative zones separated by two inlet and three outlet product streams. Both inlet

Table 4.1: SMB Modeling Parameters [49]

parameter	value	parameter	value
ϵ_b	0.389	K_{appl1} (1/s)	6.84×10^{-3}
K_{appl2} (1/s)	6.84×10^{-3}	K_{appl3} (1/s)	6.84×10^{-3}
L(m)	1.5	$C_{F,A}(\%)$	33.33
$C_{F,B}(\%)$	33.33	$C_{F,C}(\%)$	33.33
u_L (m/h)	0	u_U (m/h)	10
K_1	0.19	N_{Comp}	3
K_2	0.39	$Pur_{A,R}^{min}$	98
K_3	0.65	$Rec_{A,R}^{min}$	98
$Rec_{B,I}^{min}$	94		

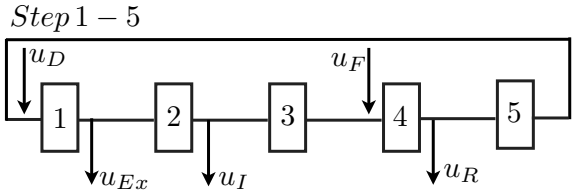

Figure 4.1: Five-zone SMB for separation of a ternary mixture [10].

and outlet streams are switched periodically in order to simulate the counter-current motion of the stationary phase. The total number of independent parameters (the velocity of desorbent, feed, extract, raffinate, steptime and one of the zone velocity) are six. These parameters have to be decided such that there is counter-current separation between B and C in columns 2 and 3, and counter-current separation between A and B in the column 4.

4.2.1.2 Four-zone SMB

The Four-zone operating scheme (Figure 4.2) is also similar to conventional four-zone SMB system [35]. However, it differs due to a break in the connection between the first and second column. Also, there is an additional desorbent stream considered at the beginning of the second column in order to retain components B and C inside SMB. The component with the least adsorption affinity, A, is, collected from the raffinate stream while the components B and C are recovered through the same extract outlet

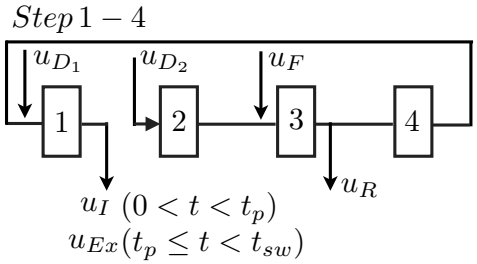

Figure 4.2: Four-zone SMB for separation of a ternary mixture [35].

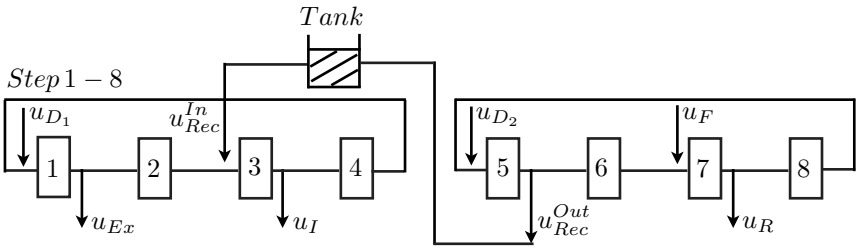

Figure 4.3: SMB cascade for separation of a ternary mixture [58].

at different intervals of time. The intermediate component is collected for $(0 < t < t_p)$ and most adsorbed component C is collected for the remainder of the switching time $(t_p \leq t < t_{sw})$. The collection time of intermediate component, t_p, is decided based on breakthrough time of component C, the time at which most strongly adsorbed component C starts to desorb [41]. Further, it is to be noted that there is no recycle of desorbent in the entire system, although stationary phase does move countercurrently because of the switching of the inlet and outlet ports. Hence the products streams can be more diluted compared to Five-zone SMB system. This process is then repeated for every switching of the ports. The total number of independent parameters (the velocity of feed, desorbent1, desorbent2, extract, switching time, t_p) are six in the four-zone SMB formulation.

4.2.2 Cascade systems

4.2.2.1 SMB cascade

This operating scheme as shown in Figure 4.3 is a sequence of two conventional four-zone SMB in series. The overall system consists of eight columns (one in each zone)

with one feed and two desorbent inlets, and three product outlets. The component A, B and C are recovered from the raffinate, intermediate stream and extract outlets respectively. In addition, there is an outlet, rich in components B and C, from column 5 which is recycled back into the SMB system at the inlet of column 3. In principle, the last four columns separate the mixture of components $B + C$ from component A, while the first four columns separate component B from C.

For practical purposes, we assume that this system has a buffer tank situated between the two SMB's. This tank ensures steady concentration input to the inlet of second SMB. In this study, we assume the tank is sufficiently large so that the dynamics of the recycled fractions are killed completely. Furthermore, this tank can function as buffer in situations where first SMB system has to be shut down. It should be noted that this tank is optional and could be removed if the switching times of both SMBs are identical. Without considering the tank, the switching times must be matched for synchronized operation. In this system, the total number of independent parameters (the velocity of feed, two desorbents, extract, recycle stream, two steptimes and one of the zone velocity in both SMBs) are nine.

It is to be noted that there exist an alternate designs of SMB cascade operating scheme in which the mixture of components $A + B$ is separated from component C first and then component A from B. However, the operating scheme considered in this study is selected based on the heuristic of easy separation first [58]. Hence, the separation of component A from B is preferred first compared to separation of component B from C.

4.2.2.2 Eight-zone SMB

The two conventional four-zone SMB configurations are integrated in order to form Eight-zone SMB as shown in the Figure 4.4. The overall system consists of eight columns (one in each zone) with one feed and two desorbent inlets, and three product

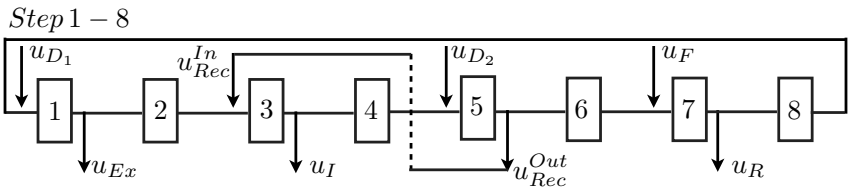

Figure 4.4: Eight-zone SMB for separation of a ternary mixture [58].

outlets similar to SMB cascade. In addition, there is an outlet, rich in components B and C, from the outlet of column 5 which is recycled back into the system at the inlet of column 3. The component A, B and C are recovered from the raffinate, intermediate stream and extract outlets, respectively. Similar to SMB cascade system, the first four columns in the Eight-zone SMB are required to separate component B from C, while last four columns are required to separate components $B + C$ from A. Both inlet and outlet ports are switched periodically to simulate the counter-current motion of the stationary phase. The total number of independent parameters (the velocities of two desorbents, feed, extract, intermediate stream, recycled stream, one of the zone velocity and steptime) are eight in the eight-zone SMB formulation.

It is to be noted that there is also an alternate design of Eight-zone SMB operating scheme. However, the operating scheme considered in this study is selected based on the heuristic of easy separation first [58]. Hence, the separation of component A from B is preferred first compared to separation of component B from C.

4.2.3 Full cycle modified SMB systems

4.2.3.1 JO process

The JO process is a unique SMB operation compared to the other isocratic modifications of standard Four-zone SMB. In this operating strategy, the entire cyclic operation of SMB is modified as shown in Figure 4.5. Figure 5(a) depicts the JO operating scheme while Figure 5(b) shows the normalized concentration profiles inside the SMB columns when the JO operation is implemented. These concentration

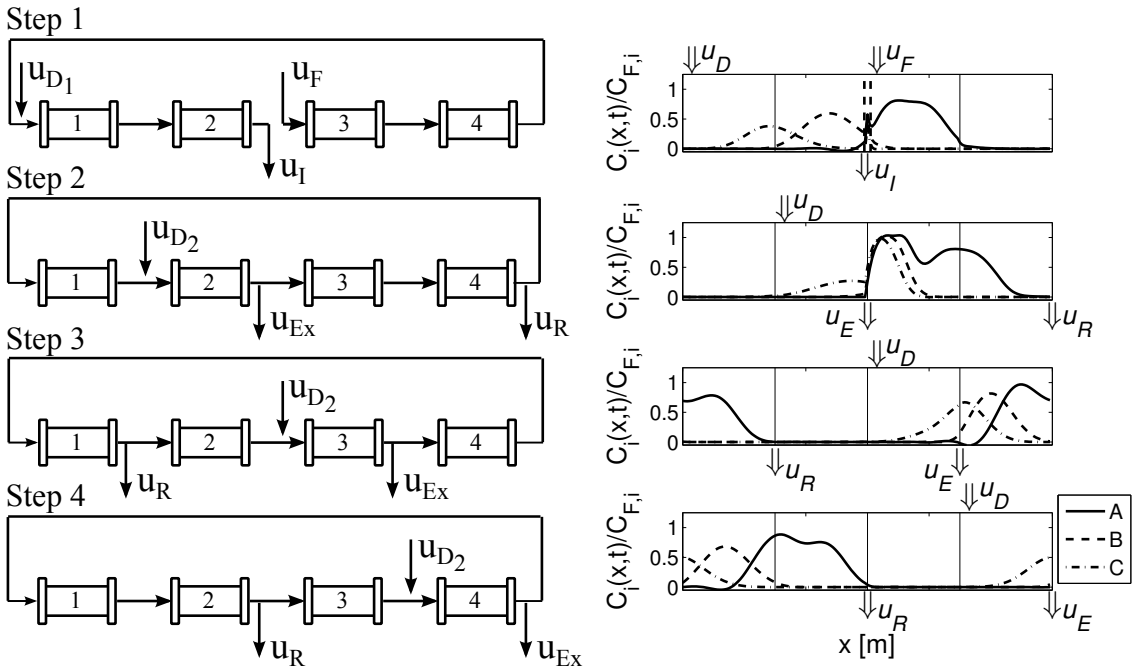

(a) JO operating scheme [48, 49]

(b) Normalized concentration profiles inside the SMB columns

Figure 4.5: JO process for the separation of a ternary mixture (a) the JO operation (b) the cyclic steady state concentration profiles at the beginning of each step of the JO operation. The component A, B and C are the fastest, intermediate and the slowest eluting components, respectively.

profiles are plotted at the beginning of each step of the JO operation after reaching cyclic steady state. In step 1, the flow connection between column 2 and 3 is broken so that the intermediate eluting component can be recovered upstream of the shut-off valve. The feed mixture is simultaneously fed to the downstream side to load the SMB system. Steps 2, 3 and 4, on the other hand, are similar to the standard SMB operation with no feed inlet. In these steps, only the fastest and the slowest eluting component are recovered while feeding the fresh desorbent during the remaining steps. Moreover, the desorbent velocity and the switching time of steps 2-4 are allowed to be different from step 1 to further add the flexibility in the collection of fastest and the slowest eluting component. The inlet and outlet streams are switched as in the standard SMB operation in the clockwise direction to simulate the counter-current

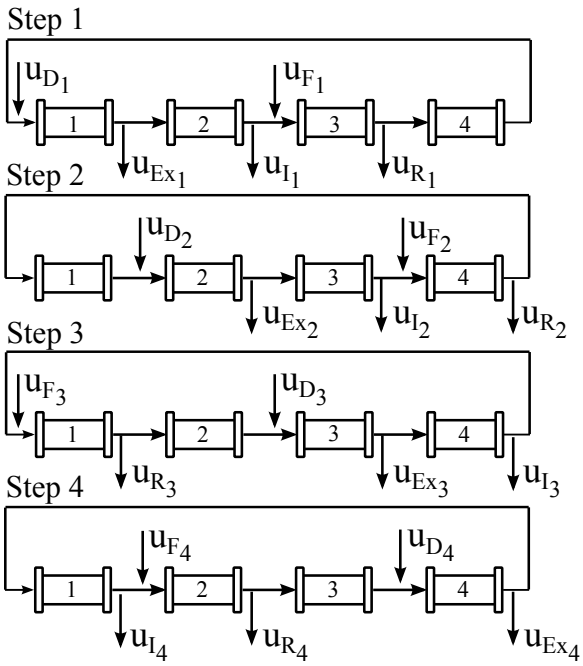

Figure 4.6: Generalized Full Cycle (GFC) formulation for the separation of a ternary mixture [3].

motion of the stationary phase. Steps 1-4 completes the cycle and this operation is repeated constantly in order to recover the pure products. The number of independent parameters that affect the performance of the JO operation are seven including the two desorbent velocities, two switching times, feed, extract and the zone 1 velocity in step 2. The more detailed information regarding the design of the JO operation and the determination of operating conditions can be found elsewhere [43, 48, 49].

It is also important to note that the JO process can be implemented experimentally on any SMB system which can implement the standard SMB operation (shown in Fig. 1.2), without any major hardware modification. We may require an additional binary valve to break the flow connection during step 1. The JO process was commercialized by Organo corporation for the separation of raffinose, sucrose, betains and salts [23]. In addition, the JO process has also been used for isolation of raffinose from beet molasses [69]. Another ternary SMB process implemented on an industrial scale is the sequential SMB [25, 26], which is not considered in this work.

4.2.3.2 Generalized Full Cycle (GFC) process

It is well known in the literature that the performance of SMB system can be dramatically improved by changing the operating conditions such as flow rates and switching time or the operation itself [3, 28, 29, 37, 94]. Moreover, numerous SMB configurations can be created by changing the relative positions of feed and desorbent inlets, or the extract, raffinate and the intermediate stream outlets. Therefore, it is very important to find the best operating strategy among various SMB configurations. The GFC process is based on this idea of identifying the best separation strategy from various different alternatives [3].

In this strategy, the JO process is generalized by introducing additional inlet and outlet streams as shown in Figure 4.6. Hence, each step of the GFC formulation consists of two inlets; one for feed and the other for the desorbent, and three outlets; one for each of the product. These inlet/outlet flow rates and the switching time are allowed to change in the different steps and thus each step can be operated in a distinct way. In addition, the inlet and outlet flow rates can also be turned off whenever required. Hence, the GFC formulation is a framework that encompasses numerous ways of operating SMB and the flow rates and the switching times are nothing but the decision variables of an optimization problem. Unlike other operating strategies, the structure of the SMB operation is not chosen here a priori. Instead, the optimizer extracts the best operating strategy that optimizes the objective function while meeting the product constraints at the same time. Since there are four columns and four steps per cycle of the GFC process, the number of independent parameters that affect the performance of the GFC operation are twenty four; six in each step including the switching time, desorbent, feed, extract, raffinate and the zone 1 velocity.

It is interesting to note that, in the GFC formulation, the connection between any two columns can be broken in any of the steps to recover a particular product similarly to the first step of the JO process. Hence, the JO process can be derived as

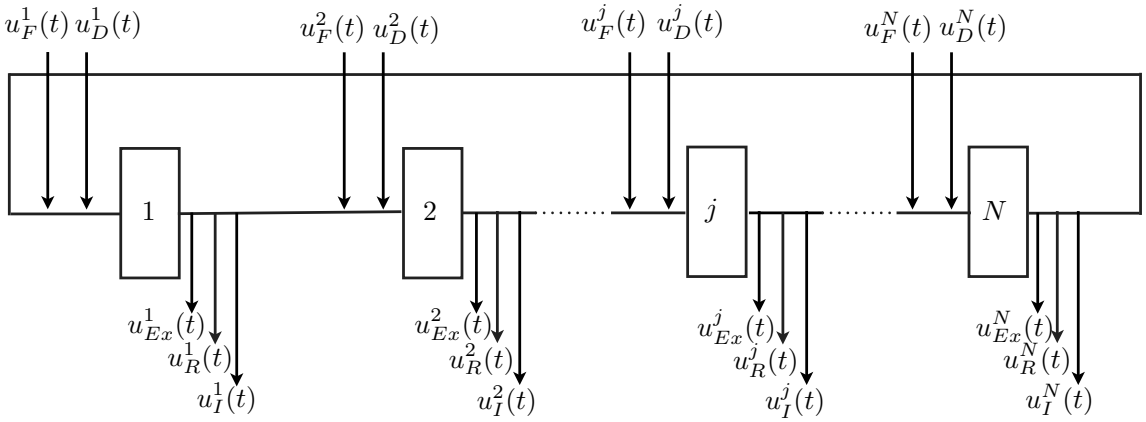

Figure 4.7: SMB full superstructure formulation for the separation of a ternary mixture.

a special case of GFC formulation. Since the optimal solution is obtained from this inclusive and general structure, the optimal operating scheme derived from the GFC formulation should always perform equivalently or better than the JO process.

4.2.3.3 SMB Full Superstructure

Similar to the GFC formulation, the full superstructure formulation is also based on identifying the best separation strategy from various alternative designs of SMB [2]. In this strategy, the GFC formulation is further expanded by relaxing the positions of the inlet and outlet ports in all the steps. A schematic of the SMB full superstructure formulation has been shown in Figure 4.7. The symbols $u_F^j(t)$ and $u_D^j(t)$ refer to the feed and desorbent inlet velocities while the symbols $u_{Ex}^j(t)$, $u_R^j(t)$ and $u_I^j(t)$ refer to the extract, raffinate and the intermediate stream outlet velocities, respectively. As can be seen from Figure 4.7, the feed and desorbent streams could be fed at the inlet of any of the columns in any of the steps. Similarly, the products could be withdrawn from the outlet of any of the columns using any of the outlet streams (raffinate, extract or intermediate) in any of the steps. As a result, the superstructure formulation considers a large number of possibilities of supplying desorbent/feed as well as for withdrawing the ternary components. Since there are four columns and

four steps per cycle of the full superstructure process, the number of independent parameters, that affect the performance of the full superstructure operation, has been drastically increased to eighty four; twenty one in each step including the switching time, five desorbent velocities, five feed, five extract, five raffinate and the zone 1 velocity.

It is interesting to note that, the GFC formulation can be derived as a special case of the full superstructure formulation. Since the optimal solution is obtained from this inclusive and general structure, the optimal operating scheme derived from the full superstructure formulation should always perform equivalently or better than the GFC process.

4.3 Mathematical model

We employ the linear driving force (LDF) model (equations (1)-(5)), which is discussed in detail in Chapter 3. In this model, both axial dispersion and diffusion into adsorbent particles, which cause band broadening, are lumped into mass transfer coefficient.

In the GFC and full superstructure formulations, it is allowed to break the connection between any two columns in any of the steps to recovery a particular product. Thus, the supply of feed and desorbent stream (downstream) should not flow against the direction of liquid flow. To prevent such kind of situation and ensure the counter-current movement of liquid and stationary phase inside the SMB columns, the following constraint (24) is implemented.

$$u^j(t) - (u_D^j(t) + u_F^j(t)) \geq 0, \quad j = 1, \ldots, N_{Column} \tag{24}$$

A pictorial representation of this constraint has been presented in an previous study [29]. If the constraint (24) is active, then the connection between jth and $(j-1)th$ column in cut open as in the first step of the JO process. In such an

operation, the outlet of the $(j-1)th$ column is directed to a product outlet while the fresh feed or desorbent solution is fed upstream of the jth column. It should be noted that the absence of this constraint leads to ill-conditioning and often the optimizer does not converge. Furthermore, logic constraints could be imposed in the SMB formulation to avoid feed/desorbent supply or extract/raffinate/intermediate stream outlets at multiple locations in the same step, which would restrict the number of pumps. In this study, however, we do not impose any such logic constraints thus inviting numerous possibilities to operate SMB.

4.4 Optimization Strategy

4.4.1 Treatment of CSS

In SMB operation the counter-current movement of the stationary phase is simulated by shifting both the inlet and outlet streams in the direction of liquid flow by valve switching. Due to this discrete shifting, SMB systems arrives at a cyclic steady state referred as CSS. The equations for formulating the CSS constraints are discussed in detail in Chapter 3. In this study, a single step formulation is considered for Five-zone, Four-zone, Eight-zone and SMB cascade where all the steps are identical except the shifting of inlet and outlet streams due to valve switching. The formulation is written as [37]:

$$\begin{aligned} C_i^j(x,0) &= C_i^{j+1}(x,t_{step}), \quad i=1,\ldots,N_{Comp}, \quad j=1,\ldots,N_{Column}-1 \\ q_i^j(x,0) &= q_i^{j+1}(x,t_{step}), \quad i=1,\ldots,N_{Comp}, \quad j=1,\ldots,N_{Column}-1 \end{aligned} \tag{25}$$

$$\begin{aligned} C_i^{N_{Column}}(x,0) &= C_i^1(x,t_{step}), \quad i=1,\ldots,N_{Comp} \\ q_i^{N_{Column}}(x,0) &= q_i^1(x,t_{step}), \quad i=1,\ldots,N_{Comp} \end{aligned} \tag{26}$$

On the other hand, a full cycle formulation is considered for JO, GFC and the full superstructure operating schemes in which the operation during all the four steps is

Table 4.2: SMB operating schemes considered for separation of a ternary mixture.

SMB operating schemes		Degrees of freedom	Number of columns	CSS formulation
Modified four-zone systems	Five-zone	6	5	Single step
	Four-zone	6	4	Single step
Cascades systems	SMB cascade	9	8	Single step
	Eight-zone	8	8	Single step
Full cycle modified systems	JO process	7	4	Full cycle
	Generalized Full Cycle (GFC)	24	4	Full cycle
	Full superstructure	84	4	Full cycle

different [59]. In the full cycle formulation, the concentration profiles are identical at the beginning and at the end of the cycle. The formulation is written as:

$$\begin{aligned} C_i^j(x,0) &= C_i^j(x,t_{cycle}), \quad i=1,\ldots,N_{Comp}, \quad j=1,\ldots,N_{Column} \\ q_i^j(x,0) &= q_i^j(x,t_{cycle}), \quad i=1,\ldots,N_{Comp}, \quad j=1,\ldots,N_{Column} \end{aligned} \tag{27}$$

Although the problem size is larger in full cycle formulation, this formulation is necessary for JO, GFC and the full superstructure operating schemes. The number of control parameters and the CSS formulation used for various SMB operating schemes is summarized in Table 4.2.

4.4.2 Problem Formulation

With the SMB model and CSS constraints, a multi-objective maximization problem is formulated subject to the desired purity and recovery requirements of the product streams. In this study, the multiple objective are considered as maximizing the productivity of the SMB system and maximizing the purity of intermediate component simultaneously. The overall optimization problem is:

$$\max_{u^j(t),u_D^j(t),u_F^j(t),u_{Ex}^j(t),u_R^j(t),u_I^j(t),t_{cycle}} \Phi_1(t) \left(= \sum_{j=1}^{N_{Column}} \int_0^{t_{cycle}} u_F^j(t)\, dt \right) \tag{28}$$

$$\max_{u^j(t),u_D^j(t),u_F^j(t),u_{Ex}^j(t),u_R^j(t),u_I^j(t),t_{cycle}} \Phi_2(t) \left(= \frac{\sum_{j=1}^{N_{Column}} \int_0^{t_{cycle}} u_I^j(t) C_{B,I}^j(L,t)\, dt}{\sum_{j=1}^{N_{Column}} \sum_{i=1}^{N_{Comp}} \int_0^{t_{cycle}} u_I^j(t) C_{i,I}^j(L,t)\, dt} \right) \tag{29}$$

subject to equations (1)-(5), (24)-(27),

Raffinate stream product purity:

$$\frac{\sum_{j=1}^{N_{Column}} \int_0^{t_{cycle}} u_R^j(t) C_{A,R}^j(L,t)\, dt}{\sum_{j=1}^{N_{Column}} \sum_{i=1}^{N_{Comp}} \int_0^{t_{cycle}} u_R^j(t) C_{i,R}^j(L,t)\, dt} \geq Pur_{A,R}^{min}, \tag{30}$$

Raffinate stream product recovery:

$$\frac{\sum_{j=1}^{N_{Column}} \int_0^{t_{cycle}} u_R^j(t) C_{A,R}^j(L,t)\, dt}{\sum_{j=1}^{N_{Column}} \int_0^{t_{cycle}} u_F^j(t) C_{A,F}^j(t)\, dt} \geq Rec_{A,R}^{min}, \tag{31}$$

Intermediate stream product recovery:

$$\frac{\sum_{j=1}^{N_{Column}} \int_0^{t_{cycle}} u_I^j(t) C_{B,I}^j(L,t)\, dt}{\sum_{j=1}^{N_{Column}} \int_0^{t_{cycle}} u_F^j(t) C_{B,F}^j(t)\, dt} \geq Rec_{B,I}^{min}, \tag{32}$$

$$u_L \leq u^j(t) \leq u_U. \tag{33}$$

where Φ_1 is the objective function corresponding to the throughput fed to the SMB process, and Φ_2 is the objective function corresponding to the purity of component B obtained in the intermediate stream outlet. The symbols $C_{A,R}^j(L,t)$ refers to the concentration of component A in the raffinate stream outlet from the jth column and $C_{B,I}^j(L,t)$ is the concentration of component B in the intermediate stream outlet from the jth column. The symbols $Pur_{A,R}^{min}$ and $Rec_{A,R}^{min}$ refers to the desired purity and recovery of component A in the raffinate stream. Similarly, $Rec_{B,I}^{min}$ refers to the desired recovery of component B in the intermediate stream. It is to be noted that in constraints (30), (31) and (32) we have assumed all the extract, raffinate and intermediate stream outlets, throughout the cycle, are combined together and collected into their respective extract, raffinate and intermediate stream ports. Further, the

constraint (33) is imposed to bound the zone velocities in order to obtain sensible operating conditions. The parameters u_U and u_L are the upper and lower bounds. This upper bound can be determined by a pressure drop equation such as Darcy's law, $u_u = k\,\frac{\Delta P_{max}}{L}$, which incorporates the maximum pressure drop that can be exerted over the entire length of the column. Here ΔP_{max} is the maximum pressure drop and k is the Darcy constant.

This multi-objective problem is converted into an epsilon-constrained single-objective problem where the second objective function, Φ_2, is imposed as a constraint [29, 31].

$$\frac{\sum_{j=1}^{N_{Column}} \int_0^{t_{cycle}} u_I^j(t) C_{B,I}^j(L,t)\,dt}{\sum_{j=1}^{N_{Column}} \sum_{i=1}^{N_{Comp}} \int_0^{t_{cycle}} u_I^j(t) C_{i,I}^j(L,t)\,dt} \geq \epsilon. \tag{34}$$

This results in a single objective problem referred as throughput maximization problem in this study. The optimal solutions of the throughput maximization problem construct the Pareto plot of the multi-objective optimization problem.

4.4.3 Solution strategy

The soulution strategy is discussed in detail in Chapter 3. The throughput maximization problem involves both spacial and time domain. In this study, the full-discretization approach is implemented where the spacial domains are discretized using central finite difference scheme, and the temporal domain is discretized using Radau collocation on finite elements [30].

The resulting problem has large number of variables and linearized Karush-Kuhn-Tucker condition tends to have a sparse structure [29]. Hence, it is crucial to choose a solver which can handle large number of variables and at the same time exploit the problem structure. To satisfy these requirements, we choose IPOPT 3.0, an interior-point solver which also utilizes exact second derivative information [88].

4.5 Results and Discussion

The optimization problem, corresponding to all the operating schemes discussed in section 4.2, is implemented within the AMPL modeling environment and solved successfully. The influence of both spatial and time domain have also been tested on the optimal operating schemes. The operating conditions i.e. flow rates and switching time are unchanged with increase in the number of finite elements. To compare modified four-zone, cascade and full cycle SMB systems together, the Pareto set of the multi-objective optimization problem is plotted. This Pareto set is generated by solving a set of constrained throughput maximization problem. The throughput obtained is translated in terms of productivity which is defined as the volume fed to the SMB process per unit volume of the adsorbent per unit time. The results are shown in Figure 4.8. The solid, dashed and dash-dotted lines correspond to full cycle modified systems, cascade systems and modified four-zone SMB systems respectively. As can

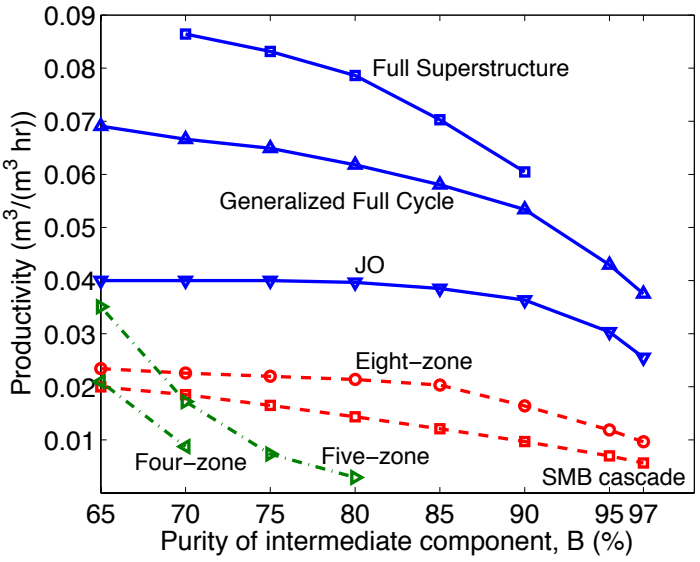

Figure 4.8: Productivity $(m^3/(m^3\,hr))$ variation with respect to the obtained purity of intermediate component for various operating schemes. The solid, dashed and dash-dotted curved lines correspond to the full cycle modified systems, cascade systems, and modified four-zone SMB systems, respectively. The purity obtained of components A is 98 %. The recoveries obtained of components A and B are 98 % and 94 %.

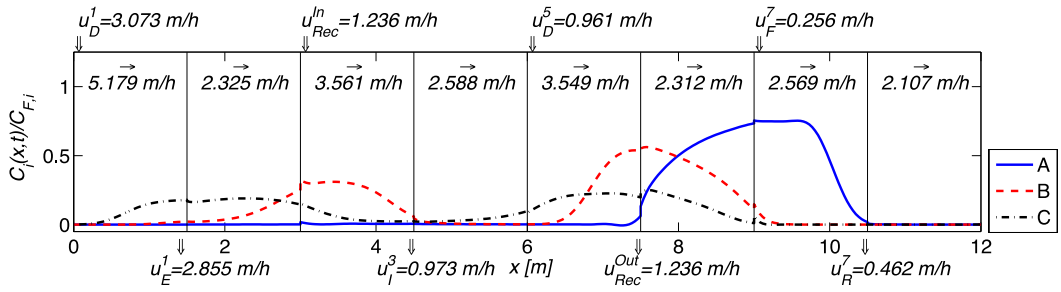

Figure 4.9: Concentration profiles within the optimized Eight-zone SMB system at the beginning of the step. The purities obtained of components A and B are 98 % and 80 %. The recoveries obtained of components A and B are 98 % and 94 %.

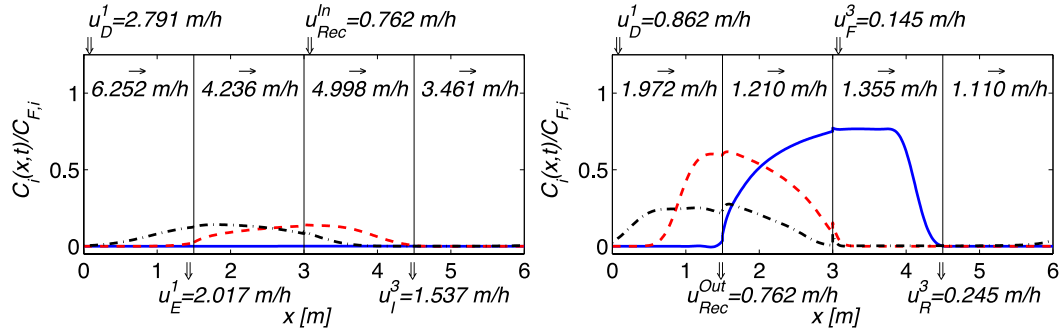

Figure 4.10: Concentration profiles within the optimized SMB cascade system at the beginning of the step. The purities obtained of components A and B are 98 % and 80 %. The recoveries obtained of components A and B are 98 % and 94 %.

be seen from the Figure 4.8, the full cycle SMB systems are found to be most efficient in carrying out a ternary separation compared to the cascade and modified four-zone SMB systems. In particular, the performance obtained from the full superstructure and the GFC operating schemes are outstanding because these operations improves the productivity of SMB system considerably compared to JO process. Also, it is interesting to note that five-zone and four-zone operating schemes are not efficient operations for this case study. In these schemes, the productivity obtained drops dramatically for higher purities of intermediate component B.

Comparing cascade systems together, from Figure 4.8, we find that Eight-zone SMB's performance is better compared to the SMB cascade operating scheme. This

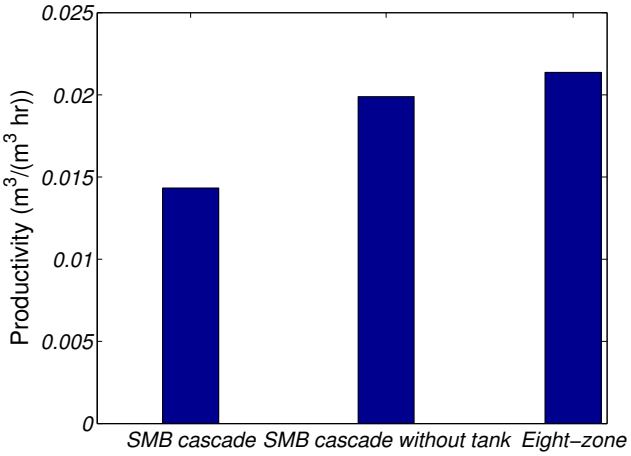

Figure 4.11: Comparison of productivity $(m^3/(m^3\,hr))$ obtained for SMB cascade, SMB cascade without considering buffer tank and Eight-zone operating schemes. The purity obtained of components A and B are 98 % and 80 % . The recoveries obtained of components A and B are 98 % and 94 %.

indicates that the dynamics inside the SMB columns have a important role in separating out the pure components. In the SMB cascade operating scheme, by placing a buffer tank between the two SMB systems, all the dynamics of the first SMB are killed. This effect is further shown with the help of concentration profiles inside each SMB at the beginning of the step (see Figure 4.9 and 4.10). The solid, dashed and dash-dotted curved lines correspond to the concentrations of components A, B and C. It is interesting to note that the difference between the productivity obtained from Eight-zone and SMB cascade operating schemes decreases progressively with increase in the purity of the intermediate component. This can be explained from the infeasibility of the triangle theory analysis; it has been shown that there does not exist any feasible point for the perfect separation of all the three components [34, 58].

In order to investigate the influence of the buffer tank, we also consider SMB cascade operating scheme without considering the buffer tank. The switching time of both SMB was kept same in order to maintain synchronized operation. The comparison of productivity obtained from SMB cascade, SMB cascade without considering

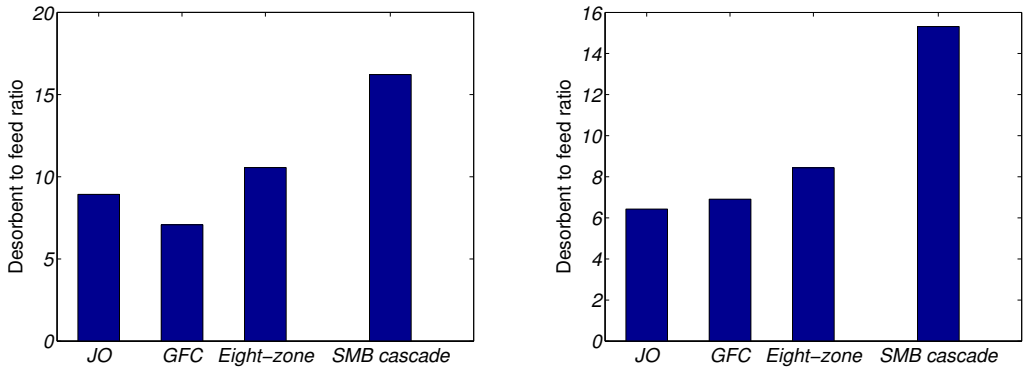

(a) $Pur_{A,R} = 98\%,\ Pur_{B,I} = 80\%$ (b) $Pur_{A,R} = 98\%,\ Pur_{B,I} = 90\%$

Figure 4.12: Optimized desorbent to feed ratio corresponding to various SMB operating schemes. The recoveries obtained of components A and B are 98 % and 94 %. (a) The purities obtained of components A and B are 98 % and 80 %. (b) The purities obtained of components A and B are 98 % and 90 %. .

the buffer tank and Eight-zone SMB is shown in Figure 4.11. This comparison corresponds to the case when 80% purity of intermediate component is obtained. As can be seen from the figure, the Eight-zone SMB is still superior compared to SMB cascade operating scheme without the buffer tank. This can be explained from the concentration profiles shown in Figure 4.9 an 4.10. The highest retained component C must be washed away completely in the fourth column (from left hand side) of SMB cascade operating scheme however, such is not the case in the Eight-zone.

The amount of desorbent consumed in the SMB process also plays an important role while assessing the performance of an operating scheme. Also, the optimum solutions of the throughput maximization problem are non-unique in terms of the desorbent consumption. Hence, in order to find the least amount of desorbent required, an optimization problem is formulated with the objective function as minimizing the amount of desorbent used while fixing the SMB throughput at its optimum value. The formulation is written as follows:

$$\min_{u^j(t),u_D^j(t),u_F^j(t),u_{Ex}^j(t),u_R^j(t),u_I^j(t),t_{cycle}} \sum_{j=1}^{N_{Column}} \int_0^{t_{cycle}} u_D^j(t)\, dt \tag{35}$$

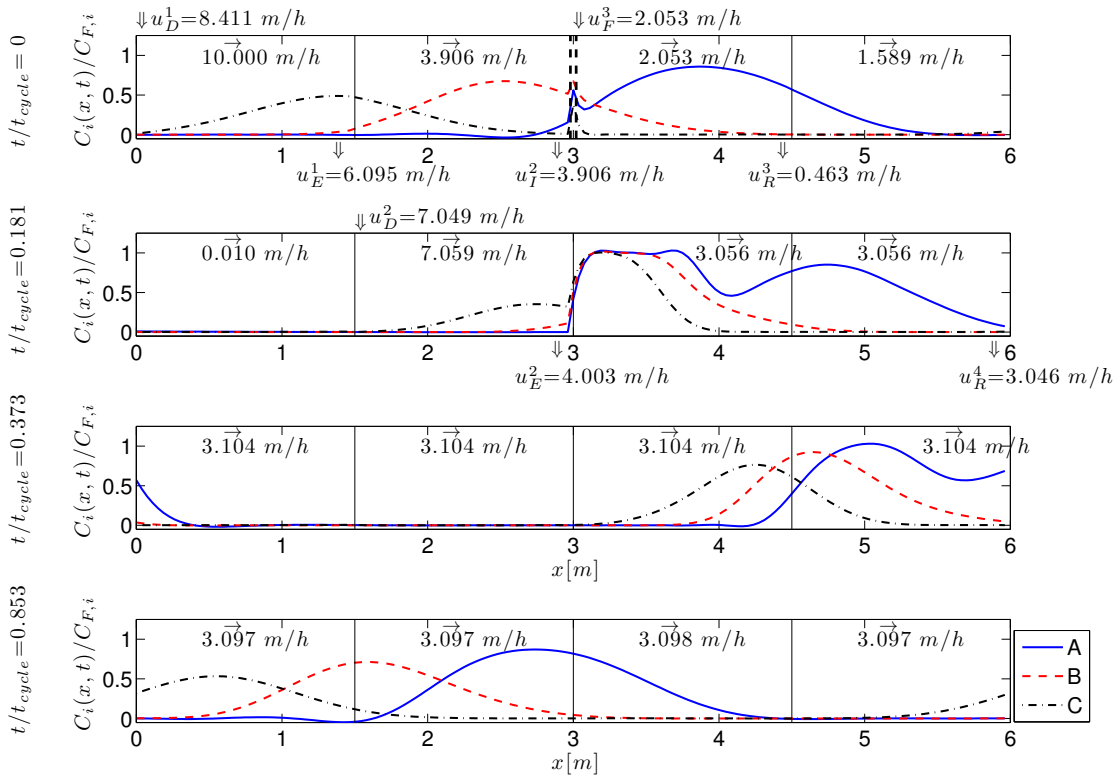

Figure 4.13: GFC operating scheme along with the normalized concentration profiles within the SMB columns. The two vertical dashed lines, closely spaced to each other, indicate the breaking of the circuit. The purities obtained of components A and B are 98 % and 80 %. The recoveries obtained of components A and B are 98 % and 94 %. The total cycle time is 4511 seconds.

subject to equations (1)-(5), (24)-(27), (30)-(34),

$$\sum_{j=1}^{N_{Column}} \int_0^{t_{cycle}} u_F^j(t)\, dt \geq \Phi_1^{opt} \tag{36}$$

where Φ_1^{opt} is the optimal throughput obtained by solving the throughput maximization problem. The results are shown in Figure 4.12. This Figure shows the comparison of optimized desorbent to feed ratio for JO, GFC, Eight-zone and SMB cascade operating schemes for two different scenarios. The purity obtained of intermediate component B is 80% and 90% for part (a) and (b), respectively. The productivity obtained from Five-zone and Four-zone operating schemes was significantly lower for purity higher than 80% of intermediate component hence they are

excluded out of discussion. As can be seen from Figure 4.12, the optimal desorbent to feed ratio for the SMB cascade system is significantly higher than Eight-zone SMB system. Hence, Eight-zone SMB operating scheme not only improves the productivity of SMB but also helps in reducing the amount of desorbent consumed. Also, the full cycle SMB systems are superior even in terms of desorbent consumption. Specially, GFC operating scheme improves productivity of the SMB process significantly without consuming much amount of desorbent. Since GFC formulation incorporates several SMB configuration (including JO process) which are potential candidates for improving productivity, the optimizer finds the best decisions to be made in order to maximize the throughput of SMB. Hence, this approach has a significant potential in identifying the best separation strategy in order to separate a ternary mixture.

The GFC optimal operating scheme is shown in Figure 4.13 along with the normalized concentration profiles at the beginning of each step. The four SMB columns are connected in a cyclic manner but separated by the solid vertical lines. The two vertical dashed lines, closely spaced to each other, indicate the breaking of the circuit, i.e., stopping the liquid flow into the next column from the previous one. The fraction of the beginning of the steps time are also shown vertically to the left side of the Figure 4.13. The total cycle time is 4511 seconds. In the first step, the circuit connecting second and third column is broken to recover the pure component B through the intermediate stream outlet. At the same time, components A and C are also recovered from the raffinate and extract stream outlets respectively. In the second step, the pure components C and A are recovered from the extract and raffinate stream outlets at the end of second and fourth column respectively. The third and fourth steps are complete recycle without any inlet and outlet stream and thus allowing concentration profiles to get separated from each other. Also, it is to be noted that the duration of third and fourth step contributes to 65 % of the total cycle time. Although there is significant amount of time spent in separating the

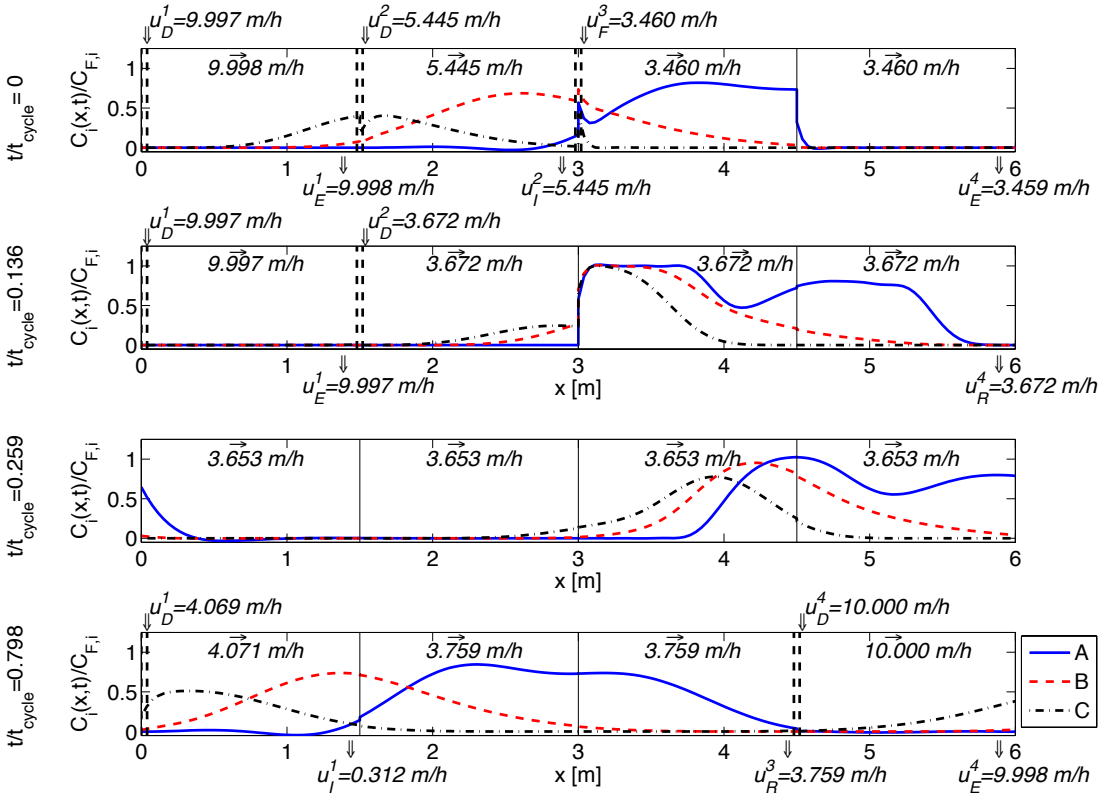

Figure 4.14: Optimal operating scheme obtained from the full superstructure formulation along with the normalized concentration profiles within the SMB columns. The two vertical dashed lines, closely spaced to each other, indicate the breaking of the circuit. The purities obtained of components A and B are 98 % and 80 %. The recoveries obtained of components A and B are 98 % and 94 %. The total cycle time is 3606 seconds.

concentration profiles inside SMB columns, it leads to high purity of products when they are withdrawn during first and second step.

The optimal operation obtained from the full superstructure formulation, as discussed in the subsection 4.2.3.3 of this Chapter, is also promising to increase the productivity of the SMB process significantly compared to the existing operations. There is almost up to 100% increase in the productivity obtained from the full superstructure compared to the JO process.

The optimal operating scheme obtained from the full superstructure formulation is shown in Figure 4.14 along with the normalized concentration profiles at the beginning

of each step. The four SMB columns are connected in a cyclic manner separated by the solid vertical lines. The two vertical dashed lines, closely spaced to each other, indicate the breaking of the circuit, i.e., stopping the liquid flow into the next column from the previous one. The fraction of the beginning of the steps time are also shown vertically to the left side of the Figure. In the first step, both columns 1 and 2 are isolated by breaking the circuit and then components B and C are purged into their respective outlet streams forcefully by feeding desorbent at the inlet of first and second column. Hence, we obtain column 4 to be dominating in terms of component A in the beginning of second step. The pure component A and B are recovered through the raffinate and intermediate stream outlets during the second step. The discontinuity in the concentration profiles at the end of second column arises due to the isolation of column 2 in the first step. The third step, on the other hand, is a complete recycle with no inlet and outlet streams. This step takes the longest time which is required for the concentration profiles to get separated from each other inside the SMB columns. Any removal stream in the third step would result in the contamination of products. In the fourth step, again purging is performed by isolating columns 4 and pure components B and C are recovered. This optimal operating scheme although results in high throughput, consumes a larger amount of dersorbent because of high amount of purging. Hence, such operating scheme of SMB could be useful in situations where desorbent is inexpensive compared to the profit obtained from the purification of products.

4.6 Conclusion

In this chapter, various ternary SMB operating schemes are compared in order to assess their performance in terms of the productivity obtained and the amount of desorbent consumed. In addition, the Generalized Full Cycle formulation (GFC) and the full superstructure formulation are presented which are optimized by considering

a large number of SMB configurations. In our case study, the full-cycle modification, which includes the JO, GFC and the full superstructure operations, has been found to be the most effective approach to achieve separation of a ternary mixture using SMB. Also, the GFC operation has shown the best performance as it improves the productivity of the SMB process significantly without consuming much amount of desorbent. Since GFC formulation incorporates several SMB configuration which are potential candidates for improving the productivity, the optimizer finds the best decisions to be made in order to maximize the throughput of SMB. Hence, this approach has a significant potential in identifying the best separation strategy in order to separate a ternary mixture.

The optimal operation scheme identified from the full superstructure formulation is also promising to increase the productivity of the SMB process significantly compared to the existing operations. However, this operation also consumes a large amount of desorbent because of high amount of purging. Hence, such operating scheme of SMB could be useful in situations where desorbent is inexpensive relative to the profit obtained from the purification of products. Further, Eight-zone SMB is found to be better operating scheme compared to SMB cascade, both in terms of performance and in terms of amount of desorbent consumed. Hence, it is concluded that dynamics in the internal recycle line are very important in separating a ternary mixture. Furthermore, Five-zone and Four-zone operating schemes have been found to be ineffective if higher purity of intermediate component is desired.

In the next chapter, we demonstrate the Generalized Full Cycle (GFC) operation experimentally, and compare its performance to the JO process.

CHAPTER V

EXPERIMENTAL VALIDATION OF TERNARY SIMULATED MOVING BED CHROMATOGRAPHY SYSTEMS

5.1 Motivation

In chemical or bioprocessing industry, we often encounter multi-component mixtures when purifying any natural or biological product [71]. Here the feed mixture consists of a large number of components of similar chemical structures and the target product is located somewhere in between the fastest and the slowest eluting components. Although a number of approaches have been suggested to perform the separation of multicomponent mixtures, the application of SMB for multi-component separation is still considered one of the major challenges. Since SMB enables high throughput and reduces desorbent consumption, there has been a continuous effort to find modified SMB schemes that allow for higher productivity yet meeting the same product specifications. Examples of such modifications are the processes called the SMB cascade, where the two standard SMB systems are connected in series [58], Eight-zone SMB, where the two standard SMB systems are integrated into one single SMB unit [58], Five-zone SMB, where the zone prior to the feed location is split into two sections and an additional outlet is provided for the recovery of the intermediate eluting component [10, 41], Four-zone SMB, where the flow connection upstream of the extract outlet is broken while the intermediate and the slowest moving components are recovered through the extract outlet at different instants of time [35, 41], ISMB where multiple components are withdrawn separately at different time instances within a step [27], and JO process, where the intermediate eluting component is fractionated

only during step 1 while step 2, 3 and 4 are similar to the standard SMB operation but without feeding [40, 43, 48, 49, 61]. In the previous chapter, various existing isocratic ternary separation strategies were compared in terms of the maximum throughout attained and the desorbent to feed ratio required [3]. This chapter had further investigated finding the best ternary separation strategy from the various available SMB configurations by considering a Generalized Full Cycle (GFC) formulation based on a systematic design. It was concluded that the JO process and the GFC operations have significant improvement over existing strategies.

In this chapter, we demonstrate the GFC operation experimentally and compare its performance to the JO process. A simultaneous optimization and model correction (SOMC) scheme is implemented in order to resolve the model mismatch [4, 8, 9, 76]. In addition, we show a systematic comparison of both JO and GFC operations by presenting a Pareto plot of the productivity achieved against the desired purity of the intermediate eluting component experimentally.

This chapter is organized as follows: Section 5.2 describes the JO and the GFC operating strategies for the separation of ternary mixtures. Section 5.3 presents the ternary separation system used in this study. Section 5.4 explains the modeling of the SMB system. Section 5.5 elaborates on the optimization strategy used in order to find the optimal operating strategies. Section 5.6 presents the experimental system considered in this study. Section 5.7 discusses the Simultaneous Optimization and Model Correction (SOMC) scheme to systematically remove the model-mismatch from the SMB system. Section 5.8 presents the experimental results with regard to the JO and the GFC operating schemes and discusses the efficacy of SOMC scheme. Section 5.9 concludes the paper and presents the scope of future work.

5.2 Operating strategies

Both JO and GFC operating strategies are discussed in detail in Section 4.2.3

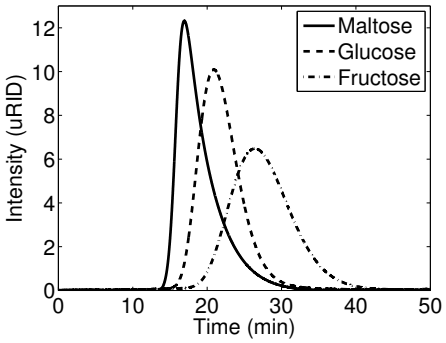

Figure 5.1: A chromatogram depicting the elution profiles of a ternary mixture consisting maltose (100 g/L), glucose (100 g/L) and fructose (100 g/L).

5.3 Chromatographic system

The ternary feed mixture in this study consists of maltose (D-(+)-Maltose monohydrate, BioXtra, >= 99%, Sigma-Aldrich), glucose (D-(+)-Glucose, anhydrous, 99%, Alfa Aesar) and fructose (D-Fructose, 99%, Alfa Aesar). A chromatogram of this feed mixture is shown in Figure 5.1. As shown in this figure, maltose is the fastest moving component, glucose is the intermediate and fructose is the slowest eluting component. The feed compositions are shown in Table 5.1. The component maltose appears as an impurity and contributes to only 10% in the feed mixture. On the other hand, both glucose and fructose contribute to 45% of the feed mixture. These compositions were selected to simulate the realistic separation problem that is encountered in the sugar industry. Deionized water (filtered using Direct-Q 3 UV, Millipore) was used as an eluent at $50°C$. The four semi-prep SMB columns (45×1.5 cm) that are used in this study were packed with DOWEX^{TM} MONOSPHERE^{TM} 99Ca/320 resin (320 μm, Dow Chemical Company).

5.4 Mathematical model

We employ the same linear driving force (LDF) model (equations (1)-(5)), which is discussed in detail in Chapter 3. In this model, both axial dispersion and diffusion into adsorbent particles, which cause band broadening, are lumped into mass transfer

coefficient. In addition, the constraint (24) is implemented to ensure the counter-current movement of liquid and stationary phase inside the SMB columns.

5.5 Optimization strategy

Since there is no short cut design approach developed for the JO and the GFC operations such as the triangle theory for binary separation, we rely on the optimizer to find the optimal operating scheme. The optimization strategy of determining the operating conditions is discussed in the following subsections.

5.5.1 Treatment of CSS

In the SMB, the inlet and outlet ports are periodically switched to mimic the counter-current motion of the stationary phase (see Figure 1.2). Due to this discrete shifting of ports, the SMB process reaches a cyclic steady state (CSS). At CSS, the concentration profiles inside the SMB columns still change within the cycle while the same operation is repeated from one cycle to another. The cycle time is calculated by summing up the duration of all the four steps. The equations for formulating the CSS constraints are discussed in detail in Chapter 3. Since JO and GFC are both asymmetric SMB operations, we consider a full cycle formulation to write the CSS [59]. In this formulation, the concentration profiles are identical at the beginning and at the end of the cycle. The formulation is written as:

$$C_i^j(x,0) = C_i^j(x,t_{cycle}), \quad i = 1,\ldots,N_{Comp}, \quad j = 1,\ldots,N_{Column} \tag{37}$$

$$q_i^j(x,0) = q_i^j(x,t_{cycle}), \quad i = 1,\ldots,N_{Comp}, \quad j = 1,\ldots,N_{Column} \tag{38}$$

5.5.2 Problem formulation

The ternary separation problem is formulated as a multi-objective optimization problem subject to the desired purity and recovery requirements of the products. The multiple objectives are maximizing the throughput of the SMB process and the glucose

purity obtained in the intermediate stream outlet. The overall optimization problem is as follows.

Maximizing throughput:

$$\max \zeta_1 = \sum_{j=1}^{N_{Column}} \int_0^{t_{cycle}} u_F^j(t)\, dt, \tag{39}$$

Maximizing glucose purity in the intermediate stream outlet:

$$\max \zeta_2 = \frac{\sum_{j=1}^{N_{Column}} \int_0^{t_{cycle}} u_I^j(t) C_{Glu,I}^j(L,t)\, dt}{\sum_{j=1}^{N_{Column}} \sum_{i=1}^{N_{Comp}} \int_0^{t_{cycle}} u_I^j(t) C_{i,I}^j(L,t)\, dt} \tag{40}$$

subject to equations (1)-(5), (37)-(38),

Maltose recovery in the raffinate stream outlet:

$$\frac{\sum_{j=1}^{N_{Column}} \int_0^{t_{cycle}} u_R^j(t) C_{Mal,R}^j(L,t)\, dt}{\sum_{j=1}^{N_{Column}} \int_0^{t_{cycle}} u_F^j(t) C_{Mal,F}^j(t)\, dt} \geq Rec_{Mal,R}^{min} + \delta, \tag{41}$$

Glucose recovery in the intermediate stream outlet:

$$\frac{\sum_{j=1}^{N_{Column}} \int_0^{t_{cycle}} u_I^j(t) C_{Glu,I}^j(L,t)\, dt}{\sum_{j=1}^{N_{Column}} \int_0^{t_{cycle}} u_F^j(t) C_{Glu,F}^j(t)\, dt} \geq Rec_{Glu,I}^{min} + \delta, \tag{42}$$

$$u_L \leq u^j(t) \leq u_U. \tag{43}$$

where ζ_1 and ζ_2 are the multiple objective functions, $C_{Glu,I}$ is the concentration of glucose in the intermediate stream outlet, $C_{Mal,R}$ is the concentration of maltose in the raffinate stream outlet, $Rec_{Mal,R}^{min}$ is the minimum recovery desired of maltose in the raffinate stream outlet, $Rec_{Glu,I}^{min}$ is the minimum recovery desired of glucose in the intermediate stream outlet and the subscript Glu, Mal, F and R refers to glucose, maltose, feed and raffinate outlet, respectively. The symbol δ corresponds to the safety factor which ensures the experimental purity and recovery values to be always higher than the desired values under the existence of minor operational and model uncertainty. It is to be noted that these purity and recovery calculations are based on one full cycle. In addition, we also introduce constraints in equation (43) on the zone velocities to obtain sensible operating conditions which avoid too high

pressure drop. The symbols u_L and u_U refer to the lower and the upper bounds. The upper bound is decided based on the maximum pressure drop that can be experienced by the pumps. In this study, u_L and u_U are set to 0 m/h and 10 m/h, respectively.

This multi-objective problem is converted into a single-objective problem by using the epsilon-constrained method where the second objective function, ζ_2, is imposed as a constraint [29, 31].

$$\frac{\sum_{j=1}^{N_{Column}} \int_0^{t_{cycle}} u_I^j(t) C_{Glu,I}^j(L,t)\, dt}{\sum_{j=1}^{N_{Column}} \sum_{i=1}^{N_{Comp}} \int_0^{t_{cycle}} u_I^j(t) C_{i,I}^j(L,t)\, dt} \geq \epsilon + \delta. \tag{44}$$

The resulting optimization problem is referred to as the throughput maximization problem in this study. The optimal solutions of the throughput maximization problem construct the Pareto plot of the multi-objective optimization problem.

The optimal operating conditions, which include pump flow rates and switching time, obtained computationally from the SMB optimization problem may need to be rounded off when they are implemented in an experimental unit. Such a round-off error may result in some deviation from the target purity. In order to guarantee that the purity converges to a value above the target purity even with the round-off error, the value of the safety margin δ in equations (41)-(44) should be sufficiently large. This is further discussed in Section 5.8.

5.5.3 Solution strategy

The simultaneous approach is adopted, which deals with the full discretization of state and control profiles, and the state equations. The spacial domains are discretized using the central finite difference scheme in the second order, and the Radau collocation on finite elements is used for the temporal discretization [30]. The resulting optimization problem has been implemented into AMPL (A Mathematical Programming Language) modeling environment [18]. The advantage of using AMPL is that it supports nonlinear programming (NLP) and provides the automatic differentiation functionality which can be used in many solvers. The resulting problem

has large number of variables and linearized Karush-Kuhn-Tucker (KKT) condition tends to have a sparse structure [29]. To deal with this challenge, we chose an interior point solver IPOPT 3.0 to solve the NLP problem [88]. Since interior-point methods can accept exact second order derivatives, they have fast convergence properties. Moreover, both structure and sparsity of the KKT system can be exploited by these solvers.

5.6 Experimental system

A Semba Octave^{TM} 100 Chromatography System was used to validate the JO and the GFC operations. The Semba Octave system carries eight column positions arranged in series and connected through an individually switchable binary pneumatic valve array. Since the binary valves can be independently switched, both JO and GFC configurations can be directly implemented on the Semba Octave system without making any modification in the hardware. We used four semi-prep columns in a 1-1-1-1 configuration. The fluid flow was controlled by four independent pumps dedicated to the feed, desorbent, extract, and recycle stream flow as shown in Figure 5.2. The extract and raffinate outlets were monitored using the two UV detectors (Shimadzu SPD-20A and Semba Octave^{TM} 4X) at the wavelength of 190nm .

The column porosity was estimated by injecting a 5 μl pulse of 100 g/L Dextran (Dextran 25000, Spectrum) in the SMB column. It was calculated to be 0.389 after subtracting the extra column volume from the retention volume of Dextran. The batch experiments were also performed for finding the initial estimates of the Henry's constants for each component by injecting 5 μl of 100 g/L glucose, 100 g/L fructose and 100 g/L maltose in the SMB column. The deionized water was used as the mobile phase at 50$^{\circ}C$ and at 1 ml/min flow rate.

A Shimadzu HPLC system was used with a BioRad Aminex HPX-87C analytical column for analyzing the sugar concentration in the feed, extract, raffinate and the

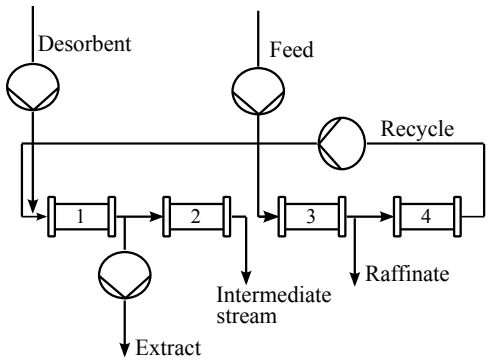

Figure 5.2: Pump configuration in the Semba Octave^{TM} Chromatography System for an operation where all the products are recovered simultaneously.

intermediate stream outlets. The analysis was performed by injecting 10 μl of each sample into the column with deionized water as an eluent flowing at $80°C$ and 0.6 ml/min flow rate. A refractive index detector (Shimadzu RID-10A) was used for both HPLC analysis and batch experiments.

5.7 Simultaneous Optimization and Model Correction scheme

The Simultaneous Optimization and Model Correction (SOMC) scheme is an iterative scheme where in each iteration the SMB model parameters are corrected by the SMB experimental data and the optimal operating conditions are predicted by re-optimizing the SMB model using the refined parameter values. The algorithm is terminated when the termination criteria is satisfied and we obtain the converged set of model parameters that predict the experimental conditions. The SOMC scheme is presented in Figure 5.3 and also summarized below in a step by step fashion [4, 8, 9, 76].

In Step 1, we start with a known set of initial model parameters. Since we have linear isotherms in our SMB model and using a linear driving force model in the solid phase, there is one equilibrium constant (Henry's constant) and one overall mass transfer coefficient for each adsorbing species in the feed mixture. Hence, there are three Henry constants and three mass transfer coefficients in our SMB model. These

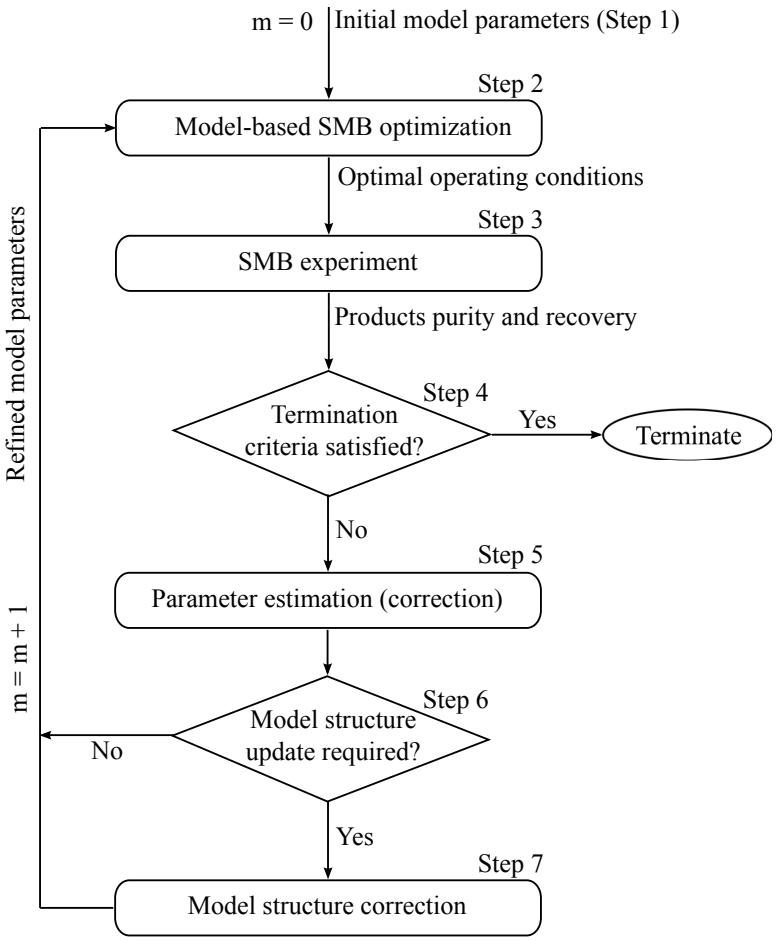

Figure 5.3: Simultaneous optimization and model correction (SOMC) scheme for the SMB process development [4, 8, 9, 76].

model parameters can be estimated by performing a set of pulse-injection experiments on a single chromatographic column, or updated from prior experiments.

In this study, these parameters are estimated from the pulse-injection experiments. Initially, the adsorption isotherm parameters and the number of theoretical plates are calculated based on the retention times and the width at the half peak height in the chromatograms obtained for each of the component. The mass transfer coefficients are then calculated by using the following equations [19].

$$K_{m,i} = \frac{2\,(NTP_i)\,u\,k_i'}{L\,(1+k_i')^2} \tag{45}$$

$$k_i' = \frac{1-\epsilon}{\epsilon}\,H_i \tag{46}$$

where the NTP_i refers to the number of theoretical plates for the ith component, k_i' is the retention factor of the ith component and u is the superficial velocity. It is to be noted that the Henry's constant is a function of porosity and the lumped mass transfer coefficient is a function of porosity, plate number and flow rate. However, the model parameters that are obtained from the batch experiments, are not evaluated by incorporating various flow conditions and also don't account for any dead volumes or mixing behaviors in the actual SMB unit [85]. In the SOMC scheme, it is not required to spend extra experimental effort to obtain very accurate model parameters because the initial model parameters are used only for obtaining the initial operating conditions. These model parameters will be corrected later on while fitting the SMB model to the experimental data in order to match the model predictions with the experimental observations. The symbol m refers to the number of iterations performed by the SOMC scheme. At this stage, m is set to zero.

In Step 2, the SMB process, as formulated in subsection 5.5.2, is optimized based on the initial model parameters. The optimizer finds the optimal operating conditions corresponding to the purity and recovery of the products enforced in the outlet streams.

In Step 3, an SMB experiment is performed using these optimal operating conditions and we wait for the SMB system to reach the cyclic steady state (CSS). Once the CSS has reached, each of the SMB product outlets is collected for one full cycle and the average product concentrations are calculated by analyzing these samples in the HPLC system. The purity and recovery values can then be calculated for each of the component in the extract, raffinate and the intermediate stream outlet. It is to be noted that such a simplified steady-state sampling strategy works for the linear systems, while it might not be sufficient for a more complex system. For instance, highly non-linear systems can show a strong correlation between the mass transfer coefficients and parameters representing non-linearity [9]. In that situation, we require

a large number of data points to obtain a reliable set of model parameters. Hence, the sampling strategy can be modified by collecting the transient concentration data where the SMB product outlets are collected into a container from which the samples are analyzed at regular intervals of time [9].

In Step 4, the termination criteria is checked. If the termination criteria is satisfied then the algorithm stops and the model parameters are assumed to be converged, otherwise we move on to the next stage of the SOMC scheme. This termination criteria is two fold; the first criteria is to satisfy the desired purity and recovery of the products in the SMB experiment performed. However, there could be a situation where the throughput of the SMB process could be further enhanced while meeting the product constraints at the same time. Hence, the second termination criteria is introduced. In this criteria, the maximum throughput attained in two consecutive iterations of the SOMC scheme are compared and if the relative difference in the throughput is less than a tolerance limit, γ_{tol}, then the algorithm is terminated $\left(\left|\frac{\zeta_1^{m+1}-\zeta_1^m}{\zeta_1^m}\right| \leq \gamma_{tol}\right)$. This is because the subsequent iterations would not lead to significant increment in the throughput value. The objective function tolerance, γ_{tol}, is set to 0.06 in this study. It should be noted that we certainly have to execute at least one iteration of the SOMC scheme in order to terminate this algorithm.

In Step 5, the model parameters are refined by fitting the model to the SMB experimental data. We use a simple least-square parameter estimation technique which minimizes the sum of the squares of the difference between the SMB model predictions and the experimental concentration data. The objective function, ϕ_{PE}, is formulated as:

$$\phi_{PE} = \min_{H_i, K_{m,i}} \sum_{k=0}^{N_{exp}} \sum_{i=1}^{N_{Comp}} \left(C_{i,R}^{k,mod} - C_{i,R}^{k,exp}\right)^2 + \left(C_{i,Ex}^{k,mod} - C_{i,Ex}^{k,exp}\right)^2 + \left(C_{i,I}^{k,mod} - C_{i,I}^{k,exp}\right)^2 \quad (47)$$

where the symbols $C_{i,R}^{k,mod}$, $C_{i,Ex}^{k,mod}$ and $C_{i,I}^{k,mod}$ refer to the averaged model predicted concentrations of the raffinate, extract and the intermediate stream outlet in the kth iteration of the SOMC scheme where $k = m$. Similarly, the symbols $C_{i,R}^{k,exp}$, $C_{i,Ex}^{k,exp}$

and $C_{i,I}^{k,exp}$ refer to the measured concentrations of the raffinate, extract and the intermediate stream outlet in the kth SMB experiment. Since each outlet stream of SMB consists of three components, we obtain nine concentration data points in total from each experiment. The number of model parameters that have to be refined are six including the three Henry constants and three mass transfer coefficients. It is to be noted that this technique might result in a non-unique set of parameters if only single experiment is considered. However, as a larger number of experiments are included, it is more likely to obtain a unique and reliable set of model parameters.

In Step 6, the consistency of the model is checked. If the present SMB model is unable to describe the experimental behavior then the model requires an update. The SMB model can be modified in several ways, a few of which include incorporating the dead volume effect around each column, including the dead volume associated with the recycle stream or modifying the adsorption isotherm models [8]. The decision of modifying the SMB model is based on the following two criteria (A) and (B):

(A) comparing the maximum percentage deviation of the experimental observations from the model predictions for the current experiment. If this value is smaller than a tolerance limit (γ_{MU_1}), then the current model is considered to be sufficiently accurate and we move on to the next step without modifying the model. The criteria is as follows:

$$\max\left(\left|\frac{Pur_{Glu,I}^{mod}-Pur_{Glu,I}^{exp}}{Pur_{Glu,I}^{exp}}\right|,\left|\frac{Rec_{Glu,I}^{mod}-Rec_{Glu,I}^{exp}}{Rec_{Glu,I}^{exp}}\right|,\left|\frac{Rec_{Mal,R}^{mod}-Rec_{Mal,R}^{exp}}{Rec_{Mal,R}^{exp}}\right|\right)\leq\gamma_{MU_1} \qquad (48)$$

where $Pur_{Glu,I}$ and $Rec_{Glu,I}$ are the purity and recovery of glucose in the intermediate stream outlet, $Rec_{Mal,R}$ is the recovery of maltose in the raffinate stream outlet and the superscripts mod and exp refer to the model predictions and experimental observations, respectively. The tolerance, γ_{MU_1}, is set to 0.05 in this study.

(B) comparing the minimized value of the objective function (ϕ_{PE}) in the equation (47), which represents the deviation of SMB model predictions from the experimental observations. The parameter estimation problem is re-solved with the

modified SMB model and the minimized sum of squared errors, ϕ_{PE}^{new}, is compared with the existing value $\phi_{PE}^{current}$. The criteria for updating the model is as follows:

$$\frac{\phi_{PE}^{current} - \phi_{PE}^{new}}{\phi_{PE}^{current}} \geq \gamma_{MU_2} \tag{49}$$

where ϕ_{PE}^{new} and $\phi_{PE}^{current}$ refers to the minimized sum of squared errors in the equation (47) corresponding to the modified and existing SMB models, respectively. The symbol γ_{MU_2} is the tolerance for the model update, which is set to 0.4 in this study. If the reduction in the parameter estimation objective function value is greater than the tolerance limit, γ_{MU_2}, then the model is updated and the modified SMB model is passed on to the Step 7. Otherwise, the model does not require an update and we come back to the Step 2 with the refined set of model parameters. The iteration index of SOMC scheme (m) receives an increment of one as we proceed for the next iteration. In the JO and the GFC operating strategies considered in this work, since there is no prior operational knowledge, the model update is considered only after one parameter correction step with the existing model. Thus, the model structure is not modified in the zeroth iteration of the SOMC scheme.

In Step 7, the corrected SMB model and the refined model parameters obtained by fitting the modified SMB model to the experimental data are passed back to Step 2.

Next, the model-based optimization of the SMB operation is repeated to obtain an updated set of optimal operating conditions. The next SMB experiment is performed using these updated optimal operating conditions and outlets concentration data are obtained. If the termination criteria is fulfilled then the algorithm is terminated, otherwise this concentration data is used to further refine the model parameters in the parameter estimation process. The algorithm continues in an iterative fashion until we obtain the converged set of model parameters.

It is to be noted that there may be significant build up of components in the recycle stream loop (see Figure 5.2). Hence, to increase the observability of the SMB process, the recycle stream can be sampled over a single step to obtain the average

concentration of each component in the recycle loop. However, such sampling perturbs the cyclic steady state and thus can be performed only after all other sampling is completed. These recycle stream concentration data can then be included while fitting the SMB model to the experimental data in the Step 5.1 of the SOMC scheme. In this study, the recycle stream was sampled for the first step of both JO and GFC operations. The flow circuit was cut by breaking the connection between the fourth and the first column and the outlet of the fourth column was sampled during the first step. The desorbent flow rate at the inlet of the first column was appropriately modified to keep the zone 1 velocity same after breaking the flow circuit. In this work, the addition of recycle stream concentration data does not influence the optimum solution of the parameter estimation problem (in Step 5). Nevertheless, increasing the observability of experiments may improve the condition of the parameter estimation problem for more complex systems.

It should be emphasized that the SOMC scheme is not a control technique to maintain the quality of the products in a full-scale process, but is an experimental technique for bench-scale experiments. Only the performance at the CSS is optimized, and the transient dynamics between CSSs or disturbance rejection are not considered. After the SMB process is designed by SOMC and scaled up, a feedback controller [20] may be implemented to maintain desired production. Building the controller based on the refined mathematical model obtained from the SOMC scheme would improve the control performance to obtain a faster response and higher degree of robustness.

5.8 Results and discussion

We now discuss the experimental validation of both JO and GFC operations using the SOMC scheme. The details of the chromatographic system are discussed in Section 5.3. The column specifications, porosity and the feed concentration are listed in Table 5.1. The product performance criteria that is imposed on the SMB system

is shown in Table 5.2. We added the constraints on the recovery of maltose obtained in the raffinate stream outlet and the recovery and purity of glucose obtained in the intermediate stream outlet. The rationale behind choosing such performance criteria was to make a systematic comparison of both JO and GFC operations. This criteria allows an analysis of Pareto front of the multi-objective optimization problem where the other product constraints are always active at the optimal solution. This Pareto plot is discussed later in this section. It is to be noted that the product performance criteria shown in Table 5.2 also ensures high purity and recovery of fructose (more than 80%) in the extract stream outlet. Hence, we do not impose any product constraints on fructose separately. Both JO and GFC operating schemes are implemented on the Semba Octave^{TM} Chromatography System. The details of the experimental setup are described in Section 5.6.

5.8.1 JO process

The experimental results obtained from the JO process are presented in Figure 5.4 which shows the comparison of the SMB model predictions and the experimental observations for each iteration of the SOMC scheme. We started with the pulse-injection experiments of the maltose, glucose and fructose and found an initial set of model parameters based on the retention time and width at the half peak height in the chromatograms (see Table 5.3, Step 1). The details of the pulse-injection experiments are mentioned in Section 5.6. The SMB model was then optimized and the optimal operating conditions were implemented on the SMB system (Step 2 and 3). While the experiment was running, the concentration profiles in the product outlets were constantly monitored to ensure the cyclic steady state. The CSS was confirmed by sampling the product outlets for two consecutive cycles at the cyclic steady state. Typically, the JO and GFC processes needed to run for 6-8 cycles to reach the CSS. Once the CSS had reached, the product outlets were fractionated for one full cycle

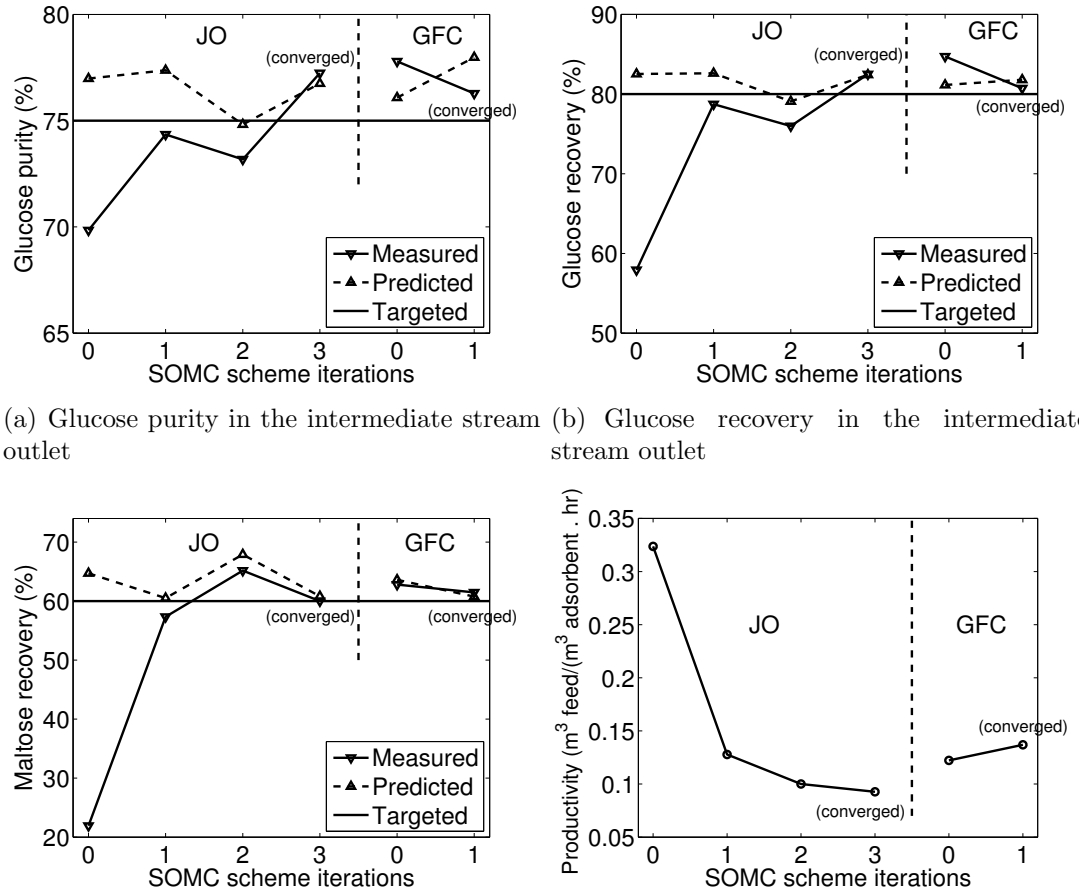

(a) Glucose purity in the intermediate stream outlet

(b) Glucose recovery in the intermediate stream outlet

(c) Maltose recovery in the raffinate stream outlet

(d) Productivity of SMB

Figure 5.4: JO and GFC process: a comparison of the model predictions and the experimental observations for each iteration of SOMC scheme. The dashed vertical line is dividing the results of the JO and the GFC processes.

and the purity and recovery calculations were performed. As shown in Figure 5.4, there was a huge deviation between the model predictions and the experimental observations that were obtained in the zeroth iteration (Step 4). In particular, the maltose recovery measured in the raffinate stream outlet was significantly lower than the desired value. Hence, the termination criteria could not be satisfied and we moved on to the next step.

The parameter estimation step was executed next (Step 5). In this step, the six model parameters were corrected by fitting the SMB model to the experimental

data. These refined model parameters are listed in Table 5.3. It is interesting to note that the SMB model, discussed in Section 5.4, does not explicitly account for the mixing and dispersion inside the tubing connecting the columns and other peripheral equipment such as detectors and switching valves. However, if this dead volume is symmetrically present on either side of the SMB columns then it could be well captured by the LDF model where the contribution to the first and second moments of concentrations from all parts of the chromatographic process are additive and directly related to the model parameters of the column [71, 21]. Here, the Henry constants and the mass transfer coefficients can then be corrected to account for the dead volume effect inside the SMB system. Hence, the refined model parameters obtained in Step 5 account for the symmetric dead volume present in the SMB system. The next step was to verify the model structure of the SMB system (Step 6). Since there is no prior operational knowledge about the JO process, we keep the model structure tentatively for the zeroth iteration of the SOMC scheme and do not change it. At this point, the zeroth iteration ($m = 0$) of the SOMC scheme has been completed.

As the first iteration proceeds ($m = 1$), the SMB model was re-optimized based on the refined model parameters and the second SMB experiment was performed by implementing the new optimal operating conditions (Step 2 and 3). The results are shown in Figure 5.4. As shown in this Figure, there was a significant difference between the experimental observations of the first and the zeroth iteration. In particular, the maltose recovery obtained in the raffinate stream outlet was drastically improved. Hence, the single iteration of SOMC scheme was able to reduce the model mismatch considerably. This observation demonstrates the efficacy of the SOMC scheme. The productivity of the SMB, however, decreased because of the dead volume that was accounted in the model parameters. The termination criteria was still not satisfied hence we moved on to the parameter estimation step (Step 5). In this step, the

six model parameters were corrected by fitting the SMB model to both the experiments simultaneously in order to obtain more reliable set of SMB model parameters. The next step was to verify the model structure of the SMB system (Step 6). The maximum percentage deviation of the experimental observations in the equation (48) was 5.5% (greater than γ_{MU_1}) hence the SMB model may need to be modified. In the SMB unit used in this study, we encounter symmetric dead volume between the SMB columns except for the flow line consisting of recycle stream pump (see Figure 5.2). Although the recycle stream pump is necessary to maintain the cyclic operation of the SMB system, this pump also results in significant asymmetric dead volume which must be separately incorporated into our SMB model. In this study, a simple plug flow model has been used to simulate the dead volume of the recycle stream. The dead volume model is:

$$\frac{\partial C_i^j(x,t)}{\partial t} + u^j(t)\frac{\partial C_i^j(x,t)}{\partial x} = 0, \quad x \in [0, L_{rec\_loop}] \tag{50}$$

Here, the axial dispersion in the recycle loop is approximated by the numerical diffusion using a first order backward finite difference scheme [64]. Hence, the resulting numerical dispersion is proportional to the length of the recycle loop. Since it is hard to accurately measure the dead volume associated with the recycle stream, the length of the recycle loop (L_{rec_loop}) is allowed to change and considered as an extra degree of freedom in the parameter estimation step. It should be be noted that the recycle stream flow line is also switched periodically to be in sync with inlet and the outlet streams of the SMB system. This corrected model structure was used in the parameter estimation in Step 5. In this step, the six model parameters and the length of the recycle loop were corrected by fitting the SMB model to both of the SMB experiments simultaneously in order to obtain more unique and reliable set of parameters (see Table 5.3). The objective function that represents model mismatch in equation (47) was reduced by 42.17% (greater than γ_{MU}) which confirms that the modified model is a more accurate representation of the existing system. The dead

volume in the recycle stream loop was found to be significant, around 20% of the single column volume based on fitting the model to the experimental data. These refined model parameters along with the modified SMB model were further passed on to Step 2 for the second iteration (Step 7).

As the second iteration proceeds ($m = 2$), the SMB model was re-optimized based on the refined model parameters and the third SMB experiment was performed by implementing the new optimal operating conditions (Step 2 and 3). As shown in the Figure 5.4, the model mismatch was further reduced however the measured purity and recovery values were still slightly lower than the desired value (Step 4). The productivity of the SMB decreased again slightly because of the recycle stream dead volume that was accounted in the SMB model. The termination criteria, however, was still not satisfied hence the parameter estimation step was executed next (Step 5). In this step, only the six model parameters were varied while fitting the SMB model to the experiments. The length of the recycle loop was kept fixed because it was found to be an insensitive parameter and changing it did not make any difference in terms of the model fitting except increasing the difficulty of the optimization problem. The six model parameters were then corrected by fitting the SMB model to all of the SMB experiments simultaneously in order to obtain more unique and reliable set of parameters (see Table 5.3). The SMB model structure is believed to be sufficiently accurate at this stage (Step 6) because the maximum percentage deviation of the experimental observations was 4.2% (less than γ_{MU_1}). The refined model parameters from the Step 5 were then further used for re-optimizing and re-implementing the optimal operations on the SMB system. Overall, it needed three iterations of the SOMC scheme to converge to the set of model parameters that predicted the experimental conditions for the JO process. Since the objective function tolerance, γ_{tol}, was set to 0.06, we confirmed that the relative throughput increment in the subsequent iteration was 2.4% (less than 6%) and therefore the algorithm can be terminated.

It can be seen in Table 5.3 that all model parameters changed relatively significantly from the $0th$ to $1st$ iteration. These changes can be attributed largely to the dead volume in the equipment. In our model, the effect of the dead volume is lumped into the mass transfer coefficients and Henry constants [54]. It is also possible that the nonlinearity of the isotherm may contributed the changes [15, 60, 62, 86] [3538]. However, we believe the influence of isotherm nonlinearity is limited considering the low feed concentrations

5.8.2 GFC process

We now proceed to the experimental validation of the GFC process. The results are presented in Figure 5.4 which shows the comparison of the SMB model predictions and the experimental observations for each iteration of the SOMC scheme. The experimental set up was exactly same as the one used for the JO process, including the dead volume associated with the recycle stream loop. Hence, the model parameters obtained from the JO process were also expected to be applicable for the GFC process. Therefore, instead of starting from the pulse-injection experiments and obtaining an initial set of model parameters, we started off with the converged parameters that were obtained from the JO process (see Figure 5.5, Step 1). The SMB optimization problem was then solved to obtain the optimal operating conditions for the GFC process. As discussed before, the GFC process is a formulation encompassing numerous SMB operations and the optimal operating scheme is found by maximizing the SMB throughput while meeting the product specifications at the same time. This throughput maximization problem is a singular control problem which is known to have non-unique solutions [30]. To avoid this non-uniqueness, we constrain the throughput maximization problem further by considering minimization of desorbent consumption, which is solved subsequently. We solve the following two problems (I) and (II) sequentially as follows:

(I) Maximizing throughput:

$$\max \zeta_1 = \sum_{j=1}^{N_{Column}} \int_0^{t_{cycle}} u_F^j(t)\, dt, \tag{51}$$

subject to equations (1)-(5), (37)-(38), (41)-(44).

(II) Minimizing desorbent consumption:

$$\min \zeta_3 = \sum_{j=1}^{N_{Column}} \int_0^{t_{cycle}} u_D^j(t)\, dt, \tag{52}$$

subject to

SMB throughput:

$$\zeta_1(t) \left(= \sum_{j=1}^{N_{Column}} \int_0^{t_{cycle}} u_F^j(t)\, dt \right) \geq \zeta_1^{opt}, \tag{53}$$

equations (1)-(5), (37)-(38), (41)-(44).

where ζ_3 is the objective function accounting for the desorbent consumption in the SMB process and ζ_1^{opt} is the optimum SMB throughput obtained by solving the throughput maximization problem in equation (51). Problem (I) is exactly same as the throughput maximization problem discussed in equation (39) of Subsection 5.5.2 while the Problem (II) seeks the solution that minimizes the desorbent consumption among multiple solutions to (I). The optimal operating conditions obtained in this manner has reduced desorbent consumption without sacrificing the maximized throughput. The SMB model was then optimized with this new problem formulation and the optimal operating conditions were found (Step 2). The similar optimization study has also been carried out for the JO process, the details of which are included in 5.8.4.

Next, the first experiment was performed by implementing the optimal operating conditions on the Semba Octave^{TM} Chromatography System (Step 3). As shown in Figure 5.4, in the zeroth iteration, the desired purity and recovery requirements

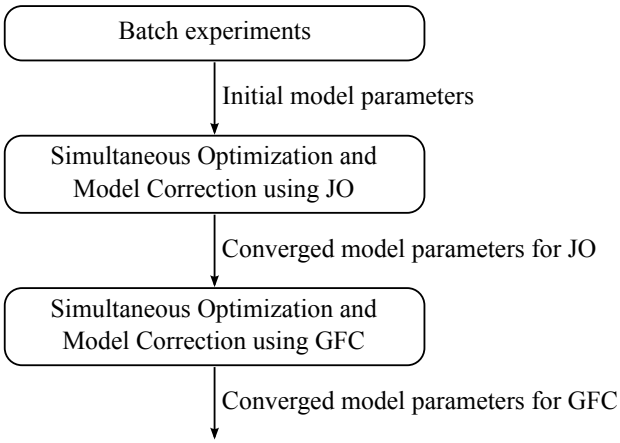

Figure 5.5: A diagram depicting the sequential order of the SOMC scheme used for the experimental validation of the JO and the GFC processes.

of the products were satisfied by the experimental observations. In fact, the purity and recovery values calculated from the experiment were higher than the predictions made from the SMB model. Hence, the first part of termination criteria was fulfilled (Step 4). However, there still exist a possibility where the throughput of the SMB process could be further enhanced while meeting the product constraints at the same time, hence we moved on. The parameter estimation step was executed next (Step 5). In this step, the six model parameters were corrected while fitting the SMB model to the experimental data (see Table 5.4). The length of the recycle loop was kept unchanged because it had already been optimized. The next step was to confirm the SMB model consistency (Step 6). The maximum percentage deviation of the experimental observations in the equation (48) was 4.2% (less than γ_{MU_1}) hence we believe the current model to be sufficiently accurate. At this point, the zeroth iteration ($m = 0$) of the SOMC scheme has been completed. The refined model parameters were then used further for re-optimizing the SMB model in the first iteration.

As the first iteration proceeds ($m = 1$), the sequential optimization problem was solved once again in order to obtain the optimal operating conditions for the GFC process (Step 2). Next, the second experiment was performed by implementing the optimal operating conditions on the Semba Octave^{TM} Chromatography System (Step 3). The results for the first iteration are presented in Figure 5.4. The throughput of the SMB process has improved considerably around 13% while still satisfying the product constraints in the outlet streams. At this stage (Step 4) however, the model parameters cannot be assumed converged because the throughput can still be improved further hence, we moved on to the parameter estimation step (Step 5). The six model parameters were then corrected by fitting the SMB model to both of the experiments simultaneously to obtain more unique and reliable set of parameters. These refined model parameters along with the existing SMB model structure were then passed back to Step 2. The SMB model was re-optimized by solving the sequential optimization formulation. We confirmed that the relative increment in the throughput was 5.2% (less than γ_{tol}) in the subsequent iteration therefore the algorithm can be terminated. Overall, it took one iterations of the SOMC scheme to converge to the set of model parameters that predicted the experimental conditions for the GFC process.

As discussed in Section 5.5.2, the optimal operating conditions need to be rounded off when they were implemented in the experimental equipment. In the Semba Octave^{TM} Chromatography system, the minimum increment of the pump flow rate is 0.1 mL/min. Thus, the optimal flow rates obtained computationally from the model must be rounded off to the nearest decimal point to be implemented in this experimental system. To guarantee that the purity converges to a value above the target purity even with the round-off error, we chose the safety margin δ to be 2%.

In order to confirm the accuracy of our computational method, we also tested the influence of the discretization both for the spatial and time domain on the optimal

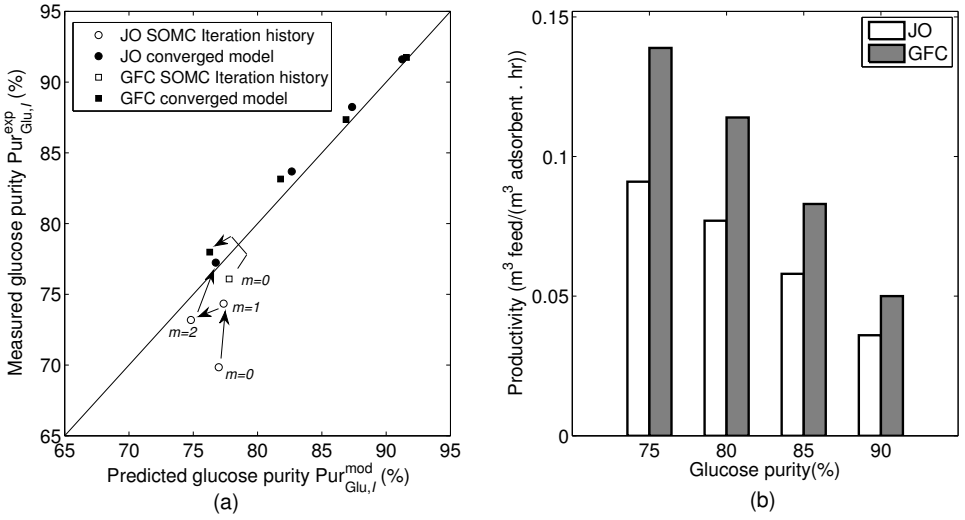

Figure 5.6: (a) Comparison of glucose purity in the intermediate stream outlet predicted by the model and measured in experiments. (b) Productivity against glucose purity in the intermediate stream outlet for JO and GFC processes.

operating schemes. The optimal operating conditions did not change with increase in the number of finite elements. The SMB optimization required around 5-20 minutes of CPU time for the JO process and 20-160 minutes of CPU time for the GFC process on a PC using an Intel Core^{TM} $i7$ processor.

5.8.3 Model validation and comparison of JO and GFC

We present the result of model validation at different purities of glucose in the intermediate stream both in the JO and GFC operations. The multi-objective optimization problem discussed in Section 5.5.2 is solved and the resulting optimal operating conditions were implemented experimentally. The comparison is plotted in Figure 5.6(a) with the iteration history of SOMC. As can be seen in this figure, once the SOMC scheme converges, a single set of converged parameters each for JO and GFC is able to predict the intermediate product purity sufficiently accurately in the range of purity from 75% to 90%. Although we believe this range covers most operations of practical interest for sugar purification, further validation may be needed if purities outside this range are required.

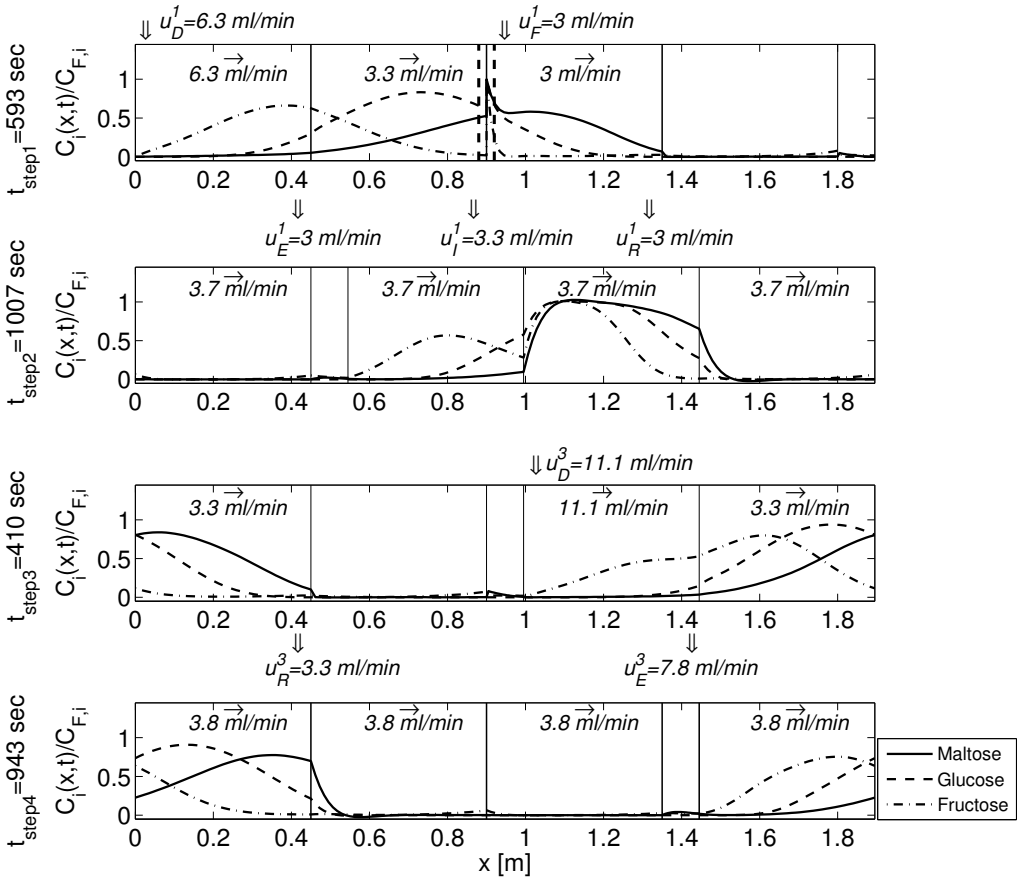

Figure 5.7: Optimal GFC structure obtained from the GFC formulation while targeting 80% glucose purity in the intermediate stream outlet. The normalized concentration profiles are also shown across the SMB columns for each of the component at the beginning of each step. The four SMB columns and the recycle stream dead volume are separated by the solid vertical lines. The two vertical dashed lines, closely spaced to each other, indicate the shutting off of the flow circuit. The times for which each step lasts are also shown vertically to the left side of Figures.

One of the objective function, throughput, is plotted in Figure 5.6(b) against the other objective function, glucose purity in the intermediate stream (Pareto plot). The productivity of the GFC process is significantly higher than that of the JO process; even the smallest difference of the productivity observed for the purity of 90% is about 40%. It should be noted that the results shown here can be system specific and may depend on the performance criteria employed in this study. Choosing a

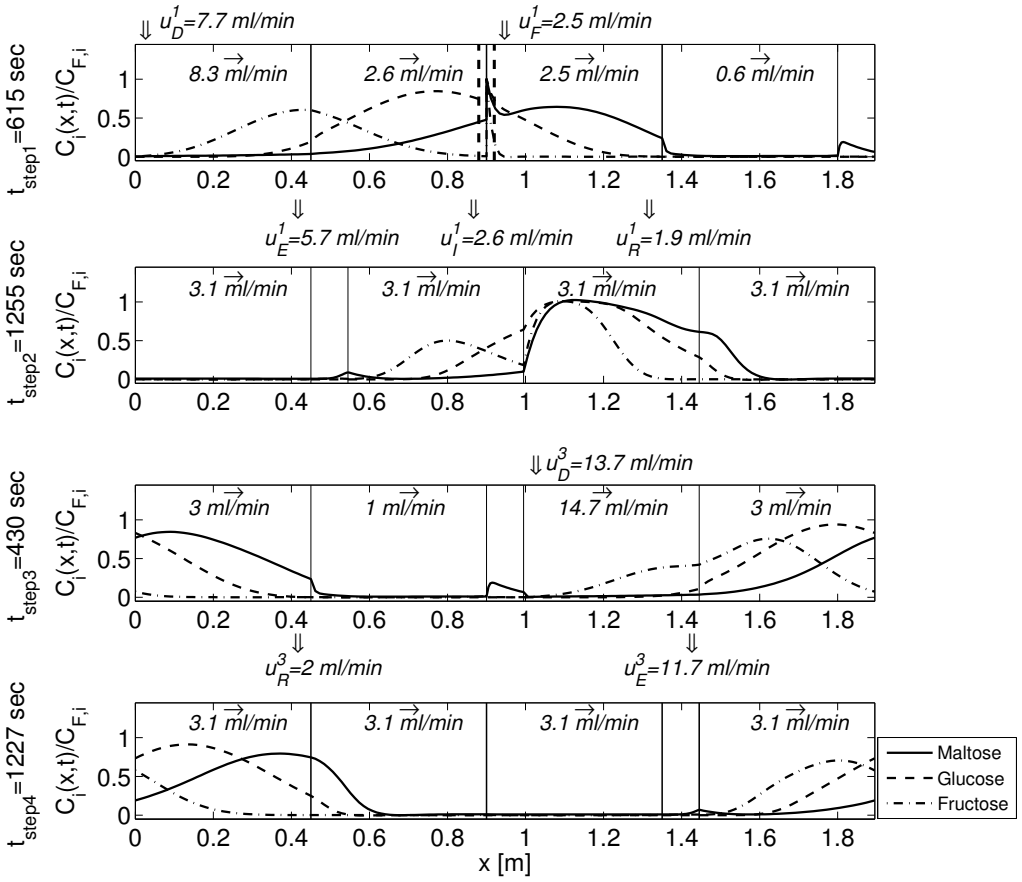

Figure 5.8: Optimal GFC structure obtained from the GFC formulation while targeting 85% glucose purity in the intermediate stream outlet. The normalized concentration profiles are also shown across the SMB columns for each of the component at the beginning of each step. The four SMB columns and the recycle stream dead volume are separated by the solid vertical lines. The two vertical dashed lines, closely spaced to each other, indicate the shutting off of the flow circuit. The times for which each step lasts are also shown vertically to the left side of Figures.

different stationary phase, experimental unit, recovery, or purity target may results in a different conclusion.

We finally present the optimal SMB operating schemes derived from the GFC formulation. The optimal GFC operations corresponding to 80% and 85% glucose purity are shown in Figures 5.7 and 5.8. The normalized concentration profiles are also shown across the SMB columns for each of the component at the beginning of

each step. The four SMB columns and the recycle stream dead volume are separated by the solid vertical lines. The two vertical dashed lines, closely spaced to each other, indicate the shutting off of the flow circuit i.e., extracting the product upstream while feeding the feed or desorbent downstream of the shut-off valve. The times for which each step lasts are also shown vertically to the left side of Figures 5.7 and 5.8.

The operations shown in Figures 5.7 and 5.8 are similar, while the flow rates and switching times are different. In step 1, the connection between second and third column is broken in order to recover glucose upstream of the shut-off valve. The faster and slower moving components, maltose and fructose, are also fractionated simultaneously from the raffinate and extract stream outlets, respectively. In step 3, only maltose and fructose are collected while feeding fresh desorbent in the SMB system. Steps 2 and 4, on the other hand, are pure recycle steps circulating the liquid flow across the SMB columns without feeding or collecting any of the products. Steps 2 and 4 are very essential since they allow the concentration profiles to get separated from each other which allows higher loading in step 1 without sacrificing high purities. Also, the duration of steps 2 and 4 contributes to 65-70% of the total cycle time indicating the importance of these steps. Although there is significant amount of time spent in separating the concentration profiles inside SMB columns, such operation leads to high throughput as well as high purity of products when they are withdrawn during steps 1 and 3. The minor difference between the operations in Figures 5.7 and 5.8 is that there are columns where the flow rates become zero (fourth column from the left in Step 1 and second column in Step 3). We observe this only in the operations where the purity of glucose is 75% and 80%.

It is to be noted that the GFC operation can be easily implemented experimentally on most SMB system that can implement the standard four-zone SMB configuration, without making any modifications in the hardware. For the SMB systems equipped with rotary valves, we may require only one additional binary valve in order to break

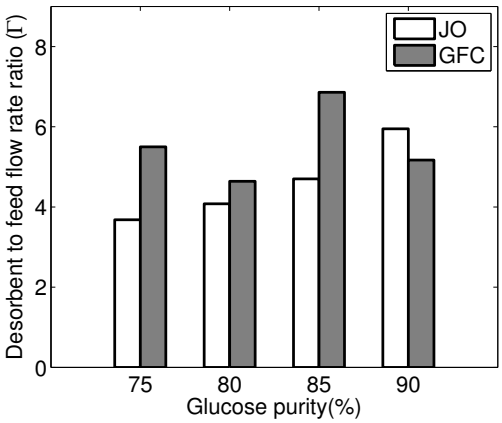

Figure 5.9: Optimized desorbent to feed flow rate ratio (Γ) comparison by varying the glucose purity in the intermediate stream outlet for both JO and GFC processes.

the flow circuits.

It should also be noticed that none of the zone velocities hit upper bound in the optimum operating schemes derived from the JO or the GFC formulation. This is because of the low value of the mass transfer coefficients in the SMB system. The increase in the flow rates leads to further expansion of the concentration profiles. As a consequence, the product outlets get contaminated and result in lower purity and recovery of the products. This observation was also confirmed by experiment, the details of which are included in Section 5.8.5.

5.8.4 Desorbent to feed flow rate ratio comparison

The desorbent consumption plays an important role while assessing the performance of the SMB operation. Therefore, the optimized desorbent to feed flow rate ratio was also compared for both JO and GFC operations as shown in Figure 5.9. We define desorbent to feed flow rate ratio, Γ, as follows:

$$\Gamma = \frac{\sum_{j=1}^{N_{Column}} \int_0^{t_{cycle}} u_D^j(t)\, dt,}{\sum_{j=1}^{N_{Column}} \int_0^{t_{cycle}} u_F^j(t)\, dt,} \tag{54}$$

The sequence of two optimization problems, (I) and (II), as discussed in Section 5.8, was solved for both JO and GFC processes to calculate the value of Γ. The

results obtained for the GFC formulation were experimentally validated, while we only pursued a computational study for the JO process. Nevertheless, the optimal model parameters, obtained from the SOMC scheme for the JO process, can be trusted over the range of operating conditions that are considered here; we confirm the reliability of the model from the fact that these operating conditions are sufficiently close to the operating conditions discussed for the JO process in Section 5.8.

As shown in the Figure 5.9, the desorbent to feed flow rate ratio increases monotonically with increase in the desired glucose purity in the intermediate stream outlet for the JO process. However, the desorbent consumed in the GFC process, on the other hand, is almost comparable to the JO process. Hence, the GFC process is more advantageous because it improves the productivity of the SMB process significantly (around 40-50%) with comparable amount of desorbent consumption.

5.8.5 Experimental validation of optimal flow rates

To verify whether the relatively low zone velocity, which does not hit upper bound, maximizes the productivity, we carry out an analysis using two different operating conditions, JO base case and JO high flow rate operations, as shown in Table 5.5. In the JO high flow rate operation, we scaled up all the flow velocities of the JO base case operation by a factor of ten so that the zone 1 velocity of step 1 reaches close to its upper bound. The switching times, on the other hand, were decreased by the same factor as shown in Table 5.5. When the simulation was performed for the JO high flow rate operation, we noticed a significant decrease in both purity and recovery values in the product outlets. This observation explains why the zone flow rates did not reach the upper bound in all the optimal operating conditions. Since we have low value of the mass transfer coefficients in our SMB system, the concentration profiles are already dispersed. The increase in the flow rates leads to further expansion of the concentration profiles and therefore the product outlets get contaminated and result

in lower purity and recovery of the products.

To confirm this observation, we further implemented the base case and the JO high flow rate operations on the experimental system. The results are presented in Table 5.5. As expected, the purity and recovery values in the product outlets were significantly lower compared to the base case. Hence, the simulation results were consistent with the experimental observations. It is to be noted that the set of model parameters used for obtaining these optimal operations was not the converged set obtained from the SOMC scheme. Hence, a minor model mismatch was present while performing these experiments and therefore the experimental observations deviate slightly from the model predictions in Table 5.5.

5.9 Conclusions

In this study, both JO and GFC operations are validated experimentally using the Semba Octave^{TM} chromatography system. A simultaneous optimization and model correction scheme (SOMC) has been used to resolve the model mismatch. The advantage of using the SOMC scheme is that it is a systematic approach to arrive at the model parameters that predict the experimental conditions. In addition, we do not have to rely on the careful descriptions such as extra-column dead volumes that exists in the actual SMB unit or the effects of the flow rates on the mass transfer inside the column. We can even start with a rudimentary set of model parameters and obtain the converged set of parameters by fitting the SMB model to the experimental data. We also present a systematic comparison of both JO and GFC processes by constructing a Pareto front involving the productivity obtained from the SMB operation and the glucose purity desired in the intermediate stream outlet. The GFC formulation has been shown to be an efficient approach for finding the best ternary separation strategy from various different alternatives. The productivity obtained from the GFC process is significantly higher (around 40-50%) compared to the JO process.

It is to be noted that both JO and GFC operations are easily implementable on most of the SMB system without making any modification in the hardware. For the SMB systems equipped with rotary valves, we may require one or more than one additional binary valves in order to break the flow circuits. However, there is no major hardware modification required for implementing such advanced operations.

In the next chapter, the optimization of simulated moving bed reactor (SMBR) systems is discussed. The focus is on developing an SMBR process for industrial-scale production of propylene glycol ethers.

Table 5.1: Experimental details of the SMB system

Parameter	Value
Column details	
Number of columns (N_{Column})	4
Length (L)	45 cm
Diameter (D)	1.5 cm
Porosity (ϵ_b)	0.389[a]
Mobile phase	
Substance	Deionized water
Temperature	$50°C$
Stationary phase	
Resin	DOWEX^{TM} MONOSPHERE^{TM} 99Ca/320
Average particle size	320 μm
Feed stream	
Number of components (N_{Comp})	3
Maltose concentration ($C_{Mal,F}$)	40 g/L
Glucose concentration ($C_{Glu,F}$)	180 g/L
Fructose concentration ($C_{Fru,F}$)	180 g/L

[a] the details are mentioned in Section 5.6.

Table 5.2: Performance criteria for the SMB optimization problem for the separation of maltose, glucose and fructose

Desired parameters	Value
Minimum maltose recovery in the raffinate stream outlet $\left(Rec^{min}_{Mal,R}\right)$	60%
Minimum glucose recovery in the intermediate stream outlet $\left(Rec^{min}_{Glu,I}\right)$	80%
Minimum glucose purity in the intermediate stream outlet $\left(Pur^{min}_{Glu,I}\right)$	75%

Table 5.3: Summary of the model parameters corrections for the JO process for each iteration of SOMC scheme

Model parameters	Iteration 0 (Batch exp.)	Iteration 1	Iteration 2	Iteration 3 (converged)
H_1	0.067	0.186	0.189	0.187
H_2	0.230	0.300	0.298	0.299
H_3	0.455	0.540	0.517	0.505
$K_{m,1}$ (sec^{-1})	6.63×10^{-3}	1.92×10^{-3}	1.84×10^{-3}	1.26×10^{-3}
$K_{m,2}$ (sec^{-1})	11.32×10^{-3}	7.75×10^{-3}	6.31×10^{-3}	5.56×10^{-3}
$K_{m,3}$ (sec^{-1})	9.23×10^{-3}	8.33×10^{-3}	9.64×10^{-3}	11.29×10^{-3}
L_{rec_loop} (cm)	–	9.50	9.50	9.50
SMB productivity (m^3 feed/(m^3 adsorbent . hr))	0.324	0.129	0.101	0.091

Table 5.4: Summary of the model parameters corrections for the GFC process for each iteration of SOMC scheme

Model parameters	Iteration 0	Iteration 1 (converged)
H_1	0.187	0.187
H_2	0.299	0.303
H_3	0.505	0.525
$K_{m,1}$ (sec^{-1})	1.26×10^{-3}	1.51×10^{-3}
$K_{m,2}$ (sec^{-1})	5.56×10^{-3}	6.69×10^{-3}
$K_{m,3}$ (sec^{-1})	11.29×10^{-3}	9.12×10^{-3}
L_{rec_loop} (cm)	9.50	9.50
SMB productivity (m^3 feed/(m^3 adsorbent . hr))	0.120	0.137

Table 5.5: Operating conditions to investigate the effect of flow rates[1]

	JO base case operation		**JO high flow rate operation**	
Operating conditions:				
Step 1				
Feed flow rate	1.9 ml/min		18.5 ml/min	
Desorbent flow rate	1 ml/min		10 ml/min	
Switching time	622 seconds		62 seconds	
Step 2-4				
Desorbent flow rate	1.1 ml/min		10.9 ml/min	
Extract flow rate	1.4 ml/min		13.6 ml/min	
Recycle flow rate	1.3 ml/min		13.1 ml/min	
Switching time	1907 seconds		191 seconds	
Results:				
Parameter	Model predictions	Experimental observations	Model predictions	Experimental observations
Glucose purity in the intermediate stream outlet	92%	88.84%	62.88%	57.68%
Glucose recovery in the intermediate stream outlet	92.5%	86.08%	50.7%	50.28%
Maltose recovery in the raffinate stream outlet	74.7%	67.36%	45.43%	50.8%

[1] the model parameters were as follows: $H_1 = 0.18$, $H_2 = 0.29$, $H_3 = 0.536$, $K_{m,1} = 1.32 \times 10^{-3}\, sec^{-1}$, $K_{m,2} = 7.24 \times 10^{-3}\, sec^{-1}$, $K_{m,3} = 8.61 \times 10^{-3}\, sec^{-1}$.

CHAPTER VI

OPTIMIZATION OF REACTIVE SIMULATED MOVING BED SYSTEMS FOR PRODUCTION OF GLYCOL ETHER ESTER

6.1 Introduction

The concept of reactive chromatography that integrates both separation and reaction inside the column has been a subject of considerable attention for last few decades [22, 24, 32, 33, 36, 45, 47, 66, 67, 70, 75, 79, 87]. Such mechanism facilitates the reversible reaction to go beyond thermodynamic equilibrium by continuously separating the products from the reaction zone. As a consequence, there is more product formation in these systems and the products can be recovered at high purities due to their separation from the reactants. Furthermore, the integration of both reaction and separation units into one single unit reduces both capital and operating costs. Because of these advantages, the potential of reactive chromatography systems has been explored by several research groups for various applications such as esterification [22, 45, 67, 79], transesterification [70], alkylation [32, 33], hydrolysis [47, 75, 87], isomerization [24], etherification [36] and dehydrogenation [66]. Although the reactive chromatography process offers several advantages, the batchwise operation may not be suitable for large-scale productions.

Simulated moving bed reactor (SMBR), on the other hand, is an extension of this process that performs reactive chromatography in a continuous and countercurrent fashion. SMBR operations can provide economic benefit for equilibrium limited reversible reactions. In such operations, in situ separation of the products drives the reversible reactions to completion beyond thermodynamic equilibrium and also helps

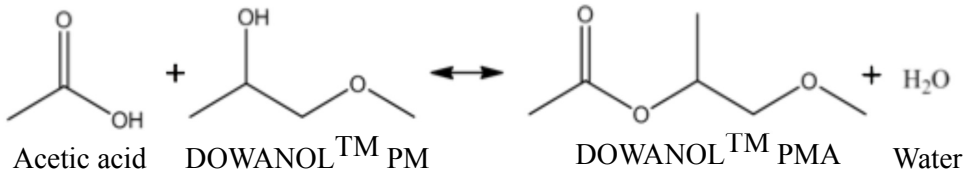

Figure 6.1: Esterification reaction of acetic acid and PM using AMBERLYST^{TM}15 as a cation exchange resin.

in the continuous recovery of the products of high purity. The advantages of SMBR systems have been highlighted in numerous studies for various industrial applications such as enzymatic sucrose inversion [6, 16, 42], MTBE synthesis [80, 95, 97], glucose isomerization [83, 96], methylacetate hydrolysis [91, 92], oxidative coupling of methane [38, 39], p-xylene production [56], methylacetate synthesis [44, 91] and esterification of acetic acid with ethanol [50]. A summary of the SMBR applications can also be found in Minceva et al. [56]. Nevertheless, to the best of our knowledge, reactive chromatography has not yet been applied to a large-scale industrial production.

In this study, we develop a novel industrial application of SMBR process. We consider the production of propylene glycol methyl ether (PMA) through the esterification of 1-methoxy-2-propanol (PM) and the acetic acid (AA) as shown in Figure 6.1. The esterification reaction is catalyzed by AMBERLYST^{TM}15, a cation exchange resin that functions both as a catalyst and an adsorbent. PMA, the product of this esterification reaction, is the second most widely used propylene glycol ether with most of its use as a solvent for industrial paints and coatings in the automotive industry [1]. It is also used in the electronic industry and formulated into various commercial products such as degreasers for the circuit boards. Conventional methods that are used to produce PMA involve reactive distillation, which limits the production of PMA due to the formation of azeotropes. SMBR systems, on the other hand, can overcome this limitation by constantly separating the products while their formation thus avoiding separation difficulties arising from the presence of azeotropes.

Modeling of reactive chromatography remains a significant challenge due to the complexity of the dynamics of a reaction, mass transfer, and chromatographic elution. Careful and laborious experiments are needed to obtain the parameters for catalyzed reaction kinetics, mass transfer, and adsorption onto the resin. These mechanisms may not necessarily be decoupled and observed separately in an experiment. In our recent study [63], we investigated reactive chromatography for the esterification shown in Figure 6.1 by carrying out a number of batch reaction and chromatographic elution experiments, and developed a preliminary model by fitting a model to experimental reactive chromatograms. Nevertheless, validity of the model under different conditions (e.g. high feed concentrations and large injection volumes) or reliability of the parameter values has not been confirmed yet.

The performance of the SMBR systems highly depends on its operating conditions. Therefore, an optimization study is required to identify the optimal operating strategy that exploits the economic potential of the SMBR system and makes its application feasible. Over the past decade, many optimization studies of SMBR systems have been performed to optimize the performance of the SMBR. Migliorini et al. [53] performed a parameter analysis of the SMBR performances and proposed maximization of productivity as the useful objective function for the optimization of the SMBR. Azevedo et al. [6] presented an optimization methodology that maximizes the SMBR productivity while enforcing the minimum reaction conversion as a design constraint. Dünnbier et al. [16] formulated a single-objective optimization problem that minimizes the specific separation costs and presented a novel model-based optimization strategy for the SMBR optimization. This study also discussed an elaborate optimization procedure based on deterministic approaches. However, these optimization studies considered only single objective in their problem formulation.

The operating conditions of the SMBR system in general affect several objectives functions including the productivity, conversion of the limiting reactant, product purity, recovery and solvent consumption. Moreover, these objective functions often conflict with each other. To deal with this challenge, instead of finding the best solution of the single-objective optimization problem, it is more insightful to investigate the trade-off between the multiple objective functions. Therefore, a multi-objective optimization study is required to construct a Pareto front that shows the trade-off between the various objective functions. Some studies in the past [42, 80, 92, 96, 97] have considered multiple objectives in their optimization problem formulation for the SMBR. However, these studies have used the heuristic based algorithms in order to obtain the solutions of the multi-objective optimization problem. Heuristic based algorithms provide only the approximate optimum solutions in comparison to the deterministic based approaches. To improve the accuracy of solutions, in this study, the deterministic nonlinear programming techniques are adopted for solving the multi-objective optimization problem for the SMBR optimization. We use a simultaneous approach, where the spacial domains are discretized using central finite difference scheme, and the Radau collocation on finite elements is used for the temporal discretization [3]. The resulting system of algebraic equations is implemented into AMPL (A Mathematical Programming Language) and solved using an interior-point solver IPOPT [18, 88].

Although several researchers have worked on optimization of reactive SMB systems, only the conventional SMBR operating strategy is discussed most of the times [44, 56, 96]. In the conventional operating strategy, the inlet feed concentration is fixed during one switching interval while optimizing the switching time, feed, desorbent, extract and one of the column flow rates. Since the feed concentration is constant throughout the operation, we call this conventional strategy as the constant feed concentration strategy.

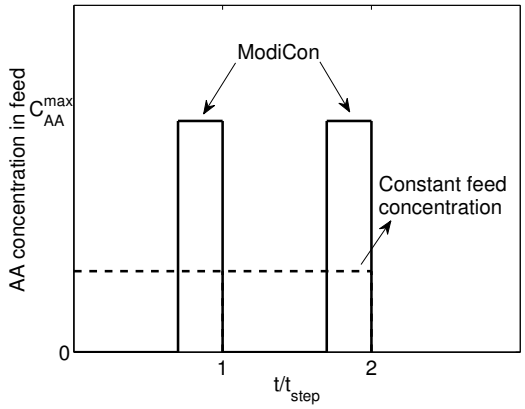

Figure 6.2: Variation of the inlet feed concentration: (1) Constant feed concentration strategy: constant composition between 0 and C_{AA}^{max} determined by the optimizer, (2) ModiCon strategy: varying feed concentration with time within the single step.

In this study, we extend this conventional operating strategy of SMBR to ModiCon operation. The ModiCon operation was first proposed by Schramm et al. [72, 73] for the separation of binary mixtures. Unlike constant feed concentration strategy, in the ModiCon operation, the feed concentration is allowed to change within a step as shown in Figure 6.2. In this example, the desorbent is fed to the SMBR at the beginning while the feed mixture is fed at a high concentration later within the same step. Such modulation of inlet feed concentration can improve the process performance by overcoming the separation limitation of the internal concentration profiles inside the SMBR [71].

The goal of this study is to develop an SMBR process for the production of PMA, and demonstrate the potential of the ModiCon operation for improving the performance of the SMBR compared to the constant feed concentration strategy. A novel industrial application involving the esterification of acetic acid and PM is considered to produce PMA as the product. We use a transport dispersive model with a linear driving force for the adsorption rate for modeling the SMBR system. The model parameters are estimated from the batch and single column pulse-injection experiments by the inverse method. A multi-objective optimization study is presented

to find the best reactive separation strategy for the production of the PMA product. We also present a Pareto plot that compares the ModiCon operation and the constant feed concentration strategy for the optimal production rate of PMA that can be achieved against the desired conversion of acetic acid.

The organization of this chapter is as follows: Section 6.2 describes the SMBR operation and the operating strategies used in this study in detail. This section also explains the various control parameters available for each operating strategy while optimizing the performance of the SMBR. Section 6.3 discusses the mathematical model adopted for modeling of the SMBR system. Section 6.4 explains the multi-objective problem formulation used for optimizing the SMBR system and the solution strategy used for obtaining the optimum solution. Section 6.5 presents the experimental system used for pulse injection experiments. This experimental data has been used for obtaining the adsorption equilibrium and kinetics parameters in the SMBR model. Section 6.6 explains the methodology used for estimating the model parameters of the SMBR model. Section 6.7 presents results of the parameter estimation and the SMBR optimization. This section further discusses the optimal operating strategies and the Pareto plot of the multi-objective optimization problem. Section 6.8 concludes the chapter and presents the scope of future work.

6.2 Operating strategies for SMBR

The reactive chromatography process is based on the concept of integrating both separation and reaction inside a chromatographic column. In this process, the limiting reactant is injected as a sharp pulse into the column and then the excess reactant is supplied. The two components react inside the column forming products that are fractionated at the outlet of the column at different intervals of time. The weakly adsorbed component moves faster in comparison to the strongly adsorbed component.

This process is operated in a batchwise manner. SMBR, on the other hand, is a continuous reactive chromatography process. The SMBR unit, as shown in Figure 6.3, consists of multiple chromatographic columns that are interconnected in a cyclic conformation. The feed is a mixture of acetic acid (AA) and PM while the desorbent only consists of PM. Both feed and desorbent are supplied continuously and at the same time extract and raffinate streams are withdrawn through the outlet ports. The acetic acid reacts with PM under acid-catalyzed conditions forming PMA and water. As this esterification reaction proceeds inside the SMBR, both PMA and water are continuously removed thus shifting the equilibrium in the forward direction. Since PMA is the faster-moving component, it is recovered from the raffinate outlet while the strongly retained component, water, is recovered through the extract outlet.

The operating conditions of SMBR must be determined to achieve the desired performance. The two inlet streams, feed and desorbent, and two outlet streams, extract and raffinate, divide the entire SMBR system into four zones. The flow rate in each zone can be controlled independently, and hence there are four degrees of freedom; feed, desorbent, extract and zone I velocity. The zone velocities are in general selected such that zone II and III become the reaction plus separation zones while zone I and IV regenerates the columns [21]. Furthermore, the countercurrent motion of the solid phase is simulated by switching both inlet and outlet ports simultaneously in the direction of liquid flow. The two consecutive switching of the ports defines a step and the time for which this step lasts is also a degree of freedom. Four consecutive steps complete a full cycle and it brings the SMBR system back to its original configuration. This cyclic operation of SMBR is constantly repeated to extract pure PMA and water from the raffinate and extract outlets. The total degrees of freedom that affect the performance of SMBR are five. However, there could also be some extra degrees of freedom depending on the SMBR operating strategy. The operating strategies that are considered in this study are given below.

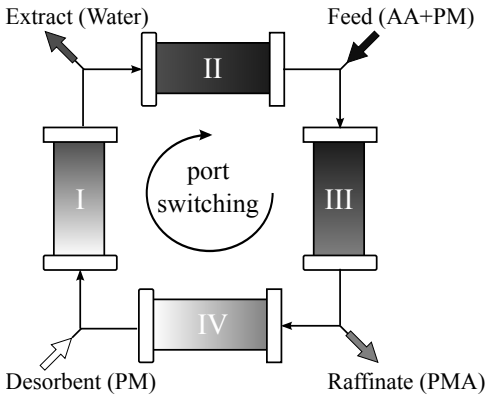

Figure 6.3: Schematic of simulated moving bed reactor unit for the production of PMA through the esterification reaction of acetic acid and PM.

6.2.1 Constant feed concentration strategy

The constant feed concentration strategy is a conventional way of operating the SMBR. In this operation, the feed concentration is kept constant during the entire step as shown in Figure 6.2. The feed composition – i.e. percentage of AA and PM – is however optimized during the SMBR optimization. Hence, the number of degrees of freedom that affect the performance of SMBR in this operating strategy is six; the optimized feed composition, switching time, and the velocities of the desorbent, feed, extract, and zone I.

It has been found that there exists the optimal feed concentration that is not necessarily 100% [45, 51]. A too high feed concentration would achieve low conversion, since the feed cannot be mixed with the desorbent effectively. In this study, we find the optimal feed concentration using the model and nonlinear optimization.

6.2.2 ModiCon strategy

The ModiCon strategy was first proposed by Schramm et al. [72, 73] for the separation of binary or multi-component mixtures by SMB chromatography. This advanced operating strategy allows periodical modulation of the feed concentration. It has been found that the productivity and specific solvent consumption can be improved from

the constant feed concentration strategy; in the ModiCon operation, the feed concentration can be manipulated in a time-varying manner so that the feed concentration has a sharp local peak, which is located away from the raffinate and extract outlets. Such a local increase of the feed mixture allows higher purity and recovery for the same productivity and solvent consumption.

In this study, we restrict the investigation to an operation where the feed concentration is changed only once in a step, as shown in Figure 6.2. The time interval (t_i) at which the inlet feed concentration changes is an extra degree of freedom. Hence, the number of degrees of freedom that affect the performance of SMBR in this operating strategy is eight; the two feed compositions in two different time intervals, intermediate time t_i, desorbent velocity, switching time, feed, extract and the velocity of zone I.

The ModiCon operation is more promising in terms of improving the PMA production rate compared to the standard SMBR operation because of its greater flexibility. The internal concentration profiles inside the SMBR can be manipulated by the modulation of the inlet feed concentration, which can improve the process performance. It should be noted that such an operation is not very difficult to implement; it can be implemented by using two pumps in parallel or by using a gradient based feed pump.

This study, to the best of our knowledge, implements the ModiCon strategy for the first time in reactive separation systems.

6.3 Mathematical model

We employ a transport dispersive model with the linear driving force for the adsorption rate (equations (6)-(15)), which is discussed in detail in Chapter 3. In this model, the axial dispersion phenomenon and diffusion into the adsorbent particles inside the columns are accounted separately using an overall axial dispersion coefficient and individual mass transfer coefficients for each component.

The reaction rate of esterification reaction is given by the second order model [63]. The net reaction rate is expressed as:

$$r^j(x,t) = k_1 \left(q^j_{AA}(x,t)\, q^j_{PM}(x,t) - \frac{1}{K_{eq}} q^j_{PMA}(x,t)\, q^j_{Water}(x,t) \right). \tag{55}$$

where k_1 is the forward reaction rate constant while K_{eq} is the equilibrium constant of the esterification reaction. The subscripts AA, PM, PMA and $Water$ refers to the acetic acid, PM, PMA and water component, respectively. It has to be noted that the reaction is assumed only in the solid phase, and hence equation (55) represents a heterogeneous catalyzed reaction.

6.4 Multi-objective optimization of the SMBR system

We formulate a multi-objective optimization problem to find the best design of the SMBR. The multiple objectives are to maximize the production rate of PMA in the raffinate outlet, maximize the conversion of esterification reaction and minimize the total PM consumption per unit weight of PMA formed. In addition, it is crucial to minimize the amount of water in the raffinate outlet because water forms an azeotrope with PMA in the downstream distillation. To deal with this difficulty, the water content in the raffinate outlet is enforced to be less than 1.0 wt%. Similarly, it is also desired to maximize the PMA recovered in the raffinate outlet. To satisfy this demand, the PMA recovery from the raffinate outlet is enforced to be more than 90 %.

6.4.1 Problem formulation

The overall optimization problem is as follows:

Maximizing PMA production rate (g/hr):

$$\max\, Pr = \frac{A_{cs}\, MW_{PMA}}{t_{step}} \sum_{j=1}^{N_{Column}} \int_0^{t_{step}} C^j_{PMA,R}(L,t)\, u^j_R(t)\, dt, \tag{56}$$

Maximizing conversion of acetic acid:

$$\max\, X = 1 - \frac{\sum_{j=1}^{N_{Column}} \int_0^{t_{step}} \left(C^j_{AA,R}(L,t)\, u^j_R(t) + C^j_{AA,Ex}(L,t)\, u^j_{Ex}(t) \right) dt}{\sum_{j=1}^{N_{Column}} \int_0^{t_{step}} C_{AA,F}\, u^j_F(t)\, dt}, \tag{57}$$

Minimizing total PM consumption per unit weight of PMA formed in the raffinate outlet (g-PM/g-PMA):

$$\min \Gamma = \frac{\sum_{j=1}^{N_{Column}} \int_0^{t_{step}} MW_{PM} \left(C_{PM,F}\, u_F^j(t) + C_{PM,D}\, u_D^j(t) \right) dt}{\sum_{j=1}^{N_{Column}} \int_0^{t_{step}} MW_{PMA} \left(C_{PMA,R}^j(L,t)\, u_R^j(t) \right) dt} \tag{58}$$

These objective functions are subject to the constraints as follows:

Equations (6)-(15),

Water content in the raffinate stream outlet (wt%):

$$Pur_{Water} = \frac{\sum_{j=1}^{N_{Column}} \int_0^{t_{step}} MW_{Water}\, u_R^j(t)\, C_{Water,R}^j(L,t)\, dt}{\sum_{i=1}^{N_{Comp}} \sum_{j=1}^{N_{Column}} \int_0^{t_{step}} MW_i\, u_R^j(t)\, C_{i,R}^j(t)\, dt} \leq 1\%, \tag{59}$$

PMA recovery in the raffinate stream outlet:

$$Rec_{PMA} = \frac{\sum_{j=1}^{N_{Column}} \int_0^{t_{step}} u_R^j(t)\, C_{PMA,R}^j(L,t)\, dt}{\sum_{j=1}^{N_{Column}} \int_0^{t_{step}} \left(u_R^j(t)\, C_{PMA,R}^j(L,t) + u_{Ex}^j(t)\, C_{PMA,Ex}^j(L,t) \right) dt} \geq 90\%, \tag{60}$$

Bounds on the zone flow rates:

$$u_L \leq u^j(t) \leq u_U. \tag{61}$$

where Pr, X and Γ are the objective functions, A_{cs} is the area of cross-section of the column and MW_i is the molecular weight of ith component and $C_{i,R}$ and $C_{i,Ex}$ are the concentrations of ith component in the raffinate and extract outlet, respectively. We also introduce lower and upper bounds on the zone velocities in equation (43) because of the restriction of maximum pressure drop that can be experienced by the pumps in the SMBR system. The symbols u_L and u_U refers to the lower and upper bounds and their corresponding values, in this study, are 0 m/min and 0.167 m/min, respectively.

6.4.2 Solution strategy

Solving the multi-objective optimization problem given in equations (6)-(15), (56)-(61) is a significant challenge. The solution is given as a surface in a three-dimensional

coordinate that consists of the three objective functions, equations (56)-(58). Since obtaining and analyzing solutions in the entire domain of the three-dimensional coordinate would be unrealistic, we consider limiting our analysis only in the region of practical interest.

In this study, we consider creating two two-dimensional projections of the three-dimensional Pareto surface: one projection where the PMA production rate Pr is plotted against the conversion X ignoring the PM consumption Γ, and another projection where Pr is plotted against Γ for a fixed conversion X. The first projection investigate the performance of the SMBR when the cost of PM (desorbent and excess reactant) is insignificant in the overall process economics. On the other hand, the second projection is for the case where the cost of PM consumption is substantial. These two projections can be obtained by solving the following two problems, which are based on the epsilon-constrained method [3, 29, 31]:

(I) Maximizing PMA production rate (g/hr):

$$\max\ Pr = \frac{A_{cs}\, MW_{PMA}}{t_{step}} \sum_{j=1}^{N_{Column}} \int_0^{t_{step}} C^j_{PMA,R}(L,t)\, u^j_R(t)\, dt,$$

subject to equations (6)-(15), (59)-(61),

The objective function corresponding to the conversion of acetic acid is implemented by using the epsilon-constrained method [3, 29, 31].

$$X \geq \epsilon_1. \tag{62}$$

By varying the value of ϵ_1 and solving problem (I) repeatedly, a Pareto plot of the optimal production rate of PMA against the conversion of acetic acid is obtained.

Next, the total PM consumption is minimized while implementing the other two objective functions as the epsilon constraints (equations (63) and (64)). The second problem is:

(II) Minimizing total PM consumption per unit weight of PMA formed in the raffinate outlet (g-PM/g-PMA):

$$\min \Gamma = \frac{\sum_{j=1}^{N_{Column}} \int_0^{t_{step}} MW_{PM} \left(C_{PM,F}\, u_F^j(t) + C_{PM,D}\, u_D^j(t) \right) dt}{\sum_{j=1}^{N_{Column}} \int_0^{t_{step}} MW_{PMA} \left(C_{PMA,R}^j(L,t)\, u_R^j(t) \right) dt}$$

subject to equations (6)-(15), (59)-(61),

The objective functions corresponding to the production rate of PMA and the conversion of acetic acid are implemented by using the epsilon-constrained method [3, 29, 31].

$$Pr \geq \epsilon_2, \tag{63}$$

$$X \geq \epsilon_3. \tag{64}$$

By varying the value of ϵ_2 and ϵ_3, and solving problem (II) repeatedly, a two-dimensional Pareto plot of the optimal PM consumption (per unit weight of PMA formed) against the production rate of PMA and the conversion of acetic acid is obtained. The values of ϵ_2 are decided based on the maximum production rate of PMA obtained from problem (I).

In this study, two projections of this three-dimensional Pareto plot are presented. The first projection investigates the trade-off between the maximum production rate of PMA against the conversion of acetic acid at the minimum PM consumption while the second projection investigates the trade-off between the production rate of PMA against the total PM consumption (per unit weight of PMA formed) at a fixed conversion.

The simultaneous approach has been used in this study to solve the system of equations for the multi-objective optimization problem [11, 30]. In this approach, both state and control profiles are fully discretized to transform the differential algebraic system to algebraic system of equations. The spatial domain is discretized using the central finite difference scheme in the second order, and the Radau collocation on finite elements is used for the temporal discretization. The spatial derivative at

the outlet of the column is discretized using three-point backward difference formula. The resulting optimization problem has been implemented into AMPL (A Mathematical Programming Language) modeling environment [18]. The advantage of using AMPL is that it supports nonlinear programming (NLP) and provides the automatic differentiation functionality, which can be used in many solvers. The resulting NLP problem is solved using an interior point solver IPOPT 3.0 [88]. Since interior-point methods can accept exact second order derivatives, they have fast convergence properties. Moreover, these solvers can exploit both structure and sparsity of the KKT (Karush- Kuhn-Tucker) system [11].

6.5 Experimental section

6.5.1 Materials

PM (1-methoxy-2-propanol, $> 99\%$) was purchased from Alfa Aesar while the acetic acid (99%) was purchased from BDH chemicals. All of chemicals were used without further purification. Sulfonated cation exchange resin, AMBERLYST^{TM} 15, was supplied from The Dow Chemical Company in a wet condition. This resin was dried at $338K$ for 12 hours and sieved before using.

6.5.2 Pulse-injection experiments

The schematic of a single column pulse-injection experiment is shown in Figure 6.4. We used a stainless steel column of an internal diameter of 0.8 cm and a length of 25 cm. The AMBERLYST^{TM} 15 cation exchange resin was swollen by keeping it in acetic acid and later used for packing the column using the slurry technique. A pulse of acetic acid and PM mixture was then injected in the column by using RH-7725i valve from Rheodyne and PM was fed as the desorbent. The PM was dehydrated using molecular sieves of type 3Å before feeding into the system. The outlet of the column was then fractionated using a fraction collector (Shimadzu, FRC-10a) and analyzed for the concentrations of acetic acid, PM, PMA and water

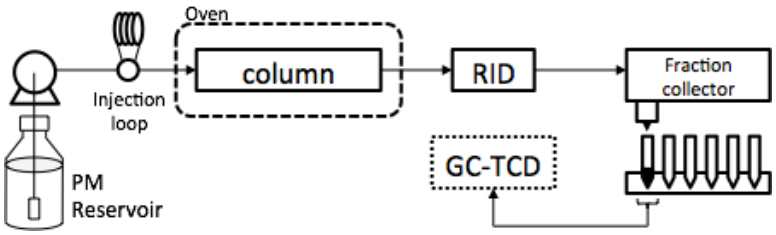

Figure 6.4: Schematic of a pulse-injection experiment.

using Gas Chromatography (GC) with a TCD detector. The TCD detector was essential for measuring the water concentration accurately below 5 vol%. When the esterification reaction was performed at the temperature higher than the boiling point of components at atmospheric pressure, a backpressure valve and an ice bath were installed right after the column to cool the effluent below the boiling point before it was exposed to atmospheric pressure. The total extra column volume was 0.343 ml.

6.5.3 Porosity estimation

The column porosity was estimated by injecting Dextran (Dextran 25000, Spectrum) as a tracer. Dextran is a high molecular weight substance that is unable to penetrate in the pores of AMBERLYST^{TM} 15. Since Dextran is not soluble in PM, the column was first saturated with water and then Dextran dissolved in water was injected into the system. The bed porosity was calculated to be 0.31 after subtracting the extra column volume from the retention time of Dextran. Although the bed porosity was calculated, this value can change in the actual system where PM, instead of water, is used as a mobile phase. To observe this change of porosity, we also calculated the swelling ratios of AMBERLYST^{TM} 15 in PM and water compared to the dry resin as shown in Table 5.1. The swelling ratio of PM is slightly lower than water thus, the actual bed porosity is expected to be slightly higher than 0.31. Therefore, we allow the porosity to change while estimating the model parameters in the Section 6.6.1.

Table 6.1: Experimental details

Parameter	Value
Column details	
Length (L)	0.25 m
Internal diameter (D)	0.008 m
Bed porosity (ϵ_b)	0.31[a]
Mobile phase	PM
Stationary phase	
Resin	AMBERLYST^{TM} 15
Particle size	$< 707\mu m$
Swelling ratios of AMBERLYST^{TM} 15 (compared to dry resin)	
PM	1.5
Water	1.55
Dead volume	0.343 ml

[a] the details are mentioned in Section 6.5.3.

6.6 Methodology for model parameters estimation

This section explains the methodology used for estimating the adsorption equilibrium, axial dispersion coefficient and kinetic parameters of the SMBR model. These model parameters are estimated by fitting the model to the multiple pulse-injection experiments (performed over a single column) simultaneously. The following subsections discuss this procedure in detail.

6.6.1 Fitting model to the pulse-injection experiments

In this study, the inverse method has been used for estimating the model parameters due to its simplicity [71]. In the inverse method, the simulated concentration profiles of the pulse-injection experiments are fitted to the experimental chromatograms while varying the values of model parameters. We use a simple least-square technique that minimizes the sum of the squares of the difference between the concentrations predicted by the model and the experimental observations. The objective function, Φ, is formulated as:

$$\Phi = \min_{H_i, K_{m,i}, D_{ax}, k_1, K_{eq}, e_b} \sum_{k=0}^{N_{exp}} \sum_{i=1}^{N_{Comp}} \sum_{l=1}^{N_{t,i}^k} \left(C_{i,l}^{k,mod} - C_{i,l}^{k,exp} \right)^2 + \rho \sum_{m=1}^{N_{reg}} \left(\theta_{reg,m}^{mod} - \theta_{reg,m}^{exp} \right). \quad (65)$$

where the subscript i and l refer to the components and the time points at which samples are collected while superscript k denotes the experimental index. The symbol N_{exp} refers to the total number of experiments considered, N_{comp} refers to the total number of components present in the system, $N_{t,i}^k$ refers to the total number of concentration data points considered for the ith component in the kth experiment, and N_{reg} is the number of regularization parameters discussed below. In the objective function, we also include Tikhonov regularization terms to prevent significant deviation of parameter values, which are estimated from separate experiments. The Tikhonov regularization is a standard approach to reduce the non-uniqueness of the estimated parameter set [82]. In this study, we include the equilibrium constant K_{eq} and bed porosity ϵ_b in θ_{reg}^{model}; i.e. $\theta_{reg}^{model} = [K_{eq}, \epsilon_b]^T$. The porosity ϵ_b was separately estimated from an experiment using dextran as described in Section 6.5.3, and the equilibrium constant K_{eq} was obtained in our previous study [63]. The coefficients of the regularization term, ρ is found by carrying over several trial-and-error runs and identifying the best compromise between the model fitting and the deviation of e_b

and K_{eq} values from the desired ones.

6.6.2 Implementation of single-column reactive chromatography model

Since the pulse-injection experiments are performed in a single column, the model equations (6)-(10) are used to simulate the pulse-injection experiment for a given set of model parameters. These modeling equations are implemented in MATLAB where the spatial domain is discretized using the central finite-difference scheme in the second order, and ode15s solver is used to integrate the system of ordinary differential equations. The parameter estimation problem is solved by using the *fmincon* optimizer in MATLAB with the interior-point algorithm.

6.7 Results and discussion

6.7.1 Parameter estimation

In this section, the model fitting results for the pulse-injection experiments are discussed. There are in total 12 model parameters; four Henry constants, four mass transfer coefficients, two reaction parameters, one axial dispersion coefficient and the bed porosity. These parameters were simultaneously estimated by fitting the single column model to two different pulse-injection experiments. The two pulse-injection experiments were performed by injecting a pulse of 50 $vol\%$ and 75 $vol\%$ acetic acid concentration in PM at $110°C$ with 5 ml injection loop and at 0.5 ml/min flow rate, respectively. Including two experimental chromatograms in equation (65) was expected to increase the reliability of the estimated parameter set ($N_{exp} = 2$).

Figure 6.5 shows the comparison of the elution profiles described by the fitted model and the experimental chromatograms. The concentration profiles of acetic acid, PMA and water are plotted on the left y-axis while PM concentration is shown on the right y-axis. The solid lines represent the predicted concentration profiles from the model and the markers represent the experimental data. As can be seen from the Figure 6.5, the model was able to fit the concentration profiles of all the components

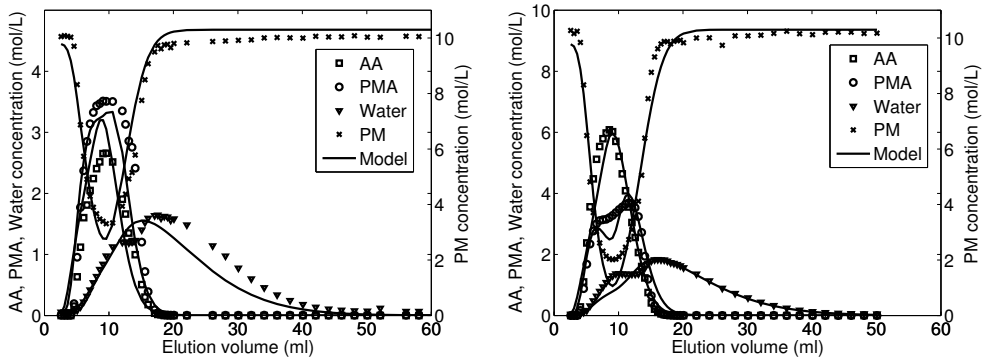

(a) Feed composition: 50-50 $vol\%$ AA and PM

(b) Feed composition: 75-25 $vol\%$ AA and PM

Figure 6.5: Model fitting results: comparison of the elution profiles predicted by the model and the experimental chromatograms obtained by injecting a pulse of acetic acid and PM at $110°C$, 5 ml injection and at 0.5 ml/min flow rate.

to a reasonable extent for both the experiments. The corresponding optimum model parameters values are summarized in Table 6.2. This parameter set is used for the multi-objective optimization study of the SMBR that is discussed in the next section.

As can be seen from Table 6.2, the values of all the estimated parameters were between their lower and upper bounds. This indicates that the optimized solution was not restricted by the bounds on the model parameters. Furthermore, the qualitative analysis of the model parameters can be performed by comparing their estimated values with the experimental observations. In our study, PMA was found to be almost a non-retained component, AA to be slightly retained while water as the strongly retained component. The Henry constant of AA, PMA and water in Table 6.2 are consistent with these observations.

The parameter values in Table 6.2 are also consistent with the results of other experiments carried out separately. The estimated value of equilibrium constant is close to its value obtained from the batch experiment, 0.86 [63]. Furthermore, the value of porosity ϵ_b is 0.334, which is slightly higher than the value measured in water, 0.310, as discussed in Section 6.5.3. Also, the value of the axial dispersion coefficient is in the same order with some of the esterification studies that are reported in the

Table 6.2: Optimized model parameters obtained by fitting the model to the pulse-injection experiments in Figure 6.5. The lower and upper bounds of the parameters that were imposed in the *fmincon* function are also listed.

Model parameters	Fitted value	Lower bound	Upper bound
H_{AA}	0.474	0	5
H_{PM}	0.226	0	5
H_{PMA}	0.001	0	5
H_{Water}	1.648	0	5
$K_{m,AA}$ (min^{-1})	0.350	0	5
$K_{m,PM}$ (min^{-1})	1.772	0	5
$K_{m,PMA}$ (min^{-1})	1.505	0	5
$K_{m,water}$ (min^{-1})	0.286	0	5
k_1 (L/mol.min)	0.195	0	100
K_{eq}	0.862	0.3	1.5
e_b	0.334	0.3	0.36
D_{ax} (m^2/min)	2.735×10^{-4}	0	50×10^{-4}

literature [79, 91]. From these observations, we believe that the parameter set shown in Table 6.2 is reasonable.

These model parameters, obtained by fitting 50 $vol\%$ and 75 $vol\%$ acetic acid pulse injections, were also validated with the elution profiles for the injection of 100 $vol\%$ acetic acid. The 100 $vol\%$ acetic acid injection experiment was also performed at $110°C$ with an injection loop of 5 ml and at the flow rate of 0.5 ml/min flow rate. The results are shown in Figure 6.6. As can be seen from the Figure, the model was able to predict the elution profiles of AA, PM and water very precisely. However,

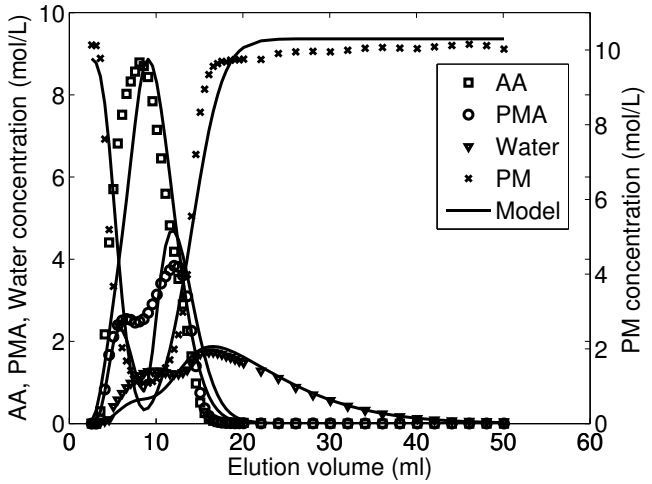

Figure 6.6: Comparison of the elution profiles predicted by the model and the experimental chromatogram obtained by injecting a pulse of 100% acetic acid at 110°C, 5 ml injection and at 0.5 ml/min flow rate.

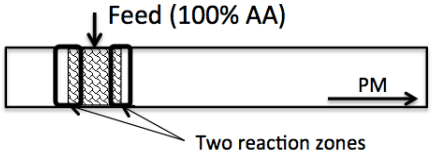

Figure 6.7: Schematic illustration of the formation of two reaction zones in the injection of 100% acetic acid.

there was some deviation observed in the PMA concentration profile, in particular, in the shoulder of PMA.

In our previous study [63], we concluded that the shoulder of the product peak was caused by the formation of two reaction zones of the pulse, as shown in Figure 6.7. When 100% acetic acid is injected, the leading and trailing boundaries between the desorbent PM and acetic acid are formed. As the pulse of acetic acid proceeds towards the end of the column, the reaction proceeds, which leads to the shoulder of the peak of the product, PMA. Thus the concentration profile of PMA may be described by the complex interplaying dynamics of axial dispersion and reaction rate, which cannot be modeled easily in our study.

Furthermore, there is also some noticeable mismatch in the water concentration profile shown in Figure 6.6. It appears that the amount of water formed in the experiments is higher than the reacted amount of acetic acid. Thus there could be a side reaction taking place. Since the pulse-injection experiments are performed at a high temperature ($110°C$), some of the dehydration reactions may have occurred leading to the additional formation of water apart from the esterification reaction. Unfortunately, we were unable to identify the potential byproducts and quantify the reaction kinetics for such a side reaction.

Besides the complex dynamics of reactive chromatography and the possibility of side reactions, there could also be some other factors that are contributing towards the model mismatch. For example, the shape of the acetic acid pulse that is injected in the column may not have been completely rectangular. In addition, there could also be viscous fingering effects resulting from the difference in the viscosity of acetic acid and PM, which are 1.22 cP and 1.7 cP at $25°C$, respectively. It has been shown in literature that such a phenomena can alter the elution profiles inside the chromatographic columns [13, 14]. Furthermore, the reaction system of acetic acid and PM might be non-ideal at high concentration of acetic acid. Thus introducing activity coefficients in the rate expression (equation (55)) may improve the model predictions in Figure 6.6 [65].

In the design of SMBR in this study, we avoid injection of 100% acetic acid, and consider concentration of acetic acid only up to 75 $vol\%$ due to the following reasons: First, as described above, modeling of the reaction zones is very difficult, leading to the model mismatch. Second, we envision using the SMBR in a comprehensive flowsheet that includes downstream processing of products with recycle. In such a flowsheet, the outlet from the SMBR unit is supplied to downstream separation units, which separate unreacted acetic acid. The unreacted acetic acid and PM recovered by such units are recycled back to the feed inlet of SMBR. In such a situation, the

Table 6.3: SMBR system details

Parameter	Value
N_{Comp}	4
N_{Column}	4
Configuration	1-1-1-1
Column length (L)	0.5 m
Internal diameter (D)	0.015 m
u_L	0 m/h
u_U	10 m/h

acetic acid may be diluted with the recycled PM.

6.7.2 SMBR optimization

The results of the SMBR optimization are presented in this section. The specification of the SMBR columns is given in Table 6.3. The multi-objective optimization problem of the SMBR that has been discussed in Section 6.4 is implemented in the AMPL modeling environment and solved using the IPOPT solver. The multiple objectives are to maximize the production rate of PMA in the raffinate outlet, maximize the conversion of acetic acid and minimize the total PM consumption per gms of PMA produced. In this study, two two-dimensional projections of this Pareto plot are presented as discussed in Section 6.4.2. The first projection investigates the trade-off between the maximum production rate of PMA against the conversion of acetic acid at the minimum PM consumption while the second projection investigates the trade-off between the production rate of PMA against the total PM consumption (per unit weight of PMA formed) at a fixed conversion.

The first projection that investigates the trade-off between the PMA production rate against the conversion of acetic acid is shown in Figure 6.8 for both constant

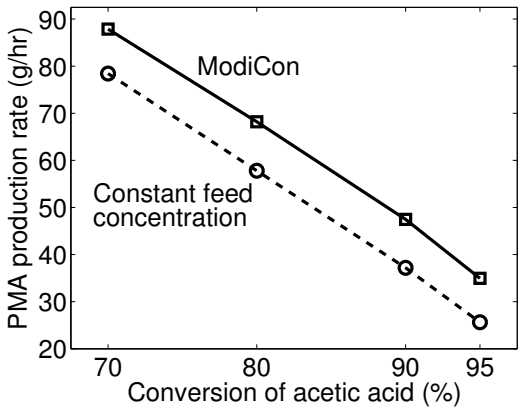

Figure 6.8: Pareto plot of the multi-objective SMBR optimization problem: PMA produced through the raffinate outlet in g/hr against the percentage conversion of acetic acid.

feed concentration and the ModiCon strategy. As can be seen from this figure, the production rate of PMA through the raffinate outlet decreases with increase in the conversion of acetic acid. Thus the higher conversion of acetic acid is not favorable to high production rates of PMA. This observation has been explained later while discussing the internal concentration profiles of the SMBR in this study. The improvement in the production rate of ModiCon over the conventional operation is nearly constant over the range of conversion considered in this study, and thus the relative improvement becomes more significant when the conversion is high. Therefore, the ModiCon operation has significant potential to improve the process performance of the SMBR.

In addition to the Pareto plot, the amount of PMA recovered and the water content (wt%) in the raffinate stream outlet are also compared with the required process specifications of the SMBR. As can be seen from Figure 9(a), the PMA recovery was always an active constraint at the optimal solution for the constant feed concentration strategy. However, such is not the case with the ModiCon operation. In the ModiCon strategy, the PMA recovery obtained was higher than 90% and its value increased with increase in the conversion of acetic acid. Thus, the ModiCon

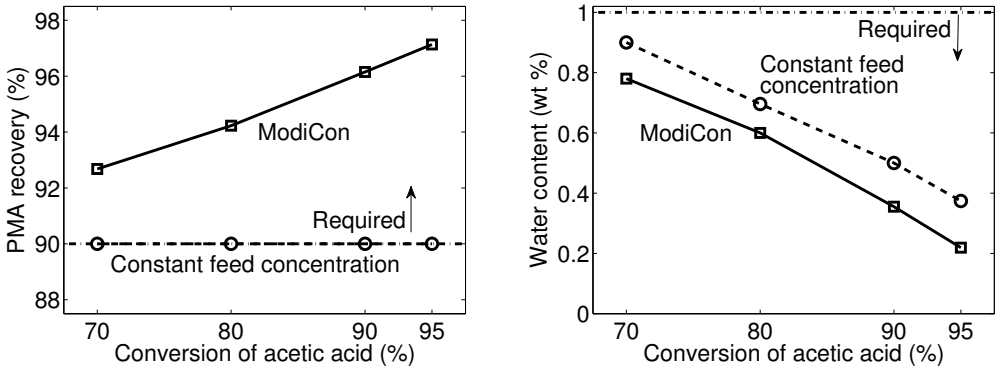

(a) PMA recovery in the raffinate outlet (b) Water content in the raffinate outlet

Figure 6.9: The optimum PMA recovery and the water content in the raffinate stream outlet compared to the required SMBR process specifications for both constant feed concentration and the ModiCon strategy.

operation is more advantageous to obtain high recovery of PMA through the raffinate outlet.

The amount of water in the raffinate stream outlet is also crucial because of the azeotrope formation between PMA and water during the downstream distillation. This water content in the raffinate stream outlet is shown in Figure 9(b), which does not become the bottleneck for achieving a high conversion. This constraint was not active for both of the operating strategies. This indicates that the water content was always below 1 $wt\%$ thus fulfilling the required process specifications across the whole operating range. Since the ModiCon operation leads to lower concentration of water compared to the constant feed concentration strategy, it is also favorable for reducing the downstream cost.

We analyze the optimal inlet feed concentration profiles obtained by optimizing both the operating strategies, where the inlet feed composition was allowed to change between 0-75% of acetic acid. The optimum feed concentration profiles for a single step are shown in Figure 6.10 for 70%, 80%, 90% and 95% conversion of acetic acid. In addition, the optimum feed concentrations values for both the operating strategies are also listed in Table 6.4. It is to be noted that these feed concentration profiles

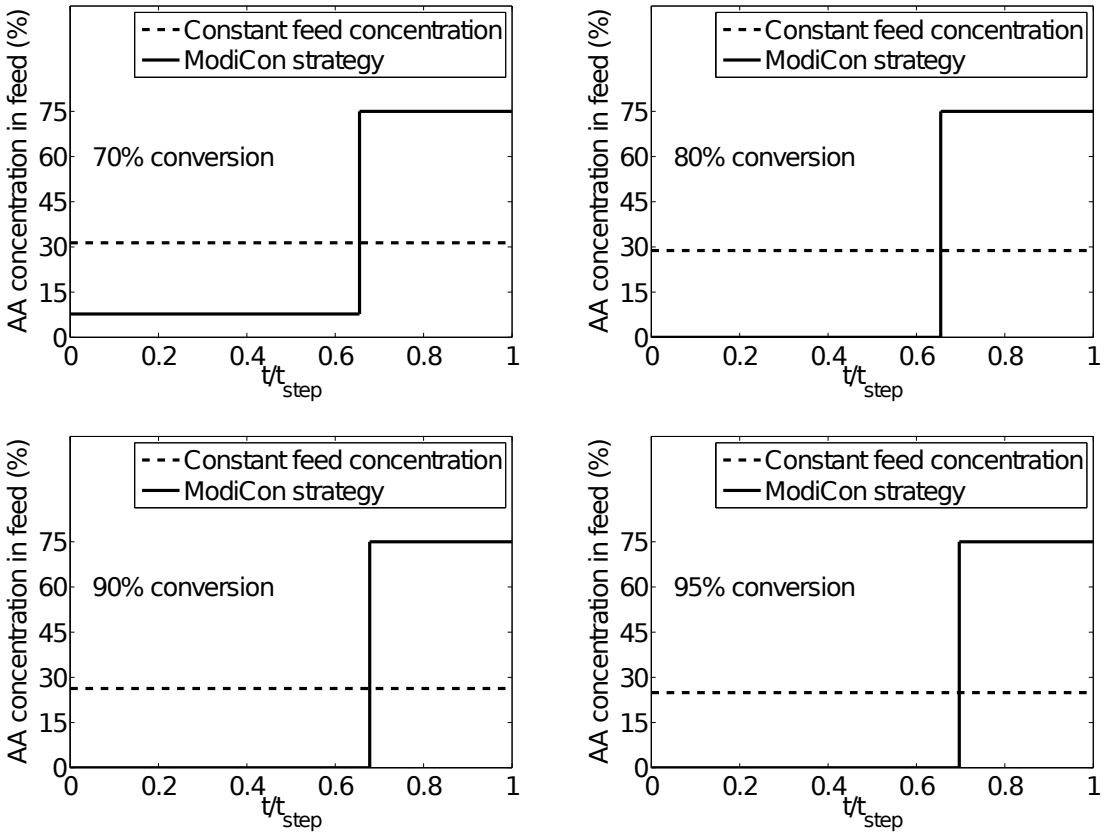

Figure 6.10: Optimum inlet feed concentration profiles within a single step for 70%, 80%, 90% and 95% conversion of acetic acid.

Table 6.4: Optimized inlet feed concentration values for the constant feed concentration and the ModiCon strategy.

Conversion of acetic acid (%)	Inlet feed concentration	
	Constant feed concentration strategy	ModiCon strategy
70	31.4% AA for $[0, t_{step}]$	7.7% AA for $[0, 0.66\,t_{step}]$ 75% AA for $[0.66\,t_{step}, t_{step}]$
80	28.8% AA for $[0, t_{step}]$	0% AA for $[0, 0.66\,t_{step}]$ 75% AA for $[0.66\,t_{step}, t_{step}]$
90	26.3% AA for $[0, t_{step}]$	0% AA for $[0, 0.68\,t_{step}]$ 75% AA for $[0.68\,t_{step}, t_{step}]$
95	24.9% AA for $[0, t_{step}]$	0% AA for $[0, 0.70\,t_{step}]$ 75% AA for $[0.70\,t_{step}, t_{step}]$

are obtained at the cyclic steady state. Hence, the end of the previous step precedes the steps shown in Figure 6.10. As can be seen from Table 6.4, the optimized feed concentration, in the constant feed concentration strategy, changes from 31.5% to 24.9% acetic acid while increasing the conversion of acetic acid from 70% to 95%. On the other hand, the optimal ModiCon strategy is very similar in all the scenarios. In the ModiCon strategy, either the PM or acetic acid at low concentration is fed at the beginning and then the feed composition is switched to 75% acetic acid, the highest concentration allowed in this optimization study. These optimum feed concentration profiles can be explained from the internal concentration profiles and the reaction rates inside the SMBR.

Figure 6.11 shows the snapshot of internal concentration profiles and the net reaction rate $r^j(x,t)$ for both constant feed concentration and the ModiCon strategies. These concentration profiles are plotted slightly after the beginning of the step ($t/t_{step} = 0.086$) at the cyclic steady state for 70% conversion of acetic acid. Thus, if the feed mixture fed at the inlet of zone III has a higher concentration compared to the outlet of zone II, we observe a sudden rise in the AA and PM concentration and corresponding drop in the PMA and water concentration at the intersection of zone II and zone III.

We analyze the reaction rates in the SMBR. As expected, in both operating strategies the net reaction rate inside the SMBR is the highest in zone II, where the acetic acid reacts with PM to form PMA and water. The strongly retained component water can be recovered from the extract outlet while the faster moving component PMA is sent to zone III, and finally recovered from the raffinate outlet.

In Figure 6.11, there are notable differences in the concentration profiles of these two different operating strategies. In particular, the concentration profile of acetic acid is significantly different; in the ModiCon strategy, the concentration of acetic acid has a significantly sharper peak in zone II. This increase in the acetic acid

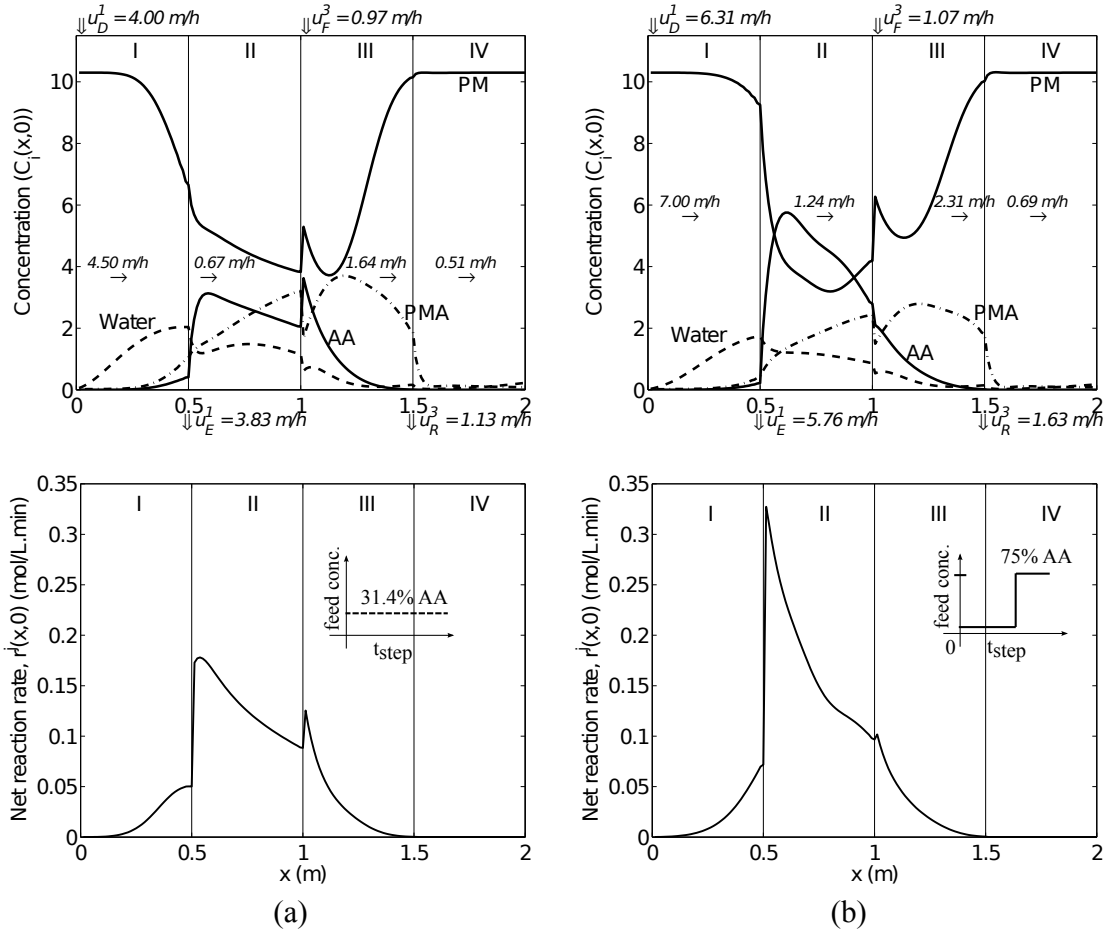

Figure 6.11: Internal concentration profiles and the net reaction rate inside the SMBR slightly after the beginning of the step ($t/t_{step} = 0.086$), for 70% conversion of acetic acid: (a) Constant feed concentration strategy, (b) ModiCon strategy.

concentration in zone II in ModiCon leads to a higher net reaction rate, while the net reaction rate in the constant feed concentration strategy has a relatively flat profile that spreads both in zones II and III.

It is to be noted that the optimal ModiCon operating strategy increases the net reaction rate in zone II only locally by modulating the feed concentration. As can be seen in Figure 6.10, at the beginning of a step, the concentration of acetic acid in the feed is zero, which prevents an increase in the net reaction rate in zone III. After all components moves downstream, the concentration of acetic acid in the feed increases. This modulation of the feed concentration allows a local increase of acetic

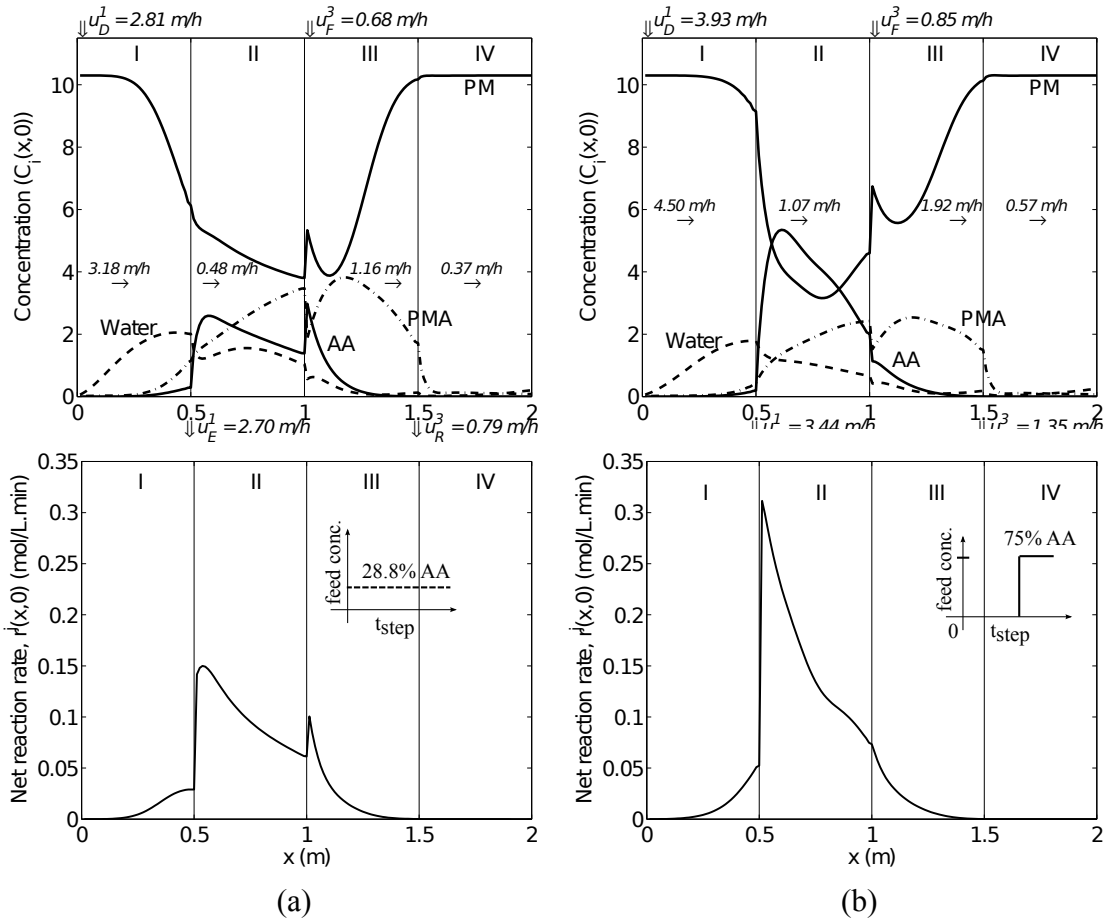

Figure 6.12: Internal concentration profiles and the net reaction rate inside the SMBR slightly after the beginning of the step ($t/t_{step} = 0.086$), for 80% conversion of acetic acid: (a) Constant feed concentration strategy, (b) ModiCon strategy.

acid concentration, which increases the net reaction rate only locally in zone II. Such a local increase of the reaction rate allows higher purity and recovery of the products when the production rate of PMA is increased at the same time.

In the ModiCon operation, the higher recovery of PMA in Figure 9(a) and smaller water content in raffinate shown in Figure 9(b) can be explained by analyzing the internal concentration profiles. Note that in the ModiCon strategy, the concentration of acetic acid in zone III is significantly lower compared to the constant feed concentration strategy. This indicates that zone III mainly functions as a separation zone while in the constant feed concentration strategy, zone III performs both reaction and separation simultaneously. Since the PMA product is isolated in the ModiCon

operation in zone III, it can be recovered with a higher flow rate in the raffinate oulet as shown in Figure 6.11. Therefore, ModiCon operation is more favorable to high recovery of PMA (see Figure 9(a)). Similarly, since the reaction is not significant in zone III of the SMBR in the ModiCon strategy, it leads to less water formation in this zone. As a consequence, the water content in the raffinate outlet also reduces as seen in Figure 9(b).

The reduction in production rate of PMA with increase in the conversion of acetic acid can also be explained from the internal concentration profiles inside the SMBR. Figure 6.11 and 6.12 show the internal concentration profiles and the net reaction rate for 70% and 80% conversion of acetic acid, respectively. The concentration profiles and the net reaction rates are similar in both figures. However the flow rates of all the inlet and outlet streams reduce for 80% conversion of acetic acid, as can be seen in Figure 6.11 and 6.12. The higher conversion in the SMBR system requires a longer residence time in the system. Consequently, the raffinate flow rate decreases and this in turn reduces the production rate of PMA.

The second projection of the Pareto plot that investigates the trade-off between the production rate of PMA against the total PM consumption (per unit weight of PMA formed in the raffinate outlet) is shown in Figure 6.13. This projection was obtained at 80% conversion of the acetic acid. As can be seen from this figure, for the same total PM consumption per unit weight of PMA formed, the ModiCon strategy achieves around 14-18% higher production rate of PMA compared to the constant feed concentration strategy. This indicates that the ModiCon operation is more efficient in utilizing the desorbent fed into the SMBR.

It should be noted that the total PM consumption include the amount of PM fed through both feed and desorbent inlets. Thus, PM is not only acting as a desorbent but also functioning as a reactant. Therefore, the amount of PM consumption is utilized in both regenerating the columns as well as in the formation of the products.

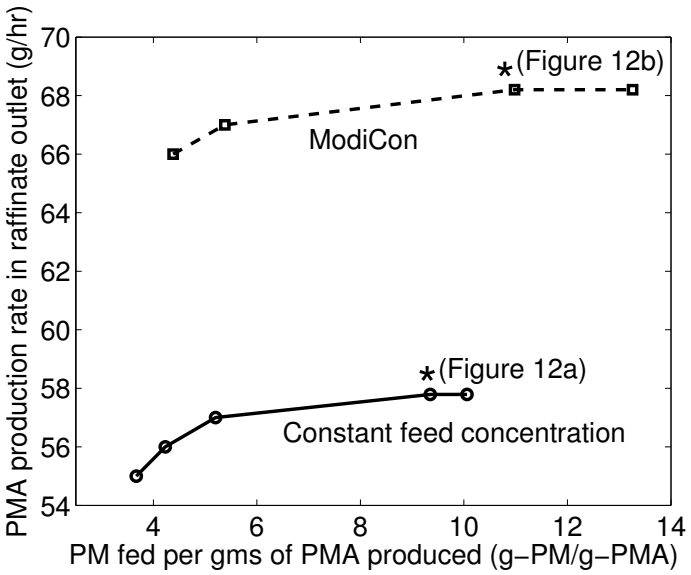

Figure 6.13: Pareto plot of the multi-objective SMBR optimization problem: PMA produced through the raffinate outlet in g/hr against the ratio of total amount of PM fed into the SMBR to the amount of PMA produced in raffinate outlet (g-PM/g-PMA) at 80% conversion of acetic acid. The points marked with an asterisk (∗) correspond to Figure 6.12.

6.8 Conclusions

In this work, a novel industrial application of SMBR for production of PMA by esterification of acetic acid and PM is developed. The SMBR system is modeled using a transport dispersive model with a linear driving force (LDF) for the adsorption rate, and the adsorption equilibrium and kinetic parameters are estimated simultaneously by fitting the single column model to the multiple pulse-injection experiments. The LDF model with axial dispersion fits the experimental chromatogram relatively well, while some mismatch is observed when the feed concentration is very high.

To design a SMBR process, a multi-objective optimization problem is formulated that investigates the trade-off between the production rate of PMA, the conversion of esterification reaction and the total PM consumption. The process specification constraints such as PMA recovery and water content in the raffinate stream outlet are also enforced in the optimization.

Two projections of the Pareto plot of the multi-objective optimization problem comparing the constant feed concentration strategy and the ModiCon strategy are presented. The production rate of PMA through the raffinate stream outlet decreases with increase in the conversion of acetic acid for both the operating strategies. Thus the higher conversion of acetic acid is not favorable to high production rates of PMA. In addition, it has been found that ModiCon operation is more advantageous to obtain high recovery of PMA through the raffinate outlet and also for reducing the downstream separation cost compared to the constant feed concentration strategy. Also, the ModiCon operation achieves higher production rate of PMA for the same amount of total PM consumed per unit weight of PMA formed. From these observations, we conclude that the ModiCon operation has significant potential to improve the process performance of the SMBR.

The ModiCon operation is based on the periodic modulation of feed concentration. It has been found that by manipulating the feed concentration in a time-varying manner, the feed concentration has a sharp local peak in zone II. Such a local increase of the feed concentration increases the net reaction rate locally and thus allows higher purity and recovery while increasing the production rate at the same time.

The next chapter concludes the entire thesis and presents the scope of future work.

CHAPTER VII

CONCLUSIONS AND FUTURE WORK

7.1 Conclusions

The results presented in this thesis have met the three main objectives stated in Chapter 2:

1. Identify the best separation strategy for the separation of a ternary mixture among various alternative designs of SMB

2. Experimentally validate both JO and Generalized Full Cycle operations for separation of sugars

3. Develop an SMBR process for industrial-scale production of propylene glycol ethers

The first objective is discussed in detail in Chapter 4, where various existing SMB separation strategies, that exist for the separation of a ternary mixture, are compared in terms of the optimal productivity obtained and the amount of solvent consumed. In addition, the concept of optimizing a superstructure formulation is proposed, where numerous SMB configurations can be incorporated into a single formulation. In the superstructure approach, the optimizer extracts the best design that maximizes the productivity of the SMB process while meeting all the product specifications at the same time. Based on this concept of superstructure optimization, in this study, the Generalized Full Cycle formulation (GFC) and the full superstructure formulation are presented. These existing as well as the proposed operating schemes are classified into three categories: modified conventional Four-zone SMB systems, cascade systems and full cycle modified SMB systems. In our case study, the full-cycle modification,

which includes the JO, GFC and the full superstructure operations, has been found to be the most effective approach to achieve the separation of a ternary mixture using SMB. In addition, the GFC operation has shown the best performance as it improves the productivity of the SMB process significantly without consuming much amount of desorbent. Further, the JO process is found to be the best operating scheme among all the existing operations. Also, the Eight-zone SMB operating scheme performs better than the SMB cascade, both in terms of the performance and in terms of the amount of desorbent consumed. Hence, it is concluded that the dynamics in the internal recycle line are very important in separating a ternary mixture. Furthermore, Five-zone and Four-zone operating schemes are identified as less productive operations if higher purity of intermediate component is desired.

The GFC and full superstructure formulations are based on a systematic framework that identifies the best ternary separation strategy based on the required process and the product specifications. Thus, these operations have significant potential for improving the productivity of SMB processes. The technologies developed using this approach could be applied in a number of pharmaceutical applications and also in the separation of sugars.

The second objective is discussed in detail in Chapter 5, which is to demonstrate the GFC operation experimentally and compare its performance to the JO process. A Semba Octave^{TM} chromatography system is used as an experimental SMB unit for implementing the optimal operations and the separation of sugars is chosen as the chromatographic system for the validation of operating strategies. When the optimal operating conditions obtained from the model optimization are implemented on the experimental unit, a model mismatch is observed in the products purity and recovery values. To resolve this model mismatch, a simultaneous optimization and model correction (SOMC) scheme has been implemented. The advantage of using the SOMC scheme is that it is a systematic approach to arrive at the model parameters

that predict the experimental conditions. In addition, we do not have to rely on the careful descriptions such as extra-column dead volumes that exist in the actual SMB unit or the effects of the flow rates on the mass transfer inside the columns. We can even start with a rudimentary set of model parameters and obtain the converged set of parameters by fitting the SMB model to the experimental data. In our case study, the converged set of model parameters obtained from the SOMC scheme were able to predict the experimental conditions sufficiently accurately in the range of glucose purity from 75% to 90%. This observation demonstrates the efficacy of the SOMC scheme.

We also present a systematic comparison of both JO and GFC processes by constructing a Pareto front of the productivity obtained from the SMB operation against the glucose purity desired in the intermediate stream outlet experimentally. The GFC formulation is shown to be an efficient approach for finding the best ternary separation strategy for the separation of sugars. The productivity obtained from the GFC process is significantly higher (around 40-50%) compared to the JO process.

It is to be noted that both JO and GFC operations are easily implementable on most of the SMB systems with only minor modifications in the hardware. For the SMB systems equipped with rotary valves, we may require one or more than one additional binary valves in order to break the flow circuits. Such a minor modification would not increase the capital cost of the equipment significantly.

The third objective is discussed in detail in Chapter 6, where an SMBR process is developed for the industrial-scale production of propylene glycol ether. The esterification of acetic acid with 1-methoxy-2-propanol (PM) is considered to produce propylene glycol methyl ether acetate (PMA) as the product. The SMBR system is modeled using a transport dispersive model with a linear driving force (LDF) for the adsorption rate, and the adsorption equilibrium and kinetic parameters are estimated

simultaneously by fitting the single column model to the multiple pulse-injection experiments. The LDF model with axial dispersion fits the experimental chromatogram relatively well, while some mismatch is observed when the feed concentration is very high.

To design an SMBR process, a multi-objective optimization problem is formulated that investigates the trade-off between the production rate of PMA, the conversion of esterification reaction and the total PM consumption. The solutions of this multi-objective optimization problem result in a three-dimensional Pareto front of the optimal PM consumption against the production rate of PMA and the conversion of acetic acid. In this study, two projections of this Pareto plot are presented that compares the ModiCon strategy, which allows periodical change of the feed composition and the constant feed concentration strategy. Based on the plots, the production rate of PMA through the raffinate stream outlet decreases with increase in the conversion of acetic acid for both the operating strategies. Thus the higher conversion of acetic acid is not favorable to high production rates of PMA. In addition, it has been found that ModiCon operation is more advantageous to obtain high recovery of PMA through the raffinate outlet and also for reducing the downstream separation cost compared to the constant feed concentration strategy. Also, the ModiCon operation achieves higher production rate of PMA for the same amount of total PM consumed per unit weight of PMA formed. From these observations, we conclude that the ModiCon operation has significant potential to improve the process performance of the SMBR.

The ModiCon operation is based on the periodic modulation of feed concentration. It has been found that by changing the feed concentration in a time-varying manner, the internal concentrations in the columns can be manipulated so that the feed concentration has a sharp local peak in zone II. Such a local increase of the feed concentration increases the net reaction rate locally and thus allows higher purity and recovery while increasing the production rate at the same time. This work, to the

best of our knowledge, implements the ModiCon strategy for the first time in reactive separation systems.

All contributions in this work shows that the model-based optimization techniques can be successfully applied in practice to make systematic decisions that optimize the performance of both SMB and the SMBR systems. In addition, such techniques can also identify novel operating strategies that improve the performance of SMB/SMBR systems significantly compared to the existing operations. Finally, this work also leads to some recommendations that could be followed up in future. The future work is discussed in the next section.

7.2 Future Work

After surveying the work done in this thesis, there are some recommendations for future research projects.

7.2.1 Extension of multi-component separation study to non-isocratic operations

In this study, only the isocratic operations are considered while comparing the various SMB operating schemes and also for finding the best separation strategy for the separation of a ternary mixture. However, a few non-isocratic SMB methods are also developed in past as discussed by Aumann et al. [5] and Wang et al. [90]. In these operations, the concentration of mobile phase is allowed to change thus introducing a solvent gradient inside the SMB system. These operations are specially useful in the purification of biomolecules such as monoclonal antibodies and polypeptides, where the adsorption strength is a function of the solvent concentration. In future, these gradient-based operations can also be optimized to explore the potential of SMB for the proteins purification.

7.2.2 Extension of experimental validation study to systems with nonlinear isotherms

In our study, both JO and GFC operating strategies are experimentally verified for the system of sugars separation. The isotherm equations, that represent the thermodynamic equilibrium between liquid and solid phase, were linear in this study due to the relatively low concentrations of sugars in the feed inlet. However, there exist several chromatographic systems that exhibit nonlinear equilibria. The nonlinearity in the system arises when the chromatographic system is overloaded either in terms of concentration or volume compared to the exchange capacity of the resin. As a result, the equilibrium between the liquid and solid phases can be no longer represented by a linear equation; and a nonlinear representation is necessary such as Langmuir, bi-Langmuir or competitive Langmuir isotherms. A recent study has validated the standard SMB systems experimentally using the Langmuir type isotherms and a predictor-corrector algorithm [9]. However, it was only pursued for the separation of a binary mixture. This work can be further extended for the separation of multi-component mixtures.

The SOMC scheme might also need to be modified to implement it for nonlinear systems. In this study (Chapter 5, Step 3 of SOMC scheme), we have used a sampling strategy that waits for the SMB system to reach the cyclic steady state and then the product outlets are collected for one full cycle. It is to be noted that such a simplified steady-state sampling strategy works for the linear systems, while it might not be sufficient for a more complex system. For instance, highly non-linear systems can show a strong correlation between the mass transfer coefficients and parameters representing nonlinearity [9]. In that situation, we require a large number of data points to obtain a reliable set of model parameters. Such a requirement can be satisfied by collecting the transient concentration data. In such a sampling strategy, the SMB product outlets are collected into a container from which the samples are

analyzed at regular intervals of time [9].

7.2.3 Experimental validation of ModiCon strategy

In this study, it has been shown that the ModiCon strategy has significant potential to improve the process performance of the SMBR compared to the conventional SMBR operating strategy. In future, this ModiCon operation will be demonstrated experimentally by using a preparative scale SMB unit. The mathematical model developed in this study will be used along with the SOMC scheme to obtain the model parameters that predict the experimental conditions.

In addition to the esterification reaction, another route is being pursued in our lab for the production of the PMA product. This new pathway involves the transesterification reaction of ethyl acetate with PM that produces the desired product, PMA, and a byproduct, ethanol. Since there are no acids present in the reactant, only the reaction with the heterogeneous catalysis is presumed to occur during transesterification. In future, the ModiCon operation will also be implemented for producing PMA via transesterification reaction.

7.2.4 Extension of SMBR to advance operations

The SMBR operation, shown in Figure 6.3, can be further extended to some of the advance operating strategies that are discussed below.

7.2.4.1 ModiCon strategy

In this study, we restricted our investigations to a ModiCon strategy where only one change of the feed concentration per step was allowed. Obviously, more frequent changes can be allowed, which may have the potential to improve the performance further. Furthermore, linear increase or decrease in the feed concentration can be implemented easily by employing a gradient pump. Such refinements of the ModiCon strategy will be studied in our future work.

7.2.4.2 PartialFeed strategy

In this study, from the optimal solutions of the GFC and full superstructure formulations, it has been found that feeding the feed solution continuously may not be advantageous all the time. From a similar observation, a modified feeding strategy is proposed by others [93]. In this strategy, the feed flow rate is varied within a single step while keeping the feed concentration constant. Since the inlet feed mixture is fed partially in the SMBR, this operation is referred as 'PartialFeed' [93]. The number of independent parameters in the PartialFeed strategy are the optimized feed composition, feed flow rates in different time intervals, switching time, desorbent, extract and the zone 1 velocity.

7.2.4.3 ModiCon plus PartialFeed strategy

The SMBR operation can be further extended to a situation where the feed concentration is also allowed to change along with the feed flow rate in a single step. Such an operation would be combination of both the PartialFeed and the ModiCon strategy. This operation may be more advantageous compared to both ModiCon and PartialFeed operations individually. The number of independent parameters in this strategy are the feed compositions and the feed velocities in different time intervals, switching time, desorbent, extract and the zone 1 velocity.

7.2.4.4 Generalized Full Cycle and Full Superstructure formulations

The concept of optimizing a superstructure formulation can also be extended to SMBR systems. In the superstructure approach, numerous SMBR configurations can be incorporated into a single formulation and the optimizer extracts the best design that optimizes the SMBR process while meeting all the process and product specifications at the same time. The number of independent parameters in these strategies can vary depending on the number of switching allowed within a cycle [43].

7.2.5 Refinement of the SMBR model

Although the mathematical model developed in this study describes the experimental chromatograms relatively well, further improvements can be expected. The reaction system of acetic acid and PM might be non-ideal at high concentration of acetic acid. Thus the reaction kinetics may need to be modeled considering the non-ideal activities. Furthermore, at a very high temperature, there is a possibility of some dehydration reactions occurring as the side reactions to the esterification reaction. Quantifying the reaction kinetics for such side reactions may also improve the mathematical model. In addition, the injection of the feed should be performed carefully to maintain a rectangular pulse, while suppressing the viscous fingering.

APPENDIX A

NOTATION

A_{cs}	cross-sectional area of column, m^2
C	liquid phase concentration, mol/L
D_{ax}	axial dispersion coefficient, m^2/min
H	Henry constant
K_m	solid phase based mass transfer coefficient, min^{-1}
k_1	reaction rate constant, L/(mol min)
K_{eq}	reaction equilibrium constant
L	column length, m
MW	molecular weight, g/mol
N_{Comp}	number of components
N_{Column}	number of columns
N_{exp}	number of experiments
N_t	number of concentration data points
N_{reg}	number of regularization parameters
Pr	production rate of PMA through the raffinate outlet, g/hr
Pr^{opt}	optimal production rate of PMA, g/hr
Pur_{Water}	water content in raffinate stream outlet, wt%
q	solid phase concentration, mol/L
q^{eq}	solid phase equilibrium concentration, mol/L
r	net reaction rate, mol/(L min)

Rec_{PMA}	PMA recovery in raffinate stream outlet, %
t	time, min
t_{step}	step time, min
u	superficial liquid velocity, m/min
u_F	feed velocity, m/min
u_D	desorbent velocity, m/min
u_R	raffinate velocity, m/min
u_{Ex}	extract velocity, m/min
u_L	lower bound on zone velocity, m/min
u_U	upper bound on zone velocity, m/min
x	axial distance, m
X	conversion of acetic acid

Greek letters

ϵ_b	bed porosity
ν	stoichiometric coefficient
Γ	total PM consumption per gms of PMA produced, g/g
Φ	objective function of the parameter estimation problem
θ_{reg}	regularization parameter
ρ	regularization coefficient

Superscripts

j	jth column
k	kth experiment
mod	model
exp	experiment

Subscripts

i	ith component
l	time points
AA	acetic acid
PM	DOWANOL^{TM} PM glycol ether
PMA	DOWANOL^{TM} PMA glycol ether
$Water$	water
F	feed
D	desorbent
R	raffinate
Ex	extract

REFERENCES

[1] *The Dow Chemical Company, Product Safety Assessment: Propylene Glycol Methyl Ether Acetate*, 2008.

[2] Agrawal, G. and Kawajiri, Y., "Optimization of ternary simulated moving bed separation by superstructure formulation," in *Foundations of Computer-Aided Process Operations (FOCAPO)*, (Savannah, GA, USA), 2011.

[3] Agrawal, G. and Kawajiri, Y., "Comparison of various ternary simulated moving bed separation schemes by multi-objective optimization," *J. Chromatogr. A*, vol. 1238, pp. 105–113, 2012.

[4] Agrawal, G., Sreedhar, B., and Kawajiri, Y., "Systematic optimization and experimental validation of simulated moving bed chromatography systems for ternary separation," *J. Chromatogr. A*, 2014. (accepted).

[5] Aumann, L., Stroehlein, G., Mueller-Spaeth, T., Schenkel, B., and Morbidelli, M., "Protein peptide purification using the multicolumn countercurrent solvent gradient purification (MCSGP) process," *Biopharm Int.*, vol. 22, no. 1, pp. 46–52, 2009.

[6] Azevedo, D. and Rodrigues, A., "Design methodology and operation of a simulated moving bed reactor for the inversion of sucrose and glucose-fructose separation," *Chem. Eng. J.*, vol. 82, no. 1-3, SI, pp. 95–107, 2001.

[7] Bentley, J. A., *Systematic process development by simultaneous modeling and optimization of simulated moving bed chromatography*. PhD thesis, Georgia Institute of Technology, 2013.

[8] Bentley, J. and Kawajiri, Y., "Prediction-Correction Method for Optimization of Simulated Moving Bed Chromatography," *AIChE Journal*, vol. 59, pp. 736–746, 2013.

[9] Bentley, J., Sloan, C., and Kawajiri, Y., "Simultaneous modeling and optimization of nonlinear simulated moving bed chromatography by the predictioncorrection method," *J. Chromatogr. A*, vol. 1280, pp. 51–63, 2013.

[10] Beste, Y. and Arlt, W., "Side-stream simulated moving-bed chromatography for multicomponent separation," *Chem. Eng. Technol.*, vol. 25, no. 10, pp. 956–962, 2002.

[11] Biegler, L. T., *Nonlinear Programming: Concepts, Algorithms, and Applications to Chemical Processes*. SIAM-Society for Industrial and Applied Mathematics, 2010.

[12] Broughton, D. B. and Gerhold, C. G. US Patent No. 2,985,589, 1961.

[13] Broyles, B. S., Shalliker, R. A., Cherrak, D. E., and Guiochon, G., "Visualization of viscous fingering in chromatographic columns," *J. Chromatogr. A*, vol. 822, no. 2, pp. 173–187, 1998.

[14] Cherrak, D., Guernet, E., Cardot, P., Herrenknecht, C., and Czok, M., "Viscous fingering: A systematic study of viscosity effects in methanol-isopropanol systems," *Chromatographia*, vol. 46, no. 11-12, pp. 647–654, 1997.

[15] CHING, C., HO, C., HIDAJAT, K., and RUTHVEN, D., "Experimental-study of a simulated countercurrent adsorption system .5. Comparison of resin and zeolite absorbents for fructose glucose separation at high-concentration," *Chem. Eng. Sci.*, vol. 42, no. 11, pp. 2547–2555, 1987.

[16] Dünnebier, G., Fricke, J., and Klatt, K., "Optimal Design and Operation of Simulated Moving Bed Chromatographic Reactors.," *Ind. Eng. Chem. Res.*, vol. 39, pp. 2290–2304, 2000.

[17] Dünnebier, G. and Klatt, K., "Modelling and simulation of nonlinear chromatographic separation processes: a comparison of different modelling approaches," *Chem. Eng. Sci.*, vol. 55, pp. 373–380, 2000.

[18] Fourer, R., Gay, D. M., and Kernighan, W., *AMPL: A Modeling Language for Mathematical Programming*. CA: Brooks/Cole Publishing Company, 2002.

[19] Grosfils, V., Levrie, C., Kinnaert, M., and Wouwer, A. V., "A systematic approach to smb processes model identification from batch experiments," *Chem. Eng. Sci.*, vol. 62, pp. 3894–3908, 2007.

[20] Grossmann, C., Erdem, G., Morari, M., Amanullah, M., Mazzotti, M., and Morbidelli, M., "'Cycle to cycle' optimizing control of simulated moving beds," *AIChE J.*, vol. 54, no. 1, pp. 194–208, 2008.

[21] Guiochon, G., Felinger, A., Shirazi, D. G., and Katti, A. M., *Fundamentals of Preparative and Nonlinear Chromatography*. Academic Press, New York, 2006.

[22] Gyani, V. C. and Mahajani, S., "Reactive chromatography for the synthesis of 2-ethylhexyl acetate," *Separ. Sci. Technol.*, vol. 43, no. 9-10, pp. 2245–2268, 2008.

[23] Hashimoto, K., *Kuromato Bunri Kogaku*. Baifukan, Tokyo, Japan, 2005.

[24] Hashimoto, K., Adachi, S., Noujima, H., and Ueda, Y., "A new process combining adsorption and enzyme reaction for producing higher-fructose syrup," *Biotechnol Bioeng*, vol. 25, no. 10, pp. 2371–2393, 1983.

[25] Heikkila, H., Hyoky, G., and Kuisma, J. US Patent No. 5,127,957, 1992.

[26] Hyoky, G., Paananen, H., and Cotillon, M., "Presentation of the fast separation technology," in *Proceedings from the 30th Biennial Meeting of the American Society of Sugar Beet Technologists*, pp. 175–185, 1999.

[27] Jermann, S., Katsuo, S., and Mazzotti, M., "Intermittent Simulated Moving Bed Processes for Chromatographic Three-Fraction Separation," *Org. Process. Res. Dev.*, vol. 16, no. 2, pp. 311–322, 2012.

[28] Katsuo, S. and Mazzotti, M., "Intermittent simulated moving bed chromatography: 1. design criteria and cyclic steady-state," *J. Chromatogr. A*, vol. 1217, pp. 1354–1361, 2010.

[29] Kawajiri, Y. and Biegler, L. T., "Nonlinear programming superstructure for optimal dynamic operations of simulated moving bed processes," *Ind. Eng. Chem. Res.*, vol. 45, no. 25, pp. 8503–8513, 2006.

[30] Kawajiri, Y. and Biegler, L. T., "Optimization strategies for simulated moving bed and PowerFeed processes," *AIChE J.*, vol. 52, no. 4, pp. 1343–1350, 2006.

[31] Kawajiri, Y. and Biegler, L. T., "Large scale nonlinear optimization for asymmetric operation and design of Simulated Moving Beds," *J. Chromatogr. A*, vol. 1133, no. 1-2, pp. 226–240, 2006.

[32] Kawase, M., Inoue, Y., Araki, T., and Hashimoto, K., "The simulated moving-bed reactor for production of bisphenol A," *Catal. today.*, vol. 48, no. 1-4, pp. 199–209, 1999.

[33] Kawase, M., Suzuki, T., Inoue, K., Yoshimoto, K., and Hashimoto, K., "Increased esterification conversion by application of the simulated moving-bed reactor," *Chem. Eng. Sci.*, vol. 51, no. 11, pp. 2971–2976, 1996.

[34] Kessler, L. and Seidel-Morgenstern, A., "Theoretical study of multicomponent continuous countercurrent chromatography based on connected 4-zone units," *J. Chromatogr. A*, vol. 1126, no. 1-2, pp. 323–337, 2006.

[35] Kim, J., Zang, Y., and Wankat, P., "Single-cascade simulated moving bed systems for the separation of ternary mixtures," *Ind. Eng. Chem. Res.*, vol. 42, no. 20, pp. 4849–4860, 2003.

[36] Klier, K., Beretta, A., Sun, Q., Feeley, O., and Herman, R., "Catalytic synthesis of methanol, higher alcohols and ethers," *Catal. Today.*, vol. 36, no. 1, pp. 3–14, 1997.

[37] Kloppenburg, E. and Gilles, E., "A new concept for operating simulated moving-bed processes," *Chem. Eng. Technol.*, vol. 22, no. 10, pp. 813–817, 1999.

[38] Kruglov, A., Bjorklund, M., and Carr, R., "Optimization of the simulated countercurrent moving-bed chromatographic reactor for the oxidative coupling of methane," *Chem. Eng. Sci.*, vol. 51, no. 11, pp. 2945–2950, 1996.

[39] Kundu, P. K., Zhang, Y., and Ray, A. K., "Multi-objective optimization of simulated countercurrent moving bed chromatographic reactor for oxidative coupling of methane," *Chem. Eng. Sci.*, vol. 64, no. 19, pp. 4137–4149, 2009.

[40] Kurup, A. S., Hidajat, K., and Ray, A. K., "Optimal operation of a pseudo-SMB process for ternary separation under non-ideal conditions," *Sep. Purif. Technol.*, vol. 51, pp. 387–403, 2006.

[41] Kurup, A., Hidajat, K., and Ray, A., "Comparative study of modified simulated moving bed systems at optimal conditions for the separation of ternary mixtures under nonideal conditions," *Ind. Eng. Chem. Res.*, vol. 45, pp. 3902–3915, 2006.

[42] Kurup, A., Subramani, H., Hidajat, K., and Ray, A., "Optimal design and operation of SMB bioreactor for sucrose inversion," *Chem. Eng. J.*, vol. 108, no. 1-2, pp. 19–33, 2005.

[43] Lee, J. W. and Wankat, P. C., "Design of pseudo-simulated moving bed process with multi-objective optimization for the separation of a ternary mixture: Linear isotherms," *J. Chromatogr. A*, vol. 1217, no. 20, pp. 3418–3426, 2010.

[44] Lode, F., Francesconi, G., Mazzotti, M., and Morbidelli, M., "Synthesis of methylacetate in a simulated moving-bed reactor: Experiments and modeling," *AIChE J.*, vol. 49, no. 6, pp. 1516–1524, 2003.

[45] Lode, F., Houmard, M., Migliorini, C., Mazzotti, M., and Morbidelli, M., "Continuous reactive chromatography," *Chem. Eng. Sci.*, vol. 56, no. 2, pp. 269–291, 2001.

[46] Ludemann-Hombourger, O., Bailly, M., and Nicoud, R. M., "Design of a simulated moving bed: Optimal particle size of the stationary phase," *Sep. Sci. Technol.*, vol. 35, no. 9, pp. 1285–1305, 2000.

[47] Mai, P., Vu, T., Mai, K., and Seidel-Morgenstern, A., "Analysis of heterogeneously catalyzed ester hydrolysis performed in a chromatographic reactor and in a reaction calorimeter," *Ind. Eng. Chem. Res.*, vol. 43, no. 16, pp. 4691–4702, 2004.

[48] Masuda, T., Sonobe, T., Matsuda, F., and Horie, M., "Process for fractional separation of multi-component fluid mixture." US Patent No. 5,198,120, 1993.

[49] Mata, V. and Rodrigues, A., "Separation of ternary mixtures by pseudo-simulated moving bed chromatography," *J. Chromatogr. A*, vol. 939, no. 1-2, pp. 23–40, 2001.

[50] Mazzotti, M., Kruglov, A., Neri, B., Gelosa, D., and Morbidelli, M., "A continuous chromatographic reactor: SMBR," *Chem. Eng. Sci.*, vol. 51, no. 10, pp. 1827–1836, 1996.

[51] Mazzotti, M., Neri, B., Gelosa, D., and Morbidelli, M., "Dynamics of a chromatographic reactor: Esterification catalyzed by acidic resins," *Ind. Eng. Chem. Res.*, vol. 36, no. 8, pp. 3163–3172, 1997.

[52] Mazzotti, M., Storti, G., and Morbidelli, M., "Optimal operation of simulated moving bed units for nonlinear chromatographic separations," *J. Chromatogr. A*, vol. 769, no. 1, pp. 3–24, 1997.

[53] Migliorini, C., Fillinger, M., Mazzotti, M., and Morbidelli, M., "Analysis of simulated moving-bed reactors," *Chem. Eng. Sci.*, vol. 54, no. 13-14, pp. 2475–2480, 1999.

[54] Migliorini, C., Mazzotti, M., and Morbidelli, M., "Simulated moving-bed units with extra-column dead volume," *AIChE J*, vol. 45, no. 7, pp. 1411–1421, 1999.

[55] Minceva, M., Pais, L., and Rodrigues, A., "Cyclic steady state of simulated moving bed processes for enantiomers separation," *Chem. Eng. Process.*, vol. 42, no. 2, pp. 93–104, 2003.

[56] Minceva, M., Gomes, P. S., Meshko, V., and Rodrigues, A. E., "Simulated moving bed reactor for isomerization and separation of p-xylene," *Chem. Eng. J.*, vol. 140, no. 1-3, pp. 305–323, 2008.

[57] Mun, S., "Improving performance of a five-zone simulated moving bed chromatography for ternary separation by simultaneous use of partial-feeding and partial-closing of the product port in charge of collecting the intermediate-affinity solute molecules," *J. Chromatogr. A*, vol. 1218, no. 44, pp. 8060–8074, 2011.

[58] Nicolaos, A., Muhr, L., Gotteland, P., Nicoud, R., and Bailly, M., "Application of equilibrium theory to ternary moving bed configurations (four+four, five+four, eight and nine zones): I. Linear case.," *J. Chromatogr. A*, vol. 908, pp. 71–86, 2001.

[59] Nilchan, S. and Pantelides, C., "On the optimisation of periodic adsorption processes," *Adsorption*, vol. 4, no. 2, pp. 113–147, 1998.

[60] Nowak, J., Gedicke, K., Antos, D., Piatkowski, W., and Seidel-Morgenstern, A., "Synergistic effects in competitive adsorption of carbohydrates on an ion-exchange resin," *J. Chromatogr. A*, vol. 1164, no. 1-2, pp. 224–234, 2007.

[61] Nowak, J., Antos, D., and Seidel-Morgenstern, A., "Theoretical study of using simulated moving bed chromatography to separate intermediately eluting target compounds," *J. Chromatogr. A*, vol. 1253, pp. 58–70, 2012.

[62] Nowak, J., Poplewska, I., Antos, D., and Seidel-Morgenstern, A., "Adsorption behaviour of sugars versus their activity in single and multicomponent liquid solutions," *J. Chromatogr. A*, vol. 1216, no. 50, pp. 8697–8704, 2009.

[63] Oh, J., Agrawal, G., Sreedhar, B., Donaldson, M. E., Schultz, A. K., Frank, T. C., Bommarius, A. S., and Kawajiri, Y., "Catalytic synthesis of propylene glycol methyl ether acetate in batch and chromatographic reactors: Experiments and parameter estimation," *Chem. Eng. J.*, 2014. (submitted).

[64] Ozisik, N., *Finite Difference Methods in Heat Transfer*. Bosa Roca, USA: CRC Press Inc, 1994.

[65] Popken, T., Gotze, L., and Gmehling, J., "Reaction kinetics and chemical equilibrium of homogeneously and heterogeneously catalyzed acetic acid esterification with methanol and methyl acetate hydrolysis," *Ind. Eng. Chem. Res.*, vol. 39, no. 7, pp. 2601–2611, 2000.

[66] Ray, A. and Carr, R., "Experimental-study of a laboratory-scale simulated countercurrent moving-bed chromatographic reactor," *Chem. Eng. Sci.*, vol. 50, no. 14, pp. 2195–2202, 1995.

[67] Reddy, B. and Mahajani, S., "Feasibility of Reactive Chromatography for the Synthesis of n-Propyl Acetate," *Ind. Eng. Chem. Res.*, vol. 53, no. 4, pp. 1395–1403, 2014.

[68] Ruthven, D. and Ching, C., "Counter-current and Simulated Counter-current Adsorption Separation Processes," *Chem. Eng. Sci.*, vol. 44, no. 5, pp. 1011–1038, 1989.

[69] Sayama, K., Kamada, T., Oikawa, S., and Masuda, T., "Production of raffinose - a new by-product of the beet sugar-industry," *Zuckerind*, vol. 117, pp. 893–898, 1992.

[70] Schmidt, J., Reusch, D., Elgeti, K., and Schomacker, R., "Kinetics of transesterification of ethanol and butyl acetate - A model system for reactive rectification," *Chem-Ing-Tech.*, vol. 71, no. 7, pp. 704–708, 1999.

[71] Schmidt-Traub, H., Schulte, M., and Seidel-Morgenstern, A., *Preparative Chromatography*. Weinheim: Wiley-VCH, 2012.

[72] Schramm, H., Kaspereit, M., Kienle, A., and Seidel-Morgenstern, A., "Improving simulated moving bed processes by cyclic modulation of the feed concentration," *Chem. Eng. Technol.*, vol. 25, no. 12, pp. 1151–1155, 2002.

[73] Schramm, H., Kaspereit, M., Kienle, A., and Seidel-Morgenstern, A., "Simulated moving bed process with cyclic modulation of the feed concentration," *J. Chromatogr. A*, vol. 1006, no. 1-2, pp. 77–86, 2003.

[74] Seidel-Morgenstern, A., Kessler, L. C., and Kaspereit, M., "New developments in simulated moving bed chromatography," *Chem. Eng. Technol.*, vol. 31, no. 6, pp. 826–837, 2008.

[75] Shieh, M. and Barker, P., "Combined bioreaction and separation in a simulated counter-current chromatographic bioreactor-separator for the hydrolysis of lactose," *J. Chem. Technol. Biot.*, vol. 66, no. 3, pp. 265–278, 1996.

[76] Sreedhar, B. and Kawajiri, Y., "Multi-column chromatographic process development using simulated moving bed superstructure and simultaneous optimization - model correction framework," *Chem. Eng. Sci.*, 2013. (in press, doi 10.1016/j.ces.2014.05.004).

[77] Storti, G., Mazzotti, M., Morbidelli, M., and Carra, S., "Robust design of binary countercurrent adsorption separation processes," *AIChE J.*, vol. 39, no. 3, pp. 471–492, 1993.

[78] Ströhlein, G., Mazzotti, M., and Morbidelli, M., "Optimal operation of simulated-moving-bed reactors for nonlinear adsorption isotherms and equilibrium reactions," *Chem. Eng. Sci.*, vol. 60, no. 6, pp. 1525–1533, 2005.

[79] Ströhlein, G., Assuncao, Y., Dube, N., Bardow, A., Mazzotti, M., and Morbidelli, M., "Esterification of acrylic acid with methanol by reactive chromatography: Experiments and simulations," *Chem. Eng. Sci.*, vol. 61, no. 16, pp. 5296–5306, 2006.

[80] Subramani, H., Zhang, Z., Hidajat, K., and Ray, A., "Multiobjective optimization of simulated moving bed reactor and its modification - Varicol process," *Can. J. Chem. Eng.*, vol. 82, no. 3, pp. 590–598, 2004.

[81] Tanimura, M., Tamura, M., and Teshima, T. Japanese Patent JP-B-H07-046097, 1995.

[82] Tikhonov, A., Goncharsky, A., Stepanov, V., and Yagola, A., *Numerical Methods for the Solution of Ill-Posed Problems.* Boston: Kluwer Academic Publishers, 1995.

[83] Toumi, A. and Engell, S., "Optimization-based control of a reactive simulated moving bed process for glucose isomerization," *Chem. Eng. Sci.*, vol. 59, no. 18, pp. 3777–3792, 2004.

[84] Toumi, A., Hanisch, F., and Engell, S., "Optimal operation of continuous chromatographic processes: Mathematical optimization of the VARICOL process," *Ind. Eng. Chem. Res.*, vol. 41, no. 17, pp. 4328–4337, 2002.

[85] Van Deemter, J. J., Zuiderweg, F. J., and Klinkenberg, A., "Longitudinal diffusion and resistance to mass transfer as causes of nonideality in chromatography," *Chem. Eng. Sci.*, vol. 5, pp. 271–289, 1956.

[86] Vente, J. A., Bosch, H., de Haan, A. B., and Bussmann, P. J., "Evaluation of sugar sorption isotherm measurement by frontal analysis under industrial processing conditions," *J. Chromatogr. A*, vol. 1066, no. 12, pp. 71 – 79, 2005.

[87] Vu, T. D. and Seidel-Morgenstern, A., "Quantifying temperature and flow rate effects on the performance of a fixed-bed chromatographic reactor," *J. Chromatogr. A*, vol. 1218, no. 44, pp. 8097–8109, 2011.

[88] Wachter, A. and Biegler, L., "On the implementation of an interior-point filter line-search algorithm for large-scale nonlinear programming," *Math. Program.*, vol. 106, no. 1, pp. 25–57, 2006.

[89] Wankat, P., "Simulated Moving Bed Cascades for Ternary Separations," *Ind. Eng. Chem. Res.*, vol. 40, pp. 6185–6193, 2001.

[90] Xie, Y., Chin, C., Phelps, D., Lee, C., Lee, K., Mun, S., and Wang, N., "A five-zone simulated moving bed for the isolation of six sugars from biomass hydrolyzate," *Ind. Eng. Chem. Res.*, vol. 44, no. 26, pp. 9904–9920, 2005.

[91] Yu, W., Hidajat, K., and Ray, A., "Determination of adsorption and kinetic parameters for methyl acetate esterification and hydrolysis reaction catalyzed by Amberlyst 15," *Appl. Catal. A:Gen.*, vol. 260, no. 2, pp. 191–205, 2004.

[92] Yu, W., Hidajat, K., and Ray, A., "Optimization of reactive simulated moving bed and Varicol systems for hydrolysis of methyl acetate," *Chem. Eng. J.*, vol. 112, no. 1-3, pp. 57–72, 2005.

[93] Zang, Y. F. and Wankat, P. C., "SMB operation strategy - Partial feed," *Ind. Eng. Chem. Res.*, vol. 41, no. 10, pp. 2504–2511, 2002.

[94] Zhang, Z. Y., Mazzotti, M., and Morbidelli, M., "Powerfeed operation of simulated moving bed units: changing flow-rates during the switching interval," *J. Chromatogr. A*, vol. 1006, pp. 87–99, 2003.

[95] Zhang, Z., Hidajat, K., and Ray, A., "Application of simulated countercurrent moving-bed chromatographic reactor for MTBE synthesis," *Ind. Eng. Chem. Res.*, vol. 40, no. 23, pp. 5305–5316, 2001.

[96] Zhang, Z., Mazzotti, M., and Morbidelli, M., "Continuous chromatographic processes with a small number of columns: Comparison of simulated moving bed with varicol, PowerFeed, and ModiCon," *Korean J. Chem. Eng.*, vol. 21, no. 2, pp. 454–464, 2004.

[97] Ziyang, Z., Hidajat, K., and Ray, A. K., "Multiobjective Optimization of Simulated Countercurrent Moving Bed Chromatographic Reactor (SCMCR) for MTBE Synthesis.," *Ind. Eng. Chem. Res.*, vol. 41, pp. 3213–3232, 2002.